AD NUMBER

AD876656

NEW LIMITATION CHANGE

TO

Approved for public release, distribution unlimited

FROM

Distribution: Further dissemination only as directed by Commanding Officer, Naval Ordnance Laboratory, White Oak, MD., Nov 1953, or higher DoD authority.

AUTHORITY

USNOL ltr, 29 Aug 1974

U.S NAVAL ORDNANCE LABOR
WHITE OAK. MARYL

250 650

DISCLAIMER NOTICE

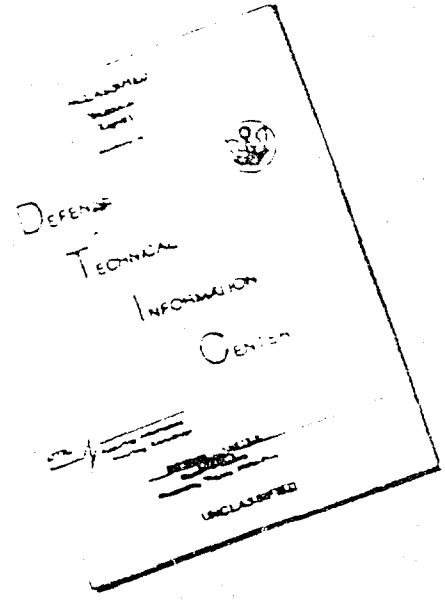

THIS DOCUMENT IS BEST QUALITY AVAILABLE. THE COPY FURNISHED TO DTIC CONTAINED A SIGNIFICANT NUMBER OF PAGES WHICH DO NOT REPRODUCE LEGIBLY.

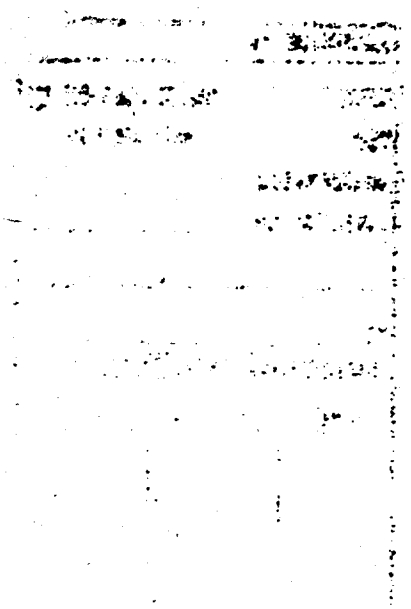

UNDERWATER ANECHOIC [illegible] LININGS

Prepared by:

A. Keller

ABSTRACT: An investigation of structured linings employing the principle of a gradual impedance transition from water to a sound-absorbent material has been made. Prototype metal loaded butyl rubber linings have been developed which consist of a molded panel of closely-packed right circular cones and an integral backing layer. Reflection characteristics were measured for three samples having this structure but differing in the type of metal loading. In addition measurements were made on plane samples of each type of rubber, and also on samples of Fafnir, Insulkrete, and canvas. The technique consisted of subjecting the test panel to normally incident pulse-modulated sound and measuring the reflected sound pressure with a rotating probe hydrophone. The test panel was backed by a perfectly-reflecting flat plate which also was used as a reference reflector. By this method it was possible to obtain the reflected sound intensity as a function of polar angle (reflectivity pattern) and from this the scattering and absorption were computed. An aluminum-loaded butyl rubber specimen with a multiple cone surface had the best overall anechoic characteristics of all samples tested, over a frequency range from 50 to 250 kc. Measurements on this sample were made from 20 kc to 1 Mc. The sound reflection coefficient (ratio of total acoustic power reflected to the total incident power) was at least -20 db over the frequency range covered and at 200 kc the coefficient had a maximum value of -32 db. The maximum reflected intensity was at least -23 db from 20 kc to 1 Mc and was -38 db at 200 kc.

U. S. NAVAL ORDNANCE LABORATORY
WHITE OAK, MARYLAND

NAVORD Report 2989 10 November 1953

This report describes the results of a research program supported by Foundational Research funds under Task No. FR-5-54. It is concerned with an investigation of several types of sound absorbent panels for use as linings in underwater anechoic tanks, and describes the development of the best wide band anechoic lining reported to date in the literature of ultrasonics. This report is intended for the information of scientific personnel concerned with the problem of doing underwater ultrasonics research or development and testing work.

EDWARD L. WOODYARD
Captain, USN
Commander

D. F. Bleil

D. F. BLEIL
By direction

References

(a) L. L. Beranek, Acoustic Measurements, (John Wiley & Sons, Inc., New York, 1949) First edition

(b) W. J. Trott and C. L. Darner, "Measurement of the Acoustic Properties of Sound Absorbent Panels at High Hydrostatic Pressures", J. Acoust. Soc. Am 22, 691 (1950)

(c) Lord Rayleigh, Theory of Sound, (Dover Publications, New York, 1945), second edition, vol 2

(d) P. M. Morse, Vibration and Sound, (McGraw-Hill, New York 1948)

(e) Erwin Meyer et al, Sound Absorption and Sound Absorbers in Water, BuShips, Dept. of Navy, Washington 25, D. C., Report No. NavShips 900, 164 (1950)

(f) American Standards Association, Inc., Acoustical Terminology (1951)

(g) P. M. Kendig and R. E. Mauser, "A Simplified Method for Determining Transducer Directivity Index", J. Acoust. Soc. Am., 19, 691 (1947)

(h) L. E. Kinsler and A. R. Frey, Fundamentals of Acoustics (John Wiley & Sons, Inc., New York, 1950), first edition

(i) Naval Ordnance Laboratory, "Theoretical Study of Underwater Sound Absorbing Layers", NAVORD Report 2303, Jun 1953 (conf)

(j) C. Zwikker and C. W. Kosten, Sound Absorbing Materials, (Elsevier Publishing Co., Inc., New York, 1949)

(k) Naval Ordnance Laboratory, "An Acoustic Technique for Measuring the Effective Dynamic Bulk Modulus of Elasticity and Associated Loss Factor of Rubber [illegible] Plastics", NAVORD Report 1534, Sep 1950

(l) M. S. Weinstein, "Some Design Considerations for High Frequency Anechoic Tanks", J. Acoust. Soc. Am., 25, 101 (1953)

(m) Underwater Sound Reference Laboratory, "An Underwater Sound Absorber for an Anechoic Tank", USRL Report No. 31, Sep 1953

References (Cont'd)

(n) W. P. Mason and F. H. Hibbard, "Absorbing Media for Underwater Sound Measuring Tanks and Baffles", J. Acoust. Soc. Am. 20,476 (1948)

(o) Admiralty Research Laboratory (Teddington), "Absorption of Acoustic Energy by Rubber Loaded Heavy Particles", ARL/N.1/95.50D, Aug 1949 (sec)

(p) Office Scientific Research and Development, Section 6, Div. 6-1, "A Calibration System in the Lower Megacycle Range" Aug 1944 (Submitted by Bell Telephone Laboratories for the Western Electric Company under Contract OSRsr-783)

CONTENTS

Part		Page
I.	Introduction	1
II.	Lining Requirements for Tanks	2
III.	Selection of Samples for Measurement	3
	A. Selection of Material	3
	B. Selection of Structure	4
IV.	Laboratory Apparatus	5
V.	Measurements	22
	A. Measurement Program	22
	B. Theory of Measurements	28
	C. Application of the Technique	34
VI.	Discussion of Results	42
	Comparison of Samples from 50 to 250 kc	42
	Measurements Considering Periodicity in ϕ	60
	Incremental Measurements on Samples No. 21 and No. 22	66
	Broad Frequency Range Measurements - Sample No. 21	69
	Interpretation and Reliability of Results	74
VII.	Conclusions and Recommendations	77
VIII.	Acknowledgments	78

ILLUSTRATIONS

		Page
Figure 1.	Test Sample of Loaded Butyl Rubber with a Cone Lattice Surface	2
Figure 2.	Measurement Tank Lined with German Pafnir	3
Figure 3.	Diagram of a Flat Lining Backed with a Perfect Reflector	5
Figure 4.	Diagram of a Flat Lining Preceded by an Impedance Transition Medium	8
Figure 5.	Normal Reflectivity Index for Loaded Butyl Rubber Samples with Metal Loading-Aluminum Powder	10
Figure 6.	Normal Reflectivity Index for Loaded Butyl Rubber Samples with Metal Loading-Lead Powder	11
Figure 7.	Normal Reflectivity Index for Loaded Butyl Rubber Samples with Metal Loading-Lead Powder (Blowing Agent Added)	12
Figure 8.	Test Sample of British Pafnir Lining	14
Figure 9.	Test Samples of Insulkrete Tank Lining	15
Figure 10.	Typical views of Pafnir Structure	16
Figure 11.	Diagram Indicating Transition Cross-Section of German Pafnir Lining	17
Figure 12.	Diagram Indicating Transition Cross-Section of Closely Stacked British Pafnir Test Sample	19
Figure 13.	Typical views of Cone Lattice Structure	20
Figure 14.	Diagram Indicating Transition Cross-Section of Cone Lattice Sample	21
Figure 15.	Block Diagram of System for the Measurement of Acoustic Absorption	25
Figure 16.	Arrangement of Apparatus	26
Figure 17.	Arrangement of Sample and Underwater Equipment	27
Figure 18.	Geometry of Experiment	29

ILLUSTRATIONS (Cont'd)

Figure 19.	Illustration Showing use of Power Charts for Calculating Reflection Indices R, Δ, and S	34
Figure 20.	Diagram of Geometric Relationship of Projector Beam to Sample and Tank	38
Figure 21.	Restriction on Projector Beam Width - Beam Width vs Frequency	39
Figure 22.	Restrictions on Projector Beam Width - Radius vs Frequency	40
Figure 23.	Typical Reflectivity Pattern-Frequency 100 kc	43
Figure 24.	Reflectivity Pattern of Sample and Reference Plate-Frequency 50 to 250 kc	45
	Reflection Characteristics versus Frequency for various Samples:	
Figure 25.	Sample No. 11	47
Figure 26.	Sample No. 21	49
Figure 27.	Sample No. 31	50
Figure 28.	Sample No. 12	51
Figure 29.	Sample No. 22	52
Figure 30.	Sample No. 32	54
Figure 31.	Sample No. 41	55
Figure 32.	Samples Nos. 51, 52, 53, and 54	56
Figure 33.	Sample No. 61	58
Figure 34.	Samples Nos. 71 and 72	59
Figure 35.	Reflectivity Index, R, for all Samples vs Frequency	61
Figure 36.	Peak Reflectivity Index, Δ, for all Samples vs Frequency	62

ILLUSTRATIONS (Cont'd)

		Page
Figure 37.	Scattering Index, S_o, for all Samples vs Frequency	63
Figure 38.	Reflectivity Patterns for Planes ψ_o and ψ_v	64
Figure 39.	Reflection Characteristics in the Planes ψ_o and ψ_v for Sample No. 21	65
Figure 40.	Reflection Characteristics in the Planes ψ_o and ψ_v for Sample No. 73	67
Figure 41.	Reflection Characteristics vs Frequency for Sample No. 22	68
Figure 42.	Reflection Characteristics vs Frequency for Sample No. 21	70
Figure 43.	Comparison of Normal Reflectivity Index and Reflectivity Index (R), Sample No. 22 - Frequency 140 to 260 kc	71
Figure 44.	Comparison of Normal Reflectivity Index and Reflectivity Index (R), Sample No. 21 - Frequency 140 to 260 kc	72
Figure 45.	Reflectivity Patterns of Sample No. 21 and Reference Plate - Frequency 35 kc to 1 Mc	73
Figure 46.	Reflectivity Patterns of Sample No. 21 vs Projector Beam Width	75
Figure 47.	Reflection Characteristics vs Frequency, Sample No. 21 Frequency 20 kc to 1 Mc.	76
Table I.	Physical Characteristics of Lining Samples	23
Table II.	Effect of Orientation on the Reflection Characteristics of British Fafnir	66

LIST OF SYMBOLS

SYMBOL	UNIT	QUANTITY
A	cm	Projector radius
a_s		Absorption of incident energy in percent.
A_p	cm^2	The area representing the total normalized power reflected from a reference plate.
A_s	cm^2	The area representing the total normalized power reflected from a sample (see par. 34)
v	cm/sec	Phase velocity
D	cm	Thickness of lining layer
D'	cm	Thickness of transition layer
D_p	cm	Distance from projector to sample
D_s	cm	Sample width
D_θ	cm	Distance in plane of sample between the two half-power points of the projector beam.
f	$(sec)^{-1}$	Frequency
$I_s(\theta)$	erg/sec cm^2	Intensity reflected from sample at a fixed distance γ, at a polar angle θ and in the plane $\psi = \psi_0 = 0$.
$I_s(\theta, \psi)$	erg/sec cm^2	Same as above, except ψ is an independent variable
$I_{s\,max}$	erg/sec cm^2	Maximum value of $I_s(\theta)$
$I_r(\theta)$	erg/sec cm^2	Intensity reflected from reference plate at a fixed distance γ, at a polar angle (θ) and in the plane $\psi = \psi_0 = 0$.
$I_r(\theta, \psi)$	erg/sec cm^2	Same as above except ψ is an independent variable

LIST OF SYMBOLS (Cont'd)

SYMBOL	UNIT	QUANTITY
I_{p} max	erg/sec cm^2	Maximum value of I_p (9)
k	radians/cm	($k = \omega/v = 2\pi/\lambda$) Acoustical phase constant
p	dynes/cm^2	Total effective pressure.
p_i	dynes/cm^2	Effective pressure of sound wave incident on a surface.
p_p max	dynes/cm^2	Pressure reflected from plate corresponding to I_{p} max.
R_p	dynes/cm^2	Effective pressure of sound wave reflected from a surface.
p_s max	dynes/cm^2	Pressure reflected from sample corresponding to I_s max.
P	erg/sec	Reflected power
P_p	erg/sec	Power reflected from reference plate
P_s	erg/sec	Power reflected from sample
r	cm	Radius
R_N		Dw/Ds
R	db	The reflectivity index, which is the reflection coefficient, R_c expressed in db
R_c		Reflection coefficient, ratio of sound energy reflected from a surface on the side of incidence to the incident energy.
R_N	db	Normal Reflectivity Index, the ratio of sound energy reflected normally from a surface to the incident energy, which is also normal.
R_ψ	db	The reflectivity index for a structure periodic in ψ (See par 36)

LIST OF SYMBOLS (Cont'd)

SYMBOL	UNIT	QUANTITY
S	db	(= $\log(A_s/A_p)$). Scattering index. Ratio of normalized power reflected from sample to the normalized power reflected from a reference plate expressed in db.
S_a	db	The scattering index for a structure periodic in Ψ
v	cm/sec	Total effective particle velocity
z_c	dyne/sec/cm^3	Specific acoustic impedance of material. The complex ratio of sound pressure to particle velocity
z_∞	dyne/sec/cm^3	Impedance of infinite thickness material.
z_T	dyne/sec/cm^3	Impedance at a point x in a transition medium
z_w	dyne/sec/cm^3	Specific acoustic impedance of water
α	nepers/cm	Attenuation constant, the real part of the acoustical propagation constant.
β	degrees or radians	Polar angle measured from the acoustic axis of a piston radiator.
β'	degrees or radians	Polar angle corresponding to half power point (Figure 20) of a piston radiator
β_0	degrees or radians	Polar angle at which the energy radiated from a piston radiator is zero.
Δ	db	Peak reflectivity index = 20 log (Pressure/Pressure). The ratio of the maximum pressures expressed in db.
$\Delta_{R_a S_a}$	db	(R_a - S_a). Δ for a hypothetical axially symmetric surface with values of R and S equal to R_a and S_a respectively.

LIST OF SYMBOLS (Cont'd)

SYMBOL	UNIT	QUANTITY
d'	db	Peak reflection index for a structure periodic in ψ
θ	degrees or radians	Polar angle measured from the acoustical axis.
λ	cm	Wave length of sound
ρ	gm/cm^3	Specific density
ψ	degrees or radians	Radial angle of the measurement plane - The angle determined by the x axis and a line which is the intersection of the measurement plane and a plane normal to the axis

UNDERWATER ANECHOIC TANK LININGS

I. INTRODUCTION

1. A problem of practical interest in the field of underwater acoustics is the development of linings or coatings which reduce sound reflections. Applications of sound absorbent linings include coverings for underwater ordnance material, linings for underwater acoustic tanks, and sound baffles in underwater acoustic devices of all types.

2. The work reported here is a preliminary study of the use of an absorbent lining with a structured surface designed to reduce the reflection of underwater sound. The surface structure of this lining consists of a closely-packed lattice of uniform right circular cones (Figure 1). The basic materials from which the structures were made were metal-loaded butyl rubbers. Three specimens were measured having this structure but differing in the type of metal loading added to the basic butyl rubber. Comparative measurements were made on flat samples of each of the above materials, and on German Fafnir, British Fafnir, Insulkrete, and canvas. The frequency range covered was from 50 kc to 250 kc for all samples. However, for the most absorbent sample, measurements were made from 20 kc to 1 Mc.

II. LINING REQUIREMENTS FOR TANKS

3. Relatively small, absorbently-lined tanks may be used in underwater acoustic measurements to simulate free field conditions over certain frequency ranges. For example, a tank, having dimensions 5 x 5 x 10 ft and lined with German Fafnir, is in use at this laboratory at the present time (Figure 2). The frequency range of the measurements normally made in this tank are from about 50 kilocycles to several megacycles. Pulse techniques are used to minimize the interference caused by reflections from the walls of the tank. The success of the pulse method is based on the ability to separate wall reflections from the desired signal by the difference in arrival times. Since the pulse repetition rate is chosen to allow many reflections between pulses, the absorption per reflection need not be great. Hence, absorption requirements for a tank lining in this type of service are not severe.

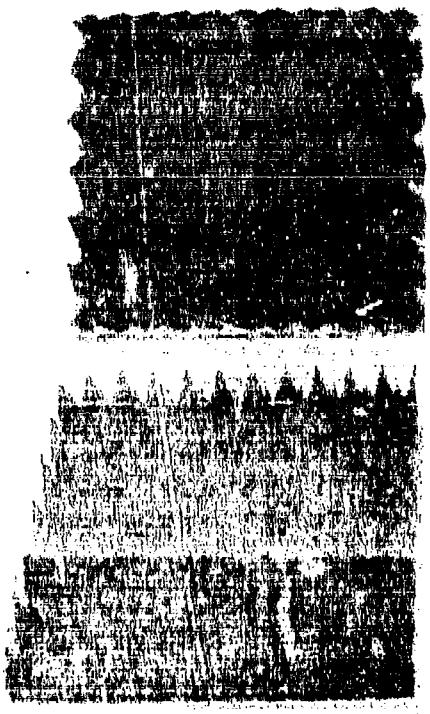

FIG. 1
TEST SAMPLE OF LOADED
BUTYL RUBBER LINING WITH
A CONE LATTICE SURFACE

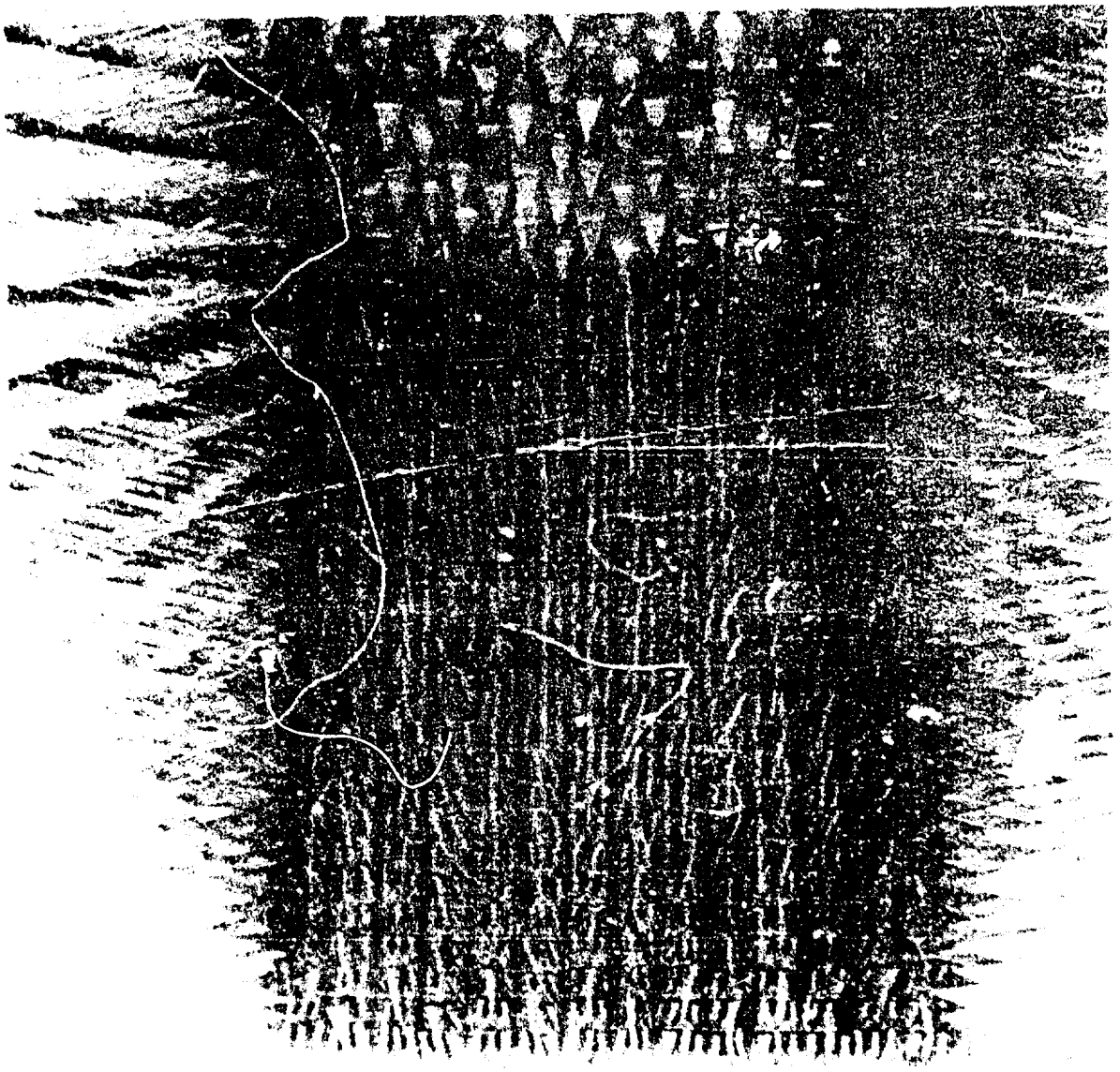

FIG. 2
[illegible] PERMANENT TANK LINED WITH GERMAN FABNIR

4. Consideration of Reflection Levels. Occasionally, however, difficulty has been experienced because of inadequate absorption by the lining, particularly when the length of the desired signal is necessarily longer than the shortest path length from a wall. Consequently, no time interval of sufficient duration for reception of the desired reflected signal is available which is free from appreciable wall reflections. For frequencies below a lower limit of about 40 kc, reflections interfere with the desired signal since the pulse length needed for good frequency resolution is of the same order as the tank dimensions. Measurements made below this frequency become progressively more difficult and require special precautions.) To alleviate this difficulty the lining must be sufficiently absorbent to reduce the initial reflections from all walls to a negligible value relative to the desired signal.

5. It is instructive to consider a spherical, absorbently-lined enclosure with a radius equal to some multiple half wavelength of the sound and a simple source located at the center. The steady-state total intensity at the center, I_T, is given by

$$I_T = I_o\left(1 + R_c + R_c^2 + R_c^3 - - - - R_c^n - - - -\right) \tag{1}$$

$$= I_o \frac{1}{1 - R_c} \tag{2}$$

where I_o is the source intensity and R_c is the reflection coefficient.

The nth-order term in the series gives the contribution to the intensity I_T of the nth reflection. If only the first order term, R_c, is considered as contributing to the reflected intensity, the remainder, γ, is

$$\gamma = \left(\frac{1}{1 - R_c} - (1 + R_c)\right) I_o \tag{3}$$

$$= \left(\frac{R_c^2}{1 - R_c}\right) I_o = R_c^2 I_o \quad \text{for } R_c << 1 \tag{4}$$

The ratio of the remainder to the first reflection is then

$$\frac{R_c^2 I_o}{R_c I_o} = R_c << 1 \tag{5}$$

That is, the error in considering only the first reflection is negligible since it is the same order of magnitude as the fraction of sound reflected on the first reflection. Since reflections in a rectangular tank tend to be more diffuse than reflections in a spherical tank (with a source at the center), consideration of only the first reflection would normally insure satisfactory operation. It should be noted that for cases where equation (5) holds, either pulse or continuous operation may be used.

6. Consideration of Mechanism of Reflection Reduction. The requirements for an effective tank lining are first, a good impedance match to water to allow the sound to enter the material; and second, the lining must be able to absorb the sound which enters. A property which can further increase the effectiveness of a lining for some types of measurements is scattering.

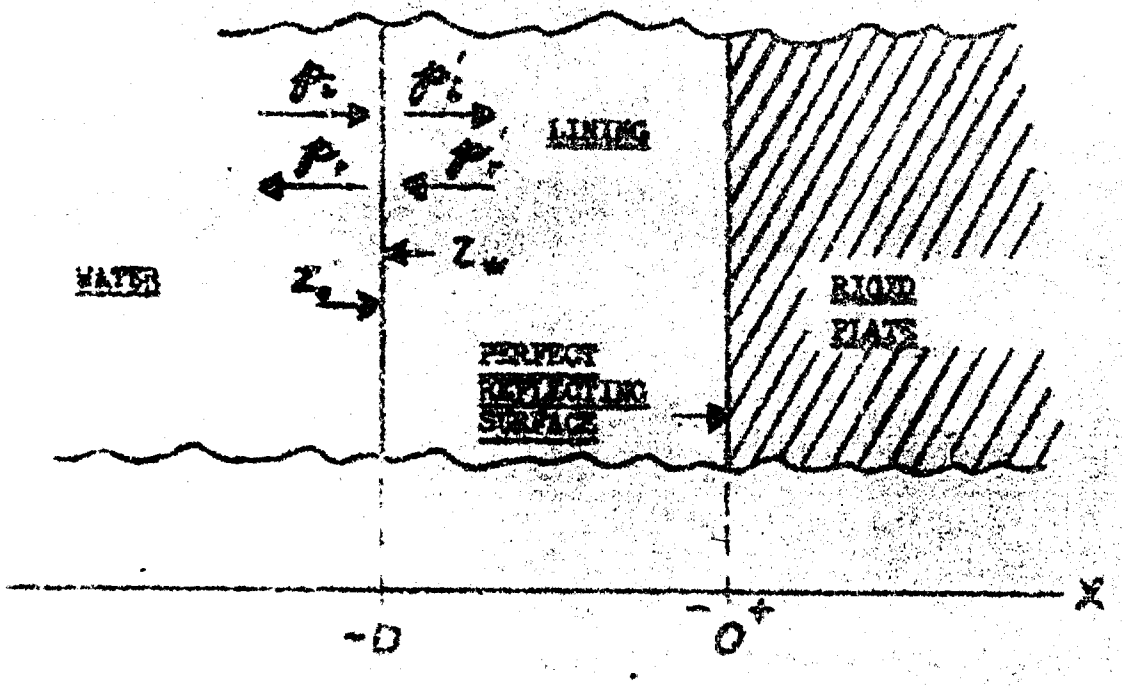

FIGURE 3
DIAGRAM OF A FLAT LINING BACKED BY A PERFECT REFLECTOR

7. One may consider a plane sound wave normally incident on a plane lining backed by a rigid plate, Figure 3. If one uses a theoretical approach similar to that of reference (a), the ratio of reflected to incident pressure at the surface of the lining is given by

$$\frac{p_r}{p_i} = \frac{Z_o - Z_w}{Z_o + Z_w} \tag{6}$$

where Z_o is the acoustic impedance of the lining surface, and Z_w is the acoustic impedance of the water.

Inside the lining the impedance at any point is given by the following equation which is discussed in considerable detail in reference (h):

$$Z(x) = \frac{p}{v} = \frac{(\rho c)_m}{1 + j(\omega/k)} \coth\left[(\alpha + jk)(-x)\right] \tag{7}$$

where p is the excess pressure at x

v is the particle velocity at x

α is the attenuation constant

k is the wave number

ρ is the density, and

c is the phase velocity

The subscript m refers to the lining. The variation of α with frequency is dependent on the nature of the loss mechanism and for loaded butyl rubbers this has not yet been determined.

8. Then for $x = -D$, where D is the lining thickness, the acoustic impedance at the interface is

$$Z_o = \frac{(\rho c)_m}{1 + j(\omega/k)} \coth\left[(\alpha + jk) D\right] \tag{8}$$

If the impedance is not to vary periodically with frequency, one must have the condition

$$e^{-2\alpha D} = p_r/p_i << 1 \tag{9}$$

for which the coth approaches unity.

One way of satisfying this condition is to make D very large and α small. If at the same time one chooses

$$(\rho c)_m \approx (\rho c)_w, \tag{10}$$

one may obtain a highly absorbent lining without appreciable mismatch. However, a lining which fulfills this condition is undesirable for the present application because of the large amount of material and space which would be required.

9. If one satisfies the condition that the product αD be large by making α very large and D small, then the expression for the impedance is

$$z_0' = \frac{(\rho c)_m}{1+(\alpha/k)^2}\left(1+j(\alpha/k)\right) \tag{11}$$

Although this impedance is complex and the impedance of water is real, one can minimize $|p_r/p_i|$ by equating the absolute values of these impedances. For a constant value of α/k one has then

$$z_0' = (\rho c)_w e^{j\tan^{-1}(\alpha/k)} \tag{12}$$

The minimum value of p_r/p_i is, therefore,

$$p_r/p_i = \frac{e^{j\tan^{-1}(\alpha/k)} - 1}{e^{j\tan^{-1}(\alpha/k)} + 1} \tag{13}$$

$$= j\tan\tfrac{1}{2}\left[\tan^{-1}(\alpha/k)\right] \tag{14}$$

for $p_r/p_i \ll 1$,

$$p_r/p_i \approx \tfrac{1}{2}(\alpha/k) = \frac{\alpha\lambda}{4\pi} \tag{15}$$

The above equation indicates that for a good match α/λ must

be small, which is contrary to the requirement that α be large for high attenuation in the material. This would be especially restrictive at low frequencies where λ is large.

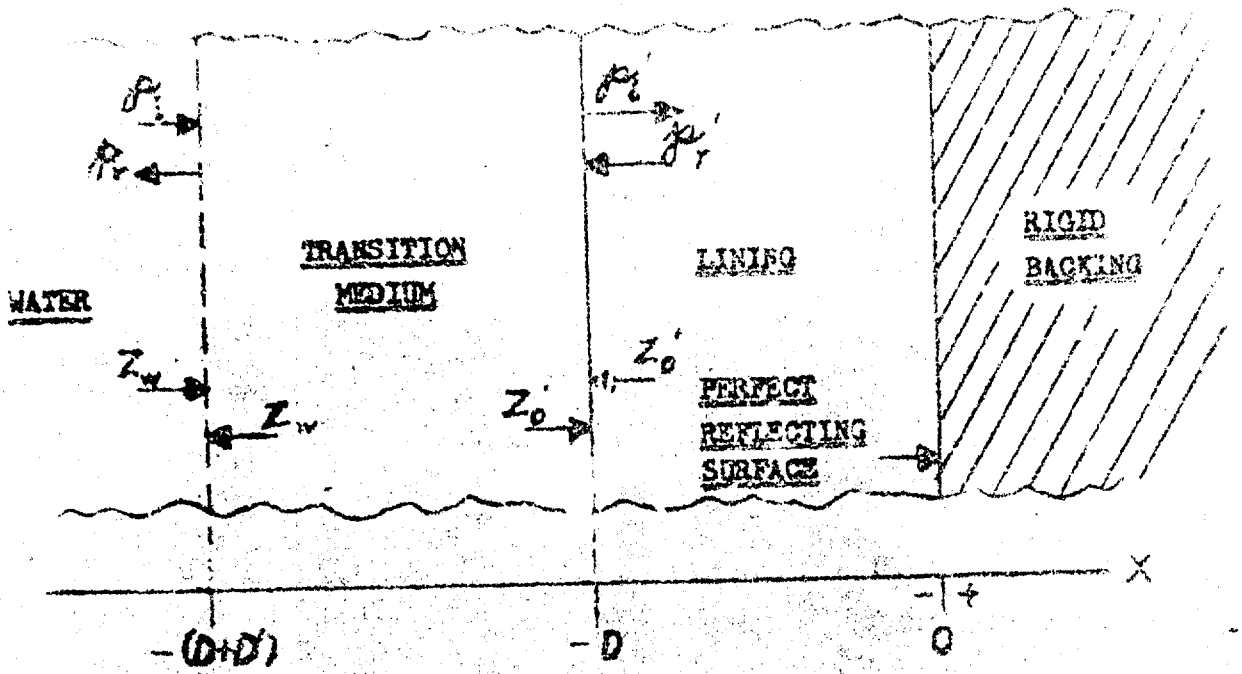

FIGURE 4.

DIAGRAM OF A FLAT LINING PRECEDED BY AN IMPEDANCE TRANSITION MEDIUM

10. Consider now a transition medium having an impedance which varies gradually with x, inserted in front of the lining, Figure 4. The impedance is continuous and at $x = -(D + D')$ the value of $Z_T(x)$ is made equal to Z_w, and at $x = -D$, it is made equal to Z_b', i.e.,

$$Z_T(-D) = Z_b' = \frac{(\rho c)_m}{1+(\beta/k)^2}\left[1 + j(\beta/k)\right] \qquad (16)$$

Since the impedance of the transition medium is a gradual continuous function of x there is practically no reflection caused by acoustic mismatch.

The use of a transition lining is an attempt to simulate [illegible]. However, the actual mechanism of

[illegible] is a simple function of [illegible] the pressure release in the translation portion of the lining are complicated functions of the shape of the structure and the properties of the media. [illegible] of structured linings is discussed in more detail in Part III. It may be added that structured linings can be designed to scatter sound, instead of matching. By such a design, the reflected intensity of narrow-beam incident sound may be lowered in a particular direction (by scattering in other directions) below that obtained by specular reflection and absorption.

III. SELECTION OF SAMPLES FOR MEASUREMENT

A. Selection of Material

12. Loaded Butyl Rubber Materials. Prior to the selection of a material for the structured samples, normal reflection measurements had been made on a large number of small flat samples of different types of metal-loaded rubber. The samples were approximately 1/4 in. thick, 2 1/2 in. in diameter and were metal backed. For each frequency a single narrow-beam transducer was used to transmit a pulse-modulated wave normal to the reflecting surface and to receive the reflected signal. The method of measurement consisted essentially of comparing the magnitude of the normally-reflected pulses from the metal-backed samples to reflections from a bare metal disc of the same normal cross section. The ratio of the reflected amplitude from the sample to that from the metal reference plate expressed in db constitutes a lumped loss occasioned by insertion of the sample. This quantity is denoted in this report as R_N, the normal reflectivity index. The measured loss does not necessarily represent the attenuation in the material, since the impedance mismatch at the water-sample interface limits the sound which can enter the material. Under these conditions, increasing the thickness of the sample does not necessarily increase the observed loss.

13. The results of these previous measurements on disc samples were used as a basis for the selection of loaded-rubber materials for the cone-lattice structured samples. Some typical results [illegible] curves of R_N versus frequency, are shown in Figures 5, 6 and 7. In these figures the variable parameter is the percentage of loading material. Other parameters considered in this early work were the type of metal loading, processing of samples, size of loading particles, and the method of fastening the samples.

14. The materials finally decided on for the present measurements were: Sample B (Figure 5) which consisted of equal parts by weight of aluminum powder and butyl rubber; Sample E (Figure 6) which consisted of 95 parts of lead powder, 9.25 parts of cumar, [illegible] parts per 100 parts of butyl rubber; and [illegible] of Sample F (Figure 7) consisting of 250 parts of

FIG. 5 NORMAL REFLECTIVITY INDEX OF LOADED BUTYL RUBBER FLAT DISK SAMPLES

METAL LOADING: ALUMINUM POWDER
VARIED PARAMETER: METAL PROPORTION

SAMPLE	PROPORTION (BY WEIGHT)
A	25 PTS/100
B	100 PTS/100
C	200 PTS/100
OA	UNLOADED

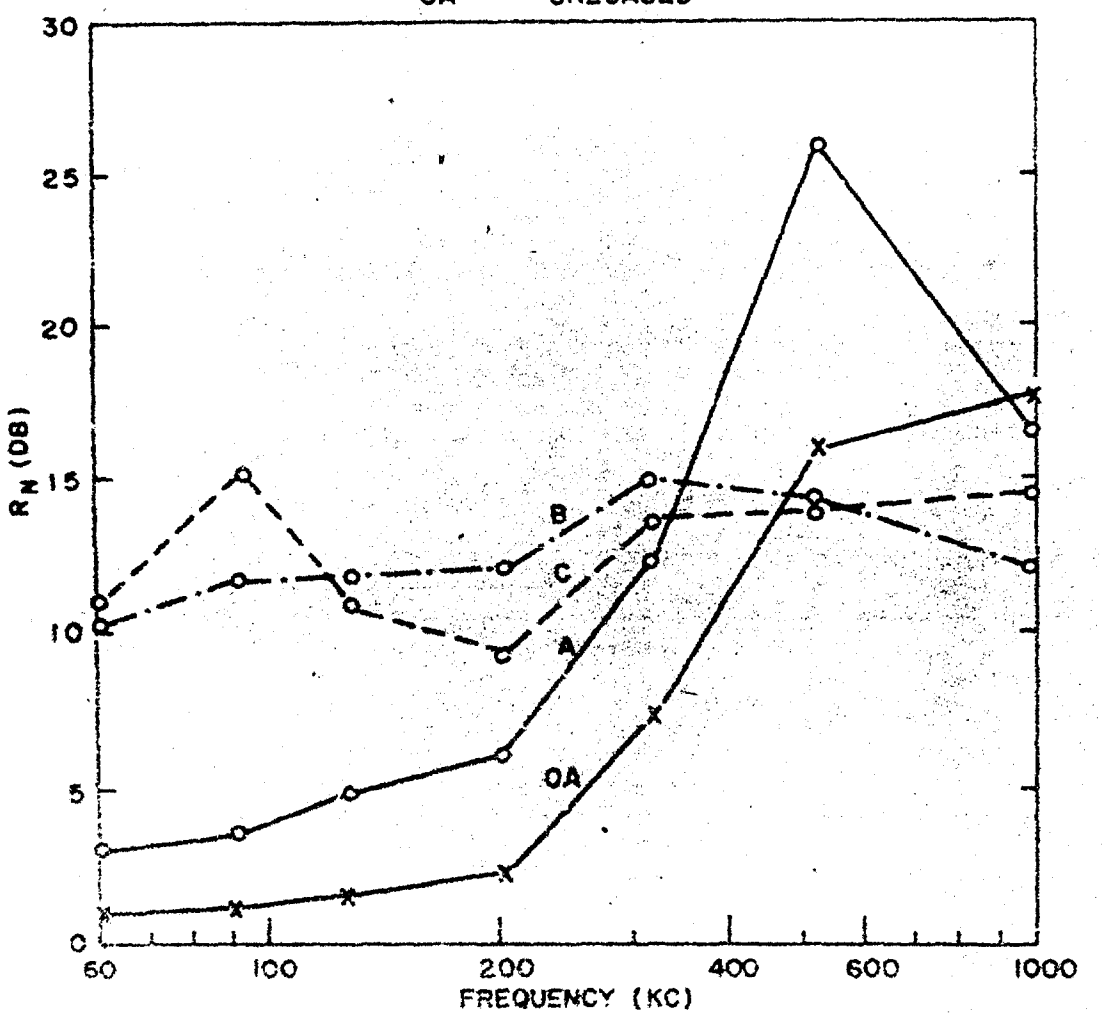

FIG. 6 NORMAL REFLECTIVITY INDEX OF LOADED BUTYL RUBBER FLAT DISK SAMPLES

METAL LOADING: LEAD POWDER (95 PTS/100)
VARIED PARAMETER: CUMAR AND BLOWING AGENT

SAMPLE	*PROPORTION (BY WEIGHT)*
D	9.25 PTS/100 CUMAR 0.1 PTS/100 BLOWING AGENT
E	9.25 PTS/100 CUMAR 1.0 PTS/100 BLOWING AGENT
F	9.25 PTS/100 CUMAR 2.0 PTS/100 BLOWING AGENT
OA	UNLOADED

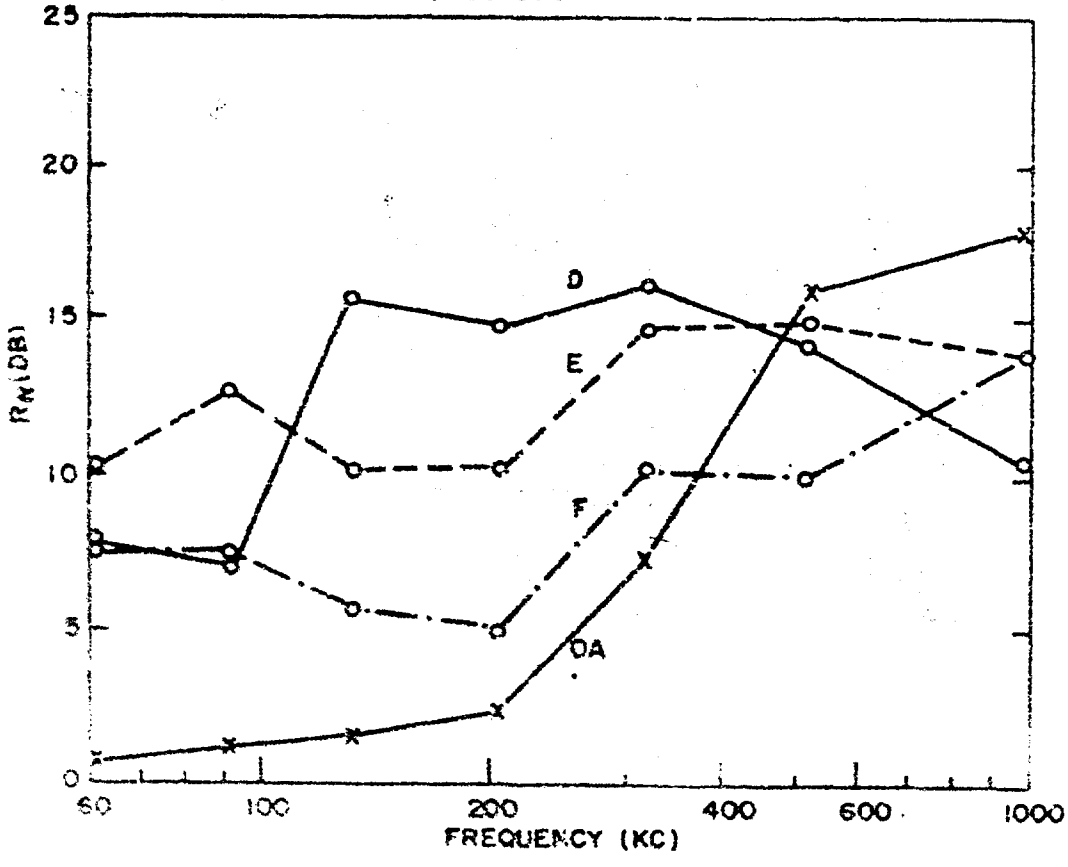

FIG. 7 NORMAL REFLECTIVITY INDEX OF LOADED BUTYL RUBBER FLAT DISK SAMPLES

METAL LOADING: LEAD POWDER
VARIED PARAMETER: METAL PROPORTION

SAMPLE	*PROPORTION (BY WEIGHT)*
G	160 PTS/100
H	25 PTS/100
I	320 PTS/100
OA	UNLOADED

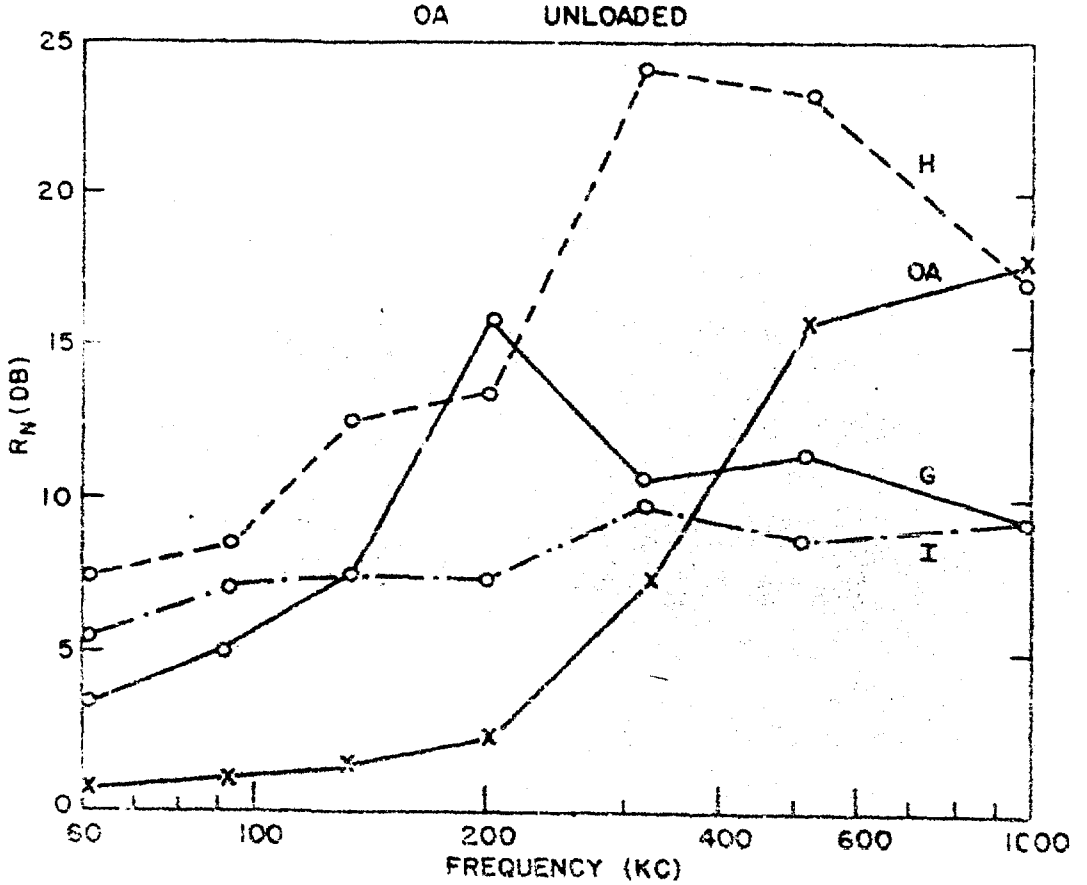

lead powder ... 100 parts of butyl rubber. The first two materials were selected on the basis of the high maximum values of attenuation over the frequency range 5 kc to 1000 kc. The heavily-loaded lead material was selected in order to study the effect of extreme loading.

15. Materials other than Loaded Butyl Rubber. The material used for the wedge elements (German Fafnir) in the existing tank lining (Figure 2) is probably buna "S" rubber. This lining was formerly used in an anechoic tank in Germany and prior to installation in our tank was stored in air for a number of years. Examination of the wedges indicates that the rubber has deteriorated and is relatively hard. Results of measurements on this lining can, therefore, be interpreted only as characteristic of existing installation and not necessarily that of Fafnir in its original condition.

16. The basic material of the wedge elements identified in this report as British Fafnir, Figure 8, is butyl rubber. Since these wedges were in good condition, the results should be representative of this material.

17. Insulkrete is a material made from coarse sawdust and cement in the proportion of 4 to 1, Figure 9. This material is being used by Underwater Sound Reference Laboratory (USRL) as a lining for a high-pressure tank. Results of measurements made at USRL, Reference (b), indicate that reflection caused by surface mismatch is rather low, of the order of -20 db compared to a reference reflection plate in the frequency range considered here. This material then constitutes one of the types mentioned in the preceding section which has a relatively low absorption per unit thickness but presents a fairly good match at the interface.

18. Canvas was included in this study because it has been used as a cheap temporary lining in small tanks. The material used for these tests was 16-ounce duck arranged in large, somewhat arbitrary pleats.

D. Selection of Structure

19. The proposal of a structure for simulating a medium with a transition layer, discussed briefly in Section I, was introduced by Rayleigh, reference (c). Rayleigh mentions the possibility of transmitting sound without reflection from one medium to another when the boundary between the two is a deeply corrugated surface with a periodicity less than the wavelength of the incident sound. Under these conditions incident sound encounters a gradual change in acoustic properties in the transition region. A minimum requirement on the normal cross section of the transition medium would appear to be that set in horn theory, namely, the

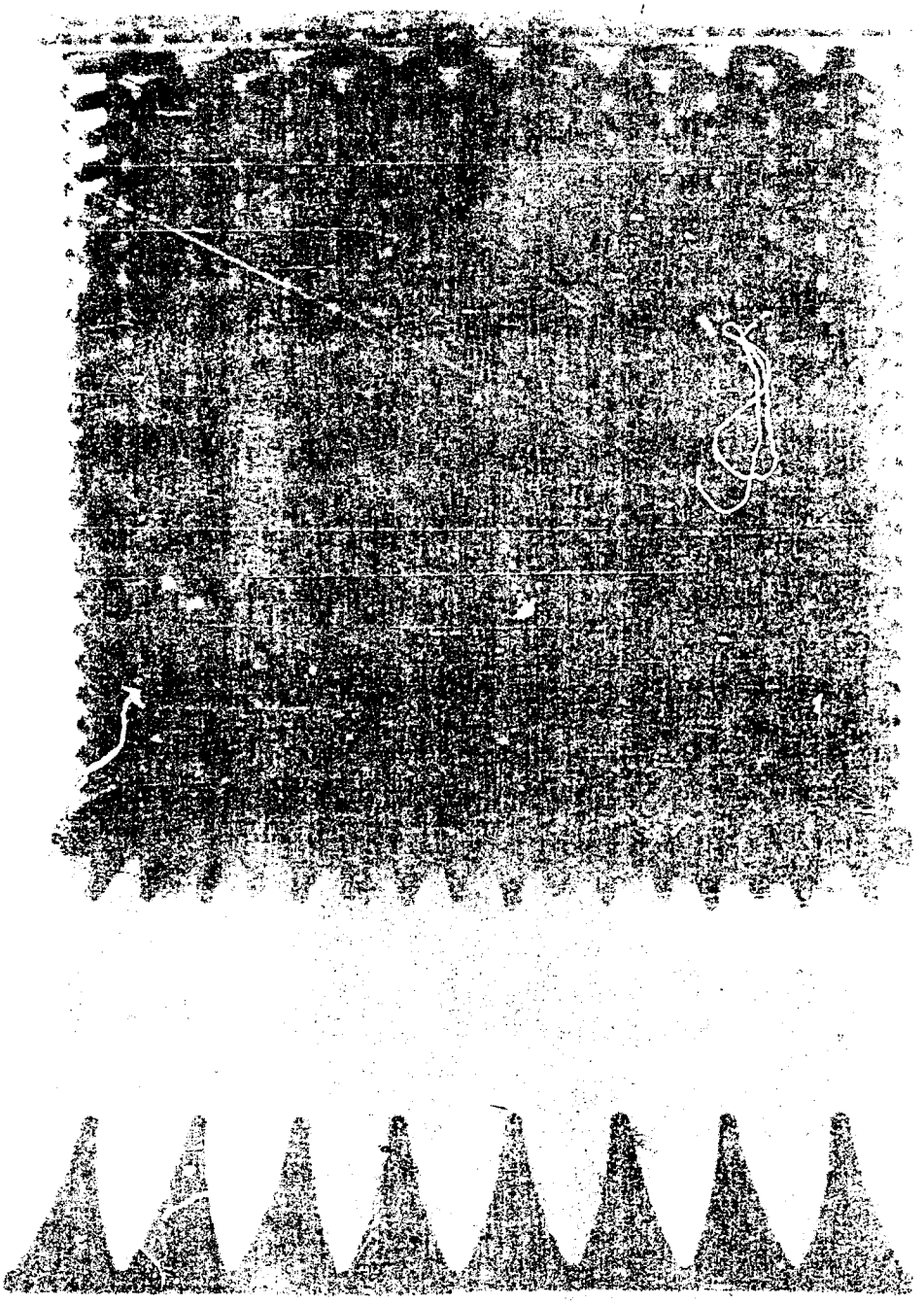

FIG. 8
TEST SAMPLE OF BRITISH FAFNIR LINING

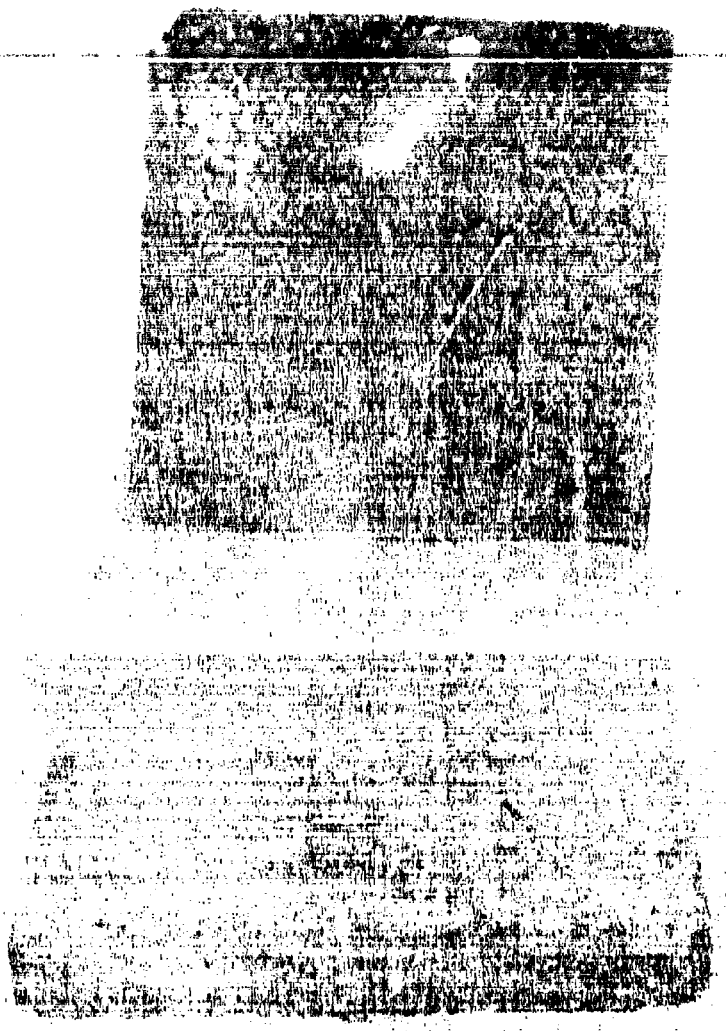

FIG. 9
TEST SAMPLES OF INSULKRETE TANK LININGS

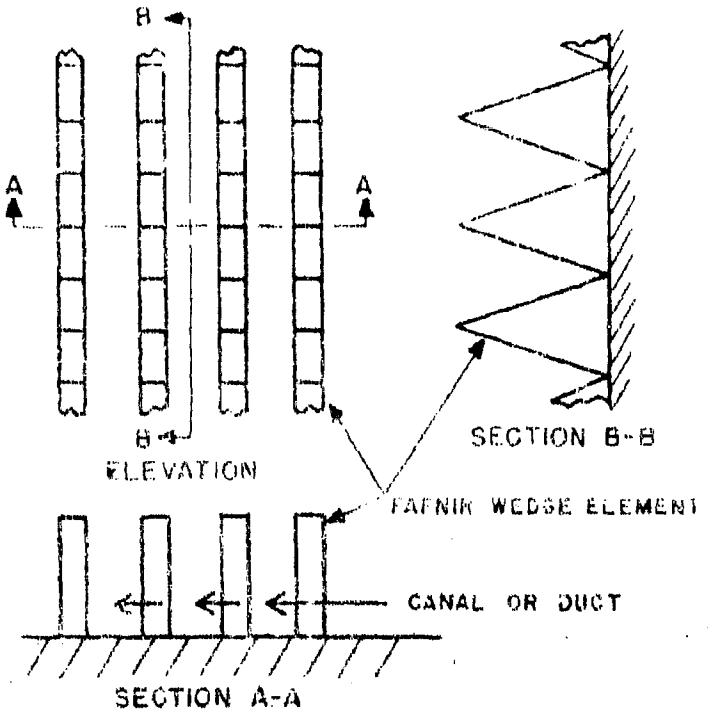

FIG. 10

TYPICAL VIEWS OF FAFNIR STRUCTURE

requirement that the change of section and rate of change of section occur in a gradual continuous manner throughout the transition length, including the boundaries, reference (d). Then, also, as in horn theory, one can state that such a change of section implies a gradual continuous change of impedance.

20. German Fafnir. The principle of gradual transition has been successfully applied to the experimental development of sound-in-air absorbent linings, and more recently as reported by Meyer in reference (e) to the development of underwater sound absorbent linings. In the development of these underwater sound linings, various materials with elastic hysteresis and various shaped structures were tried. The final version of the lining, called Fafnir, was constructed of flat triangular rubber wedges with included air spaces.

21. The structure consists of rows of these elements mounted on a wood backing plus the water canals or ducts in the spaces between the rows (see Figures 2 and 10).

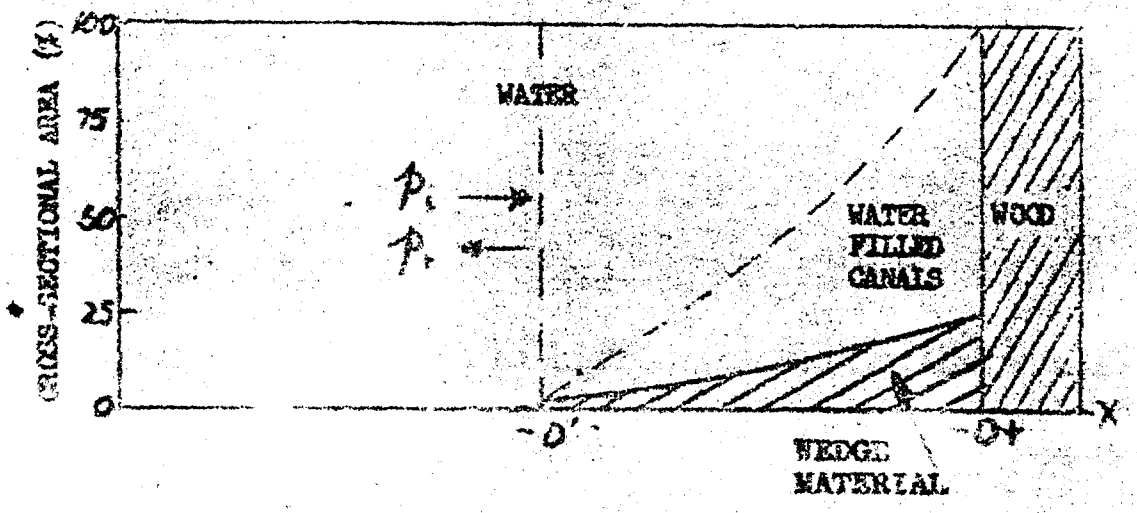

FIGURE 12

DIAGRAM INDICATING TRANSITION CROSS-SECTION OF GERMAN FAFNIR LINING

The factors involved in this particular case of graded transition may be inferred from a study of the variation of the cross section of the lining with the distance from the backing, Figure 11. If one considers only the wedges, a discontinuity in impedance exists at x = 0 due to a change in the cross section and at x = -D due to the rate of change of cross section. The problem was to select dimensions and spacing of the wedges which would minimize these discontinuities by adjusting the acoustic properties of the water-filled canals. The final selection was made after many tests in which a single parameter was varied while the others were held constant. For a wedge cross section of 25% of the total area at x = 0, the structure, according to reference (e) resulted in reflection pressures of 10% of those of the incident sound wave. This reduction held between a lower cutoff frequency for which the wedge length equals a half wave length and an upper cut-off frequency for which the spacing of the canals was equal to a half wave length. It was indicated in reference (e) that the properties of the canals affect the lower and higher frequencies. Near the lower cutoff frequency, the small ratio of spacing to wave length caused the velocity of water in the canals to be decreased which, in turn, caused an impedance mismatch at the tip of the wedge. At the high-frequency cutoff the increased ratio of spacing to wave length allowed sound to enter the structure and to be reflected from the wood backing. An array consisting of a sequence of two rows of wedges 11 cm long and 1 cm thick followed by a row of wedges 25 cm long and 1 cm thick and spaced approximately 3 cm apart was found in reference (e) to increase the band width, so that the lining was effective from about 5 to 40 kc.* Another factor considered in reference (e) and used for determining the parameters of our structure was that for a cross-sectional area of wedge of 50% of the total area at x = 0, the effect of the backing was not appreciable for wedge lengths equal to or greater than a quarter wave length. This percentage of material could not be used for the Fafnir array of reference (e) without introducing an appreciable increase in the effect of the discontinuity at x = -D' (Figure 11) occasioned by an increase in the rate of change of cross section of the wedge structure.

22. British Fafnir. In order to investigate the effect of increasing the cross section of approximately 100%, a structure was made from wedges of British Fafnir such that adjacent rows of elements were in contact with one another (Figure 8). The structured sample is about 40 cm square over-all. These wedge elements differ from those described in the preceding paragraph in that the edges are portions of large circles, 12.5" radii, terminating in a semicircle of radius of approximately 3/32 in.

* The Fafnir material installed in the NOL tank consisted of right triangular rubber wedges of lengths 10 and 20 cm with a spacing of 2 cm instead of the dimensions mentioned in the text and in reference (e). This would increase the upper cutoff frequency of the lining, as indicated in the text.

The base, thickness, and height are respectively 2 cm, 1 cm, and 10 cm corresponding to the smaller wedges discussed previously. The included air spaces are formed by slots parallel to the base, reference (e). In the present sample alternate rows of the elements are displaced one-half the width of a wedge parallel to the rows. The canals formed between the wedges are thus narrowed to the thickness of an element of about one cm, which should raise the upper cutoff frequency to approximately 70 kc. The resulting cross-sectional area versus distance from the wedge backing plate is shown in Figure 12.

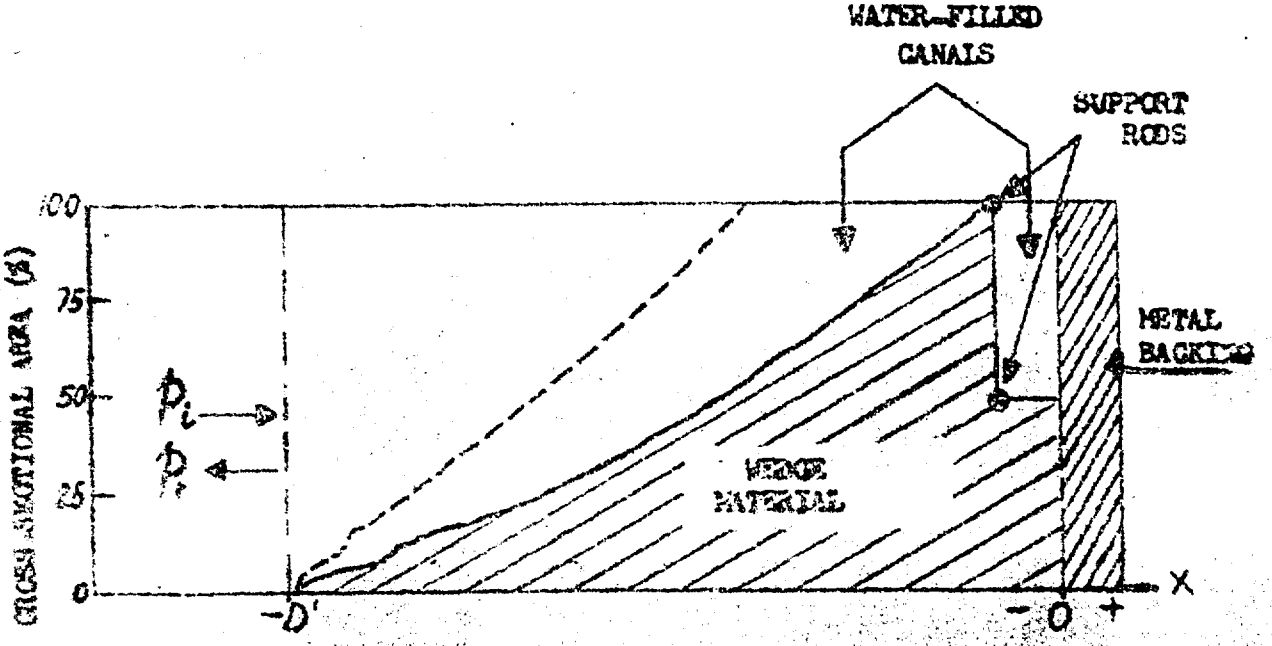

DIAGRAM INDICATING TRANSITION CROSS-SECTION OF CLOSELY STACKED BRITISH PAPER SAMPLE

FIGURE 12

The discontinuity at the base of the wedge, effective above the high-frequency cutoff, is considerably reduced by this arrangement.

22. Cone-Lattice Structure. From a consideration of the frequency limitation of Fafnir mentioned in paragraph 21, it appeared impractical to attempt to design a lining with this type of structure which would cover the desired frequency band, namely 10 kc to several megacycles. Accordingly, a structure was designed which eliminated impedance discontinuities in the transition medium to a large extent. The structure consists of a lattice of

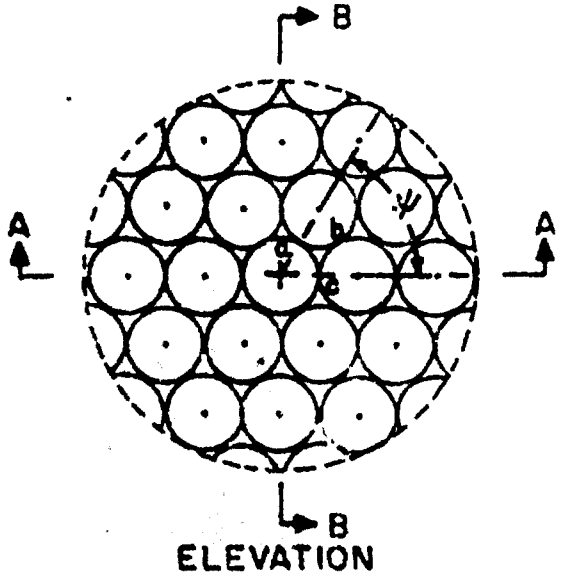

FIG. 13
TYPICAL VIEWS OF CONE LATTICE STRUCTURE

cones, illustrated by Figures 1 and 13, so positioned as to minimize the exposed flat area of the backing. The cones and backing consist of one molded unit of loaded butyl rubber. The dimensions of the cone elements were selected by using the results of reference (e) as a general guide. A length of 3.75 cm was chosen, which corresponds to a lower cutoff frequency of approximately 10 kc. The cone generating angle was chosen as small as practical, namely 15°. The radius of the cone base is approximately one cm. The test panels are approximately 22 cm square and 5 cm deep which includes a thickness of 1.25 cm for the base. In Figure 13 it will be observed that each cone is surrounded by six tangent cones. The exposed areas of the plane backing approximate small triangles. The percentage of area exposed is approximately 9% of the total section. Although it is possible to eliminate this flat area with the associated discontinuity, it was felt that for the purposes of this preliminary investigation it would be instructive to measure the reflection characteristics with the discontinuity present and to note the frequency at which the effect of the discontinuity becomes noticeable. From reference (e) one might expect this frequency to be around 250 kc, since at this frequency the maximum dimension of one of the "triangles" is equal to a half wave length. Also one would expect the level of the reflected sound to be of the order of 10 db below that for a flat sample of the same material. This is based on the percent of total area exposed. An additional consideration in the selection of this structure was the simple geometrical relationship between surface and volume versus distance from the cone tips which would be of value in any future theoretical study of the mechanism of gradual transition.

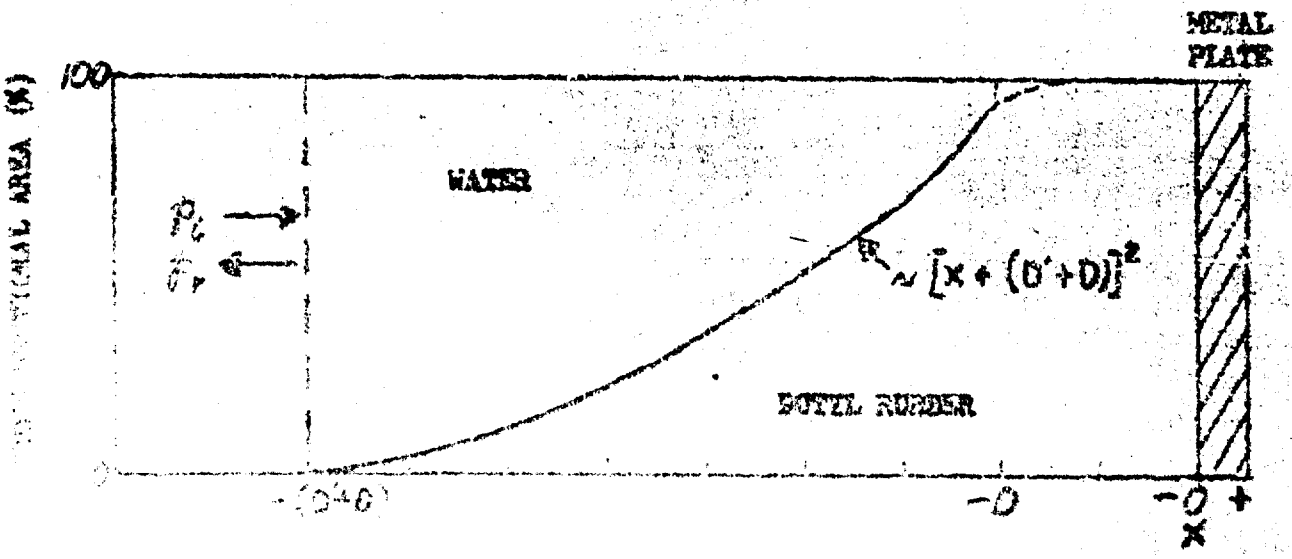

FIGURE 14

[illegible] ROOM [illegible]TORING TRANSITION CROSS-SECTION OF CONE LATTICE SAMPLE [illegible]

24. Figure 14 gives the cross-sectional area versus distance from the cone tip of the multiple cone sample. Observe that there is a smooth transition at the cone tips ($x = -(D + D')$), both the change of section and the rate of change of section approximate zero at this point. The plane area at the back of the structure ($x = -D$) is reduced to approximately one-seventh of that shown in Figure 11 for German Fafnir and can be practically eliminated by incorporating conical holes in the exposed sections of the backing (note dotted lines). The section of water included between the cones gradually tapers with distance from the wedge tips so that the discontinuity encountered with the Fafnir linings due to the canals is not present.

25. It is realized that the structures studied here are proposed for use at much lower wave length-to-dimension ratios than those included in Rayleigh's work on gradual transition. The phase surfaces at these frequencies are no longer plane and the mechanism of sound transmission from water into the material is very complicated both because of the involved shape of the structure and the complex behavior of the material. Hence, this investigation has been essentially experimental.

26. The physical characteristics of the samples studied are summarized in Table I. The table also gives code numbers and figure numbers which illustrate the respective samples. The first digit of the code number refers to the sample material and the second digit denotes common physical characteristics where practical.

TABLE 1 PHYSICAL CHARACTERISTICS OF LINING SAMPLES

FIG. NO.	SAMPLE CODE	SURFACE STRUCTURE	STRUCTURE ELEMENT				SAMPLE DIMENSIONS			MATERIAL	REMARKS
			TYPE	HEIGHT	BASE WIDTH	THICKNESS	HEIGHT	WIDTH	THICKNESS		
				(CM)			(CM)				
	01	PLANE					21	22	0.3	BRASS	BACKED WITH 0.6 CM COMPRENE
	03	PLANE					40	40	0.3	BRASS	BACKED WITH 0.6 CM COMPRENE
	04	PLANE					45	45	0.3	BRASS	BACKED WITH 0.6 CM COMPRENE
1 & 13	11	LATTICE	RIGHT CONE	3.75	2.0 (DIA)		21	22	5	LEAD-LOADED BUTYL RUBBER	ρ = 2.614
	12	PLANE					21	22	1.25	LEAD-LOADED BUTYL RUBBER	ρ = 2.61
1 & 13	21	LATTICE	RIGHT CONE	3.75	2.0 (DIA)		21	22	5	ALUMINUM-LOADED BUTYL RUBBER	ρ = 1.227
	22	PLANE					21	22	1.25	ALUMINUM-LOADED BUTYL RUBBER	ρ = 1.25
1 & 13	31	LATTICE	RIGHT CONE	3.75	2.0 (DIA)		21	22	5	LEAD-LOADED BUTYL RUBBER WITH CUMAR AND BLOWING AGENT	ρ = 1.075
	32	PLANE					21	22	1.25	LEAD-LOADED BUTYL RUBBER WITH CUMAR AND BLOWING AGENT	ρ = 1.63
8 & 10	41	(FAPHIR) RIBBED	WEDGE	10.0	5.0	1.0	40	40	6	(BRITISH FAPHIR) BUTYL RUBBER	
9	51	LATTICE	RIGHT CONE	1.0	2.0 (DIA)		45	45	5	INSULBRITE	IMMERSED IN WATER AT 180°F FOR THREE DAYS BEFORE MEASURING
9	52	PLANE					45	45	5	INSULBRITE	
9	53	PLANE					45	45	5	INSULBRITE	IMMERSED IN WATER AT 180°F FOR THREE DAYS BEFORE MEASURING
9	54	PLANE					45	45	5	INSULBRITE	IMMERSED IN WATER AT 180°F FOR THREE DAYS BEFORE MEASURING
	61	IRREGULAR	FIRATS	3		40	40	40	5	CANVAS	
2 & 10	71	(FAPHIR) RIBBED	WEDGE	10 20*	5.0 10*	1.0 1.0	110	110	20	(GERMAN FAPHIR) BUNA (S) RUBBER	ENDS OF TANK BACKED WITH 5 CMS OF WOOD.
2 & 10	72	(FAPHIR) RIBBED	WEDGE	10 20*	5.0 10*	1.0 1.0	110	110	20	(GERMAN FAPHIR) BUNA (S) RUBBER	ENDS OF TANK BACKED WITH 5 CMS OF WOOD
2 & 10	73	(FAPHIR) RIBBED	WEDGE	10 20*	5.0 10*	1.0 1.0	90	60	20	(GERMAN FAPHIR) BUNA (S) RUBBER	BACKED WITH 3 CMS OF WOOD

*SEE NOTE PAGE 18

IV. LABORATORY APPARATUS

27. Description of System. The apparatus for producing normally incident, pulse-modulated sound waves and for measuring the reflectivity pattern is illustrated in Figure 15.

28. A delayed trigger from a Tektronix oscilloscope, Type 512, initiates a square pulse which modulates the carrier from the signal generator. This pulse-modulated wave is amplified and then drives the projector through a matching network. The projector produces a narrow beam of pulse-modulated sound waves which are normally incident on the specimen. Reflections from the specimen are received by the rotating probe hydrophone and the voltage generated is sent through a matching network to the gated receiver which is triggered by the oscilloscope. The receiving gate can be set to correspond to the beginning of the desired reflected signal by an adjustable time delay. After amplification the signals are applied to the polar recorder which is designed to produce a continuous logarithmic plot. The angular position indicated by the recorder is made to correspond to the hydrophone orientation by the use of a selsyn system.

29. Arrangement of Apparatus. The arrangement of the apparatus is illustrated in Figures 16 and 17. Reference reflection plates were made of 1/8 inch brass plate backed by 1/4 inch corprene. They were suspended vertically from the rotation framework by a 1/32 inch wire rope. The plate was held vertical by a weight which was covered with sound-absorbent material. The specimen was fastened to the reflecting plate by gum-rubber bands. The center of the sample was positioned at 50 cm below the surface of the water to allow for approximate centering of the sample between the water surface and the positioning weight (which was covered with an acoustic absorber).

V. MEASUREMENTS

A. Measurement Program

30. The measurement program consisted of the four parts outlined below. All measurements were made with sound normally incident on the reflecting surface, and unless specified otherwise were made in a single plane ($\psi = 0$). (The orientation of the ψ planes are explained later.)

a. The measurement of all samples in the frequency range from 50 to 250 kc in increments of 50 kc.

b. Measurements on a cone-lattice sample and the German and British Fafnir samples in the radial plane $\psi = 0$ and $\psi = 90°$ to determine the effect on reflection characteristics caused by axial asymmetry of the sample surface.

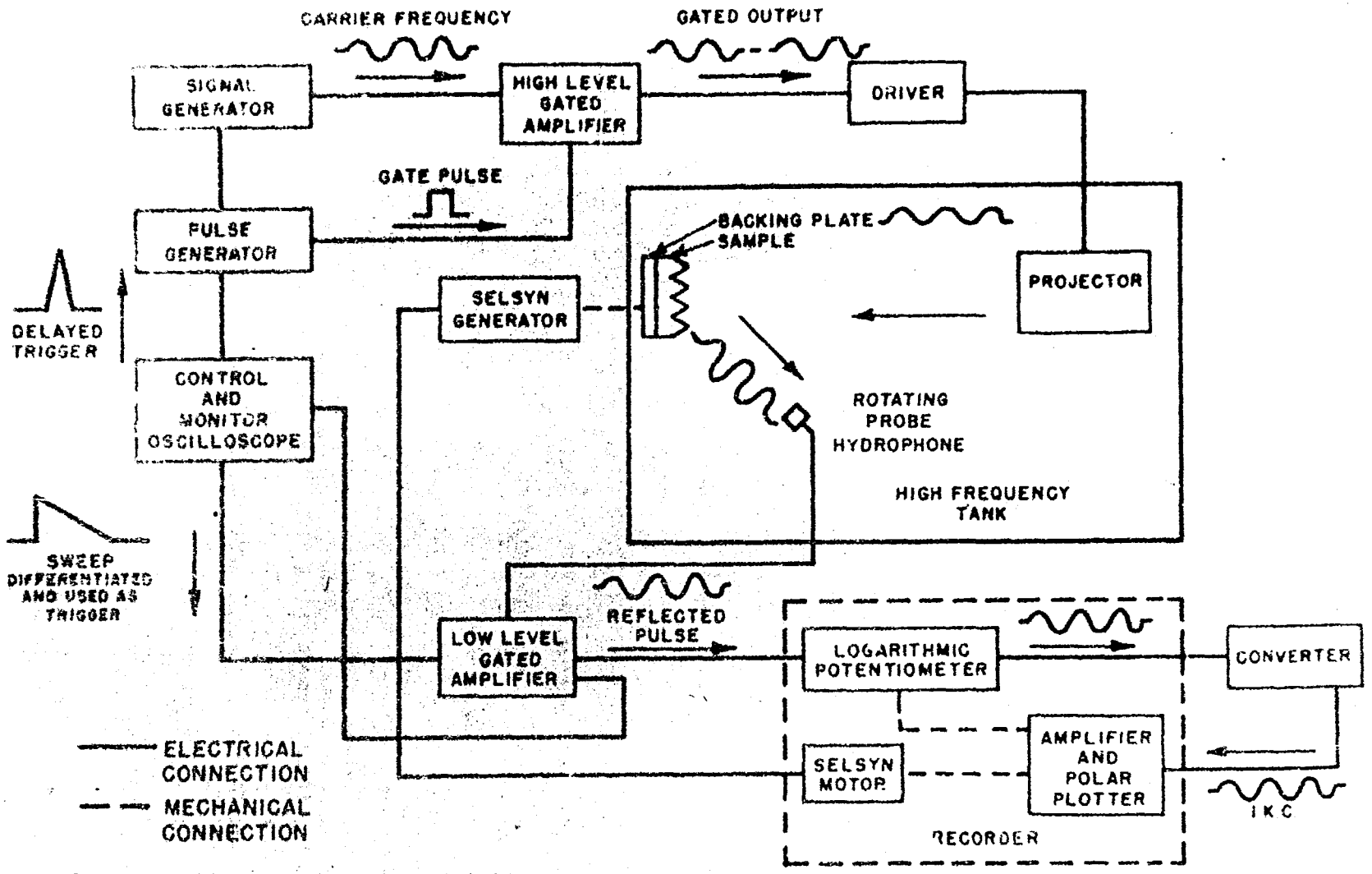

PULSE LENGTH 0.1 TO 1.0 MILLISECOND
PULSE REP. FREQ. 50 TO 200 C.P.S.

FIG. 15 SYSTEM FOR MEASUREMENT OF ACOUSTIC ABSORPTION

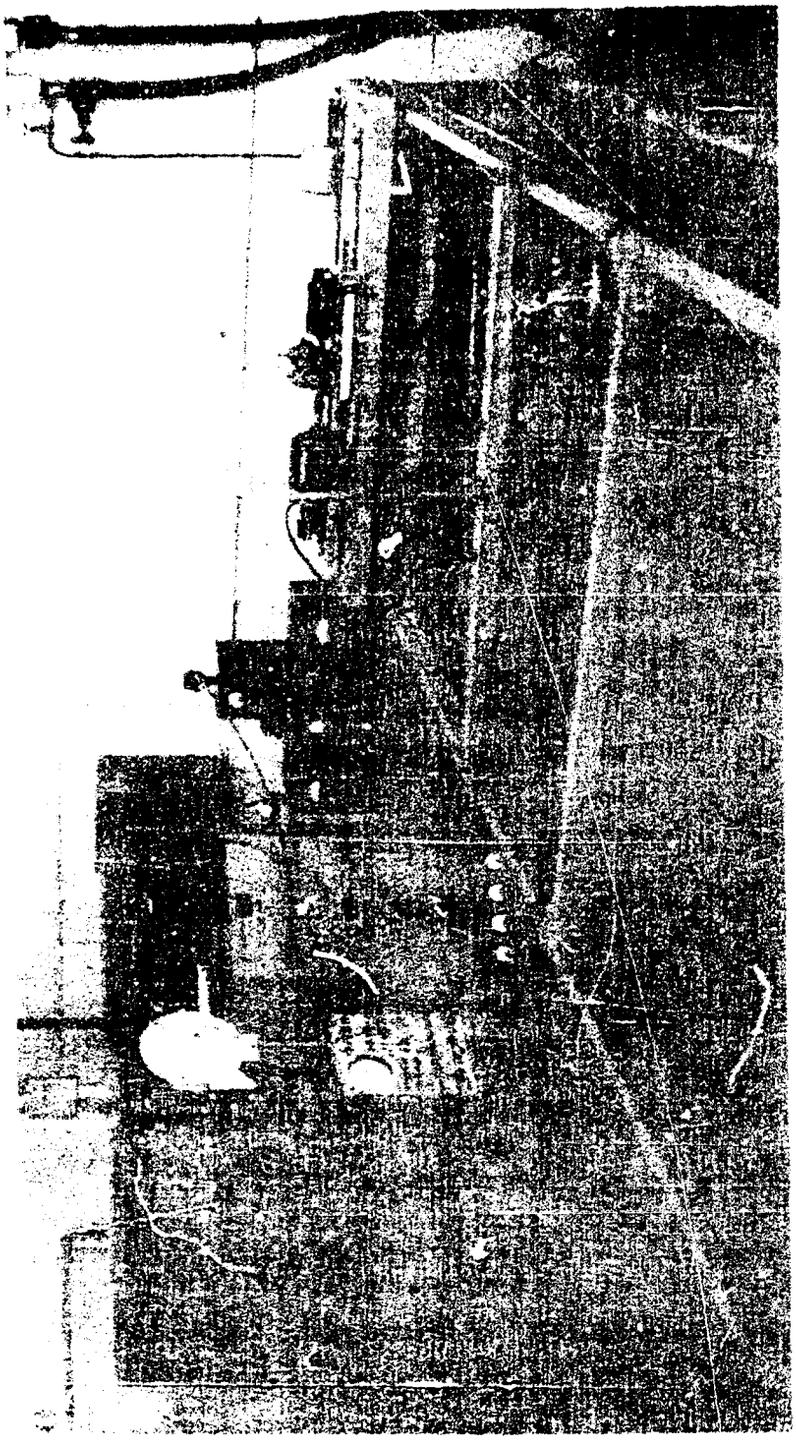

FIG. 16 ARRANGEMENT OF APPARATUS

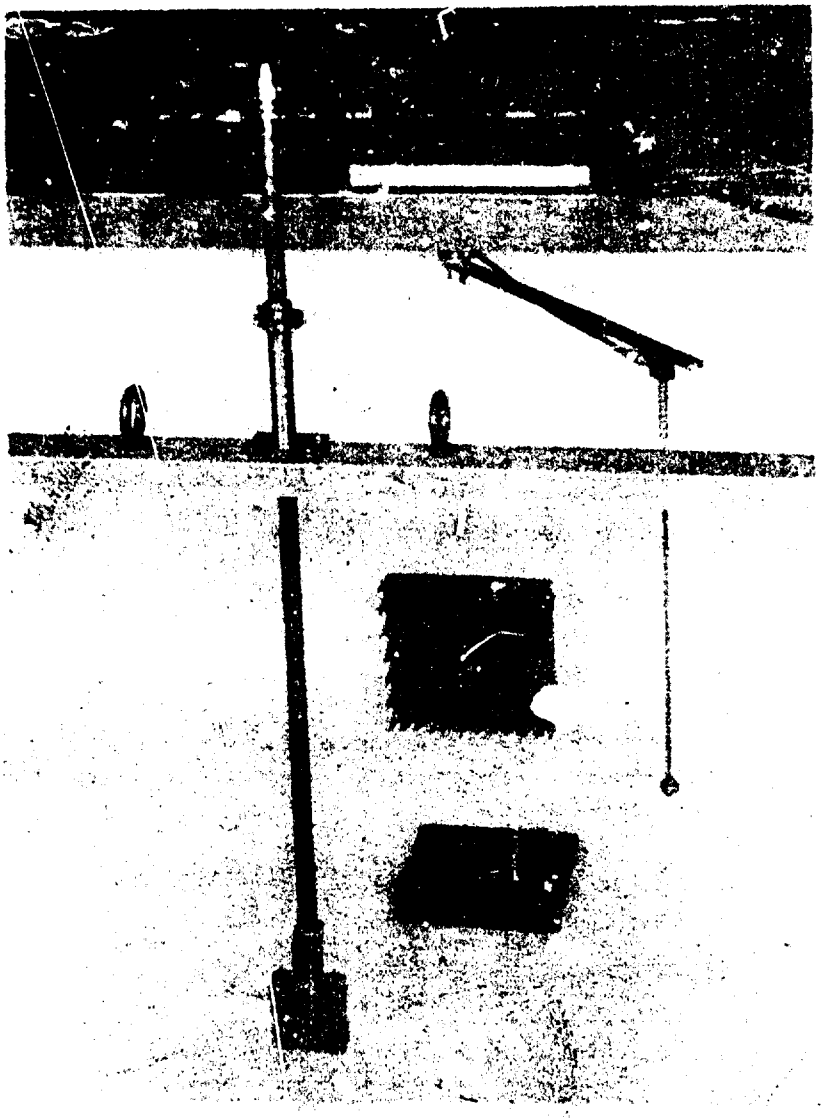

FIG. 17
ARRANGEMENT OF SAMPLE AND
UNDERWATER EQUIPMENT

c. The measurement of the most promising structured sample, No. 21, the aluminum loaded one, and the corresponding flat sample, No. 22, at smaller frequency increments. This provided detailed information on the reflection characteristics versus frequency in the region between the 50 kc spot frequencies.

d. Measurement of Sample No. 21 at points 50 kc apart over a frequency range from 20 kc (the lowest practical frequency) to 1 Mc, to determine the expected useful frequency range of a tank lined with this material.

B. Theory of Measurements

31. The method of measuring the reflection coefficient described in paragraph 8 is practical if the reflectivity pattern of the specimen is not substantially different from the reflectivity pattern of the plate; this was the case for the flat samples previously discussed. However, a structured specimen can introduce a substantial change in the reflectivity pattern. The reflectivity pattern is critically dependent on the proper alignment of projector and sample, and this is difficult to achieve. Maximum reflection does not ordinarily occur normal to the sample. Furthermore, there is sufficient scattering so that even if we compared this maximum reflection to the maximum reflection from a plate, it would not accurately indicate the absorption characteristics of the specimen. A technique devised to take account of these difficulties consists of utilizing a separate hydrophone for measuring the reflected signals. The hydrophone is rotated in a plane which passes through the axis of symmetry of the projector and normal to the sample or reference plate, Figure 18. The reflectivity patterns thus obtained, first with a reflecting plate and then with a specimen, together with the values of maximum reflection, are used for calculating the reflection and scattering coefficients from the structured samples.

32. If sound from a projector falls on a surface, the reflected power, P, through a hemisphere of radius r is given by (see Figure 15)

$$P = r^2 \int_0^{\pi/2} \int_0^{2\pi} I(\theta,\psi) \sin\theta \, d\psi \, d\theta \qquad (17)$$

where

θ is the polar angle measured from the projector axis of symmetry about an origin on the surface of the sample.
ψ is the radial angle measured from the x axis in the plane about the projector axis of symmetry (y axis).
$I(\theta,\psi)$ is the reflected intensity, a function of both θ and ψ.
r is the beam from the projector and the reflecting surface are both

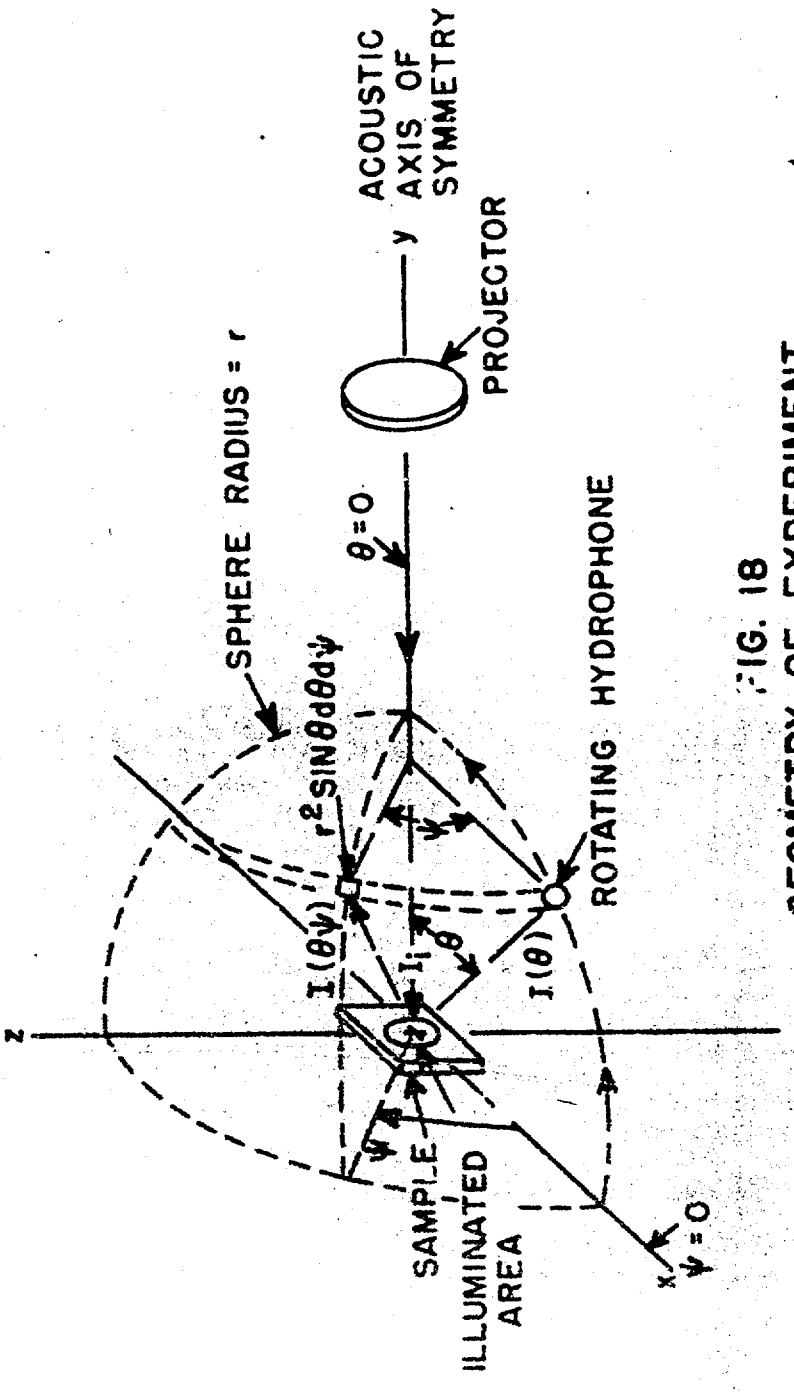

FIG. 18
GEOMETRY OF EXPERIMENT

axially symmetric about a common axis, then the reflected pattern will be axially symmetric about this axis. In this case the intensity, I, is independent of φ. The reflected power from a metal reference plate, P_p, is

$$P_f = 2\pi r^2 \int_0^{\pi/2} I_p(\theta) \sin\theta \, d\theta \qquad (18)$$

33. Axially Symmetric Samples. For a sample for which one can assume axially symmetric reflections, the reflected power, P_s, is similarly

$$P_s = 2\pi r^2 \int_0^{\pi/2} I_s(\theta) \sin\theta \, d\theta \qquad (19)$$

$I(\theta)$ in equations (18) and (19) may be measured by rotating the probe hydrophone shown in Figure 18, in the xy plane from $\theta = 0$ to $\pi/2$. According to reference (f) the reflection coefficient is defined as: "The sound reflection coefficient of a surface not a generator is the ratio of the rate of flow of sound energy reflected from the surface, on the side of incidence, to the incident rate of flow". If the metal reference plate is a perfect reflector, the reflected power P_p is equal to the incident power. The reflection coefficient, R_c may be then defined as

$$R_c = \frac{P_s}{P_p} = \frac{\int_0^{\pi/2} I_s(\theta) \sin\theta \, d\theta}{\int_0^{\pi/2} I_p(\theta) \sin\theta \, d\theta} \qquad (20)$$

R_c can be defined more generally if the single integrations in equation (20) are replaced by the double integrations appearing in equation (17).

34. Kendig and Mueser, reference (g), have devised a means of computing the power radiated from an axially symmetric source, such as given by equations (18) or (19), by a planimeter measurement of the area under a reflectivity pattern plotted on special coordinate paper (Figure 19). The angle is plotted as the abscissa expressed in degrees and scaled in terms of the function $(1 - \cos\theta)$. The intensity is plotted as the ordinate expressed in db down from the peak reflection, and is scaled to give a linear

FIG 19 ILLUSTRATION SHOWING USE OF POWER CHARTS FOR CALCULATING REFLECTION INDICES, R, Δ, AND S

FREQUENCY 150 KC
SAMPLE NO 21 ALUMINUM LOADED BUTYL RUBBER
STRUCTURE CONE LATTICE

REFLECTIVITY PATTERN OF SAMPLE NO 21
PATTERN NO 21-161

S+ 8.7 db
Δ=-40.5 db
R= 39.8 db

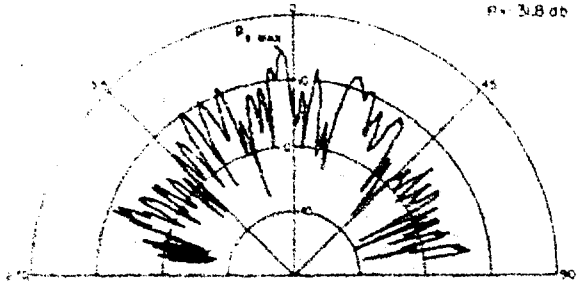

(RECORDING LEVEL 39.5 db ABOVE THAT OF THE REFERENCE PLATE)

REFLECTIVITY PATTERN OF REFERENCE PLATE NO 01
PATTERN NO. 01-155

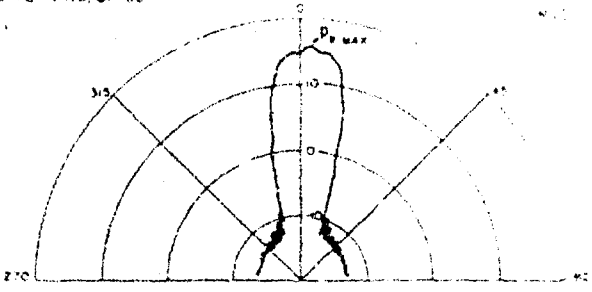

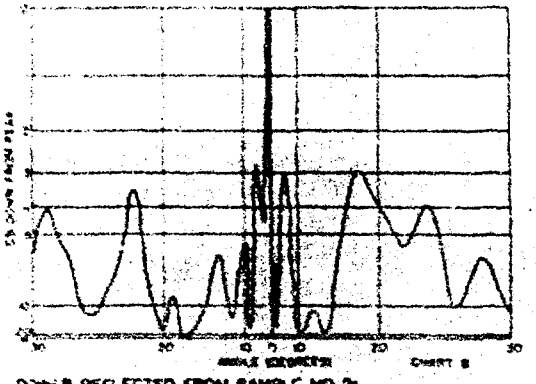

POWER REFLECTED FROM SAMPLE NO 21
(-30 DEGREES TO +30 DEGREES)
A_s = 3.21 SQ IN

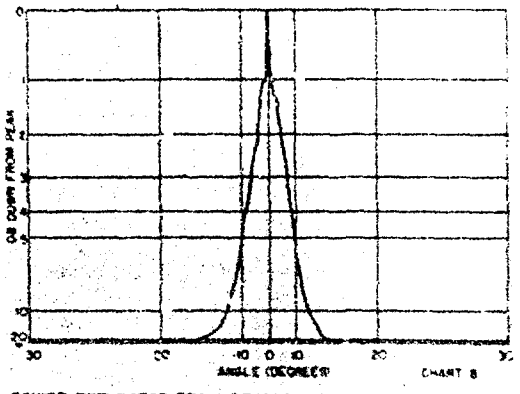

POWER REFLECTED FROM REFERENCE PLATE NO 01
(-30 DEGREES TO +30 DEGREES)
A_p = 5.21 SQ IN.

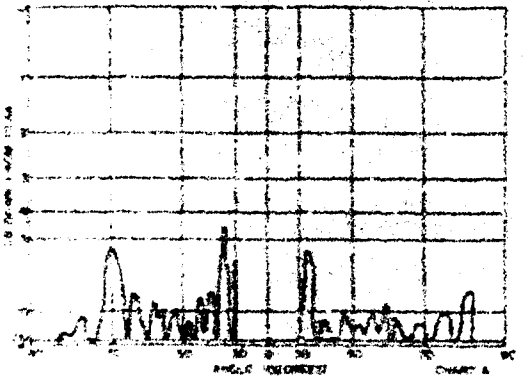

POWER REFLECTED FROM SAMPLE NO 21
(-90 DEGREES TO +90 DEGREES)
A_s = 3.44 SQ IN

ILLUSTRATIVE COMPUTATION

$$S = 10 \log \frac{A_s}{A_p} + 10 \log \frac{A_s + .75\,A_{s_2}}{A_p} + 8.7 \text{ db}$$

$$\Delta = 20 \log_{10} \frac{D_{s\,max.}}{D_{p\,max.}} = -40.5 \text{ db}$$

$$R = 8.7 - 40.5 = -31.8 \text{ db}$$

THE .75 IN THE FIRST EQUATION IS A SCALE FACTOR BETWEEN CHARTS A AND S

intensity plot. We can rewrite equation (4) to conform more closely to the computations as follows:

$$R_c = \frac{R_s}{R_o} = \frac{I_{s\,max} \int_0^{\pi/2} \left(\frac{I_s(\theta)}{I_{s\,max}}\right) \sin\theta \, d\theta}{I_{p\,max} \int_0^{\pi/2} \left(\frac{I_p(\theta)}{I_{p\,max}}\right) \sin\theta \, d\theta} \qquad (21)$$

or for brevity

$$R_c = \frac{I_{s\,max}}{I_{p\,max}} \frac{A_s}{A_p} \qquad (22)$$

Expressed in db,

$$R = 10 \log_{10} \frac{I_{s\,max}}{I_{p\,max}} + 10 \log_{10} \frac{A_s}{A_o} \qquad (23)$$

$$= A + S \qquad (24)$$

where R is the reflectivity index (the reflection coefficient expressed in db)

A is the peak reflectivity index, the first term in equation (23) and

S is the scattering index, the second term in equation (23)

35. It is obvious that of the three quantities, R, A, and S only two are independent. For example, any condition which would cause a strong reflection from the sample to occur without appreciably increasing R would mean an increase in A and a corresponding decrease in S. The two latter parameters then indicate in a general way the distribution of sound reflection introduced by the lining. The peak reflectivity index, A, indicates the maximum reflection one might expect from a sample in any direction. Since A_o represents specular reflection from the plate the scattering index S provides a measure of the deviation from specular reflection of sound reflected from the sample. The reflectivity index, R, is an overall measure of the absorption. One may obtain the absorption loss in per cent from the equation

$$\alpha = 1 - 10^{-0.1\left(\frac{R}{10}\right)} \cdot 100$$

3.5. Axially Periodic Samples. A structure such as that of the cone-lattice sample, Figure 13, is not axially symmetric but varies with ψ in a periodic manner. The power reflected from the sample as given by the exact general expression, equation (17), may be approximated in this case by making pattern measurements at small equal divisions extending over a half period. Thus, the approximate power reflected P_s is given by

$$P_s^{\psi} = \frac{2\pi r^2}{\eta \delta\psi} \sum_{i=1}^{n} \left[\int_0^{\pi} I_s^i(\theta) \sin\theta \, d\theta \right] \delta\psi \qquad (25)$$

where:

n is the number of increments $\delta\psi$ in a half period.

i as a superscript indicates that values of the parameter are measured in the plane of ψ_i.

Through a procedure similar to that followed for the axially symmetric case the new reflectivity index R is

$$R_a = 10 \log_{10}\left(\frac{P_s^{\psi}}{P_p}\right) = 10 \log_{10}\left[\frac{\sum_{i=1}^{n} I_{s\,max}^i \, A_s^i}{n I_{p\,max} A_p}\right] \qquad (26)$$

The scattering index is

$$S_a = 10 \log_{10}\left[\frac{\sum_{i=1}^{n} A_s^i}{n A_p}\right] \qquad (27)$$

The peak reflectivity indices are defined as:

$$A^i = 10 \log_{10} \frac{I_{s\,max}^i}{I_{p\,max}} \qquad (28)$$

and

$$A_a = R_a - S_a \qquad (29)$$

where Δ_a can be thought of as the peak reflectivity index for a hypothetical axially symmetric structure with values of R and S equal to R_a and S_a respectively. The index, Δ, is the maximum peak-reflectivity measured for any angle ψ. For a particular sample the number of increments, n, necessary for a specified accuracy depends on frequency, the directional characteristics of a hydrophone, and the dimensions of the setup; this may be determined experimentally. Also, measurements may be made over the polar angle range from $\theta = -\pi/2$ to $\theta = \pi/2$ in the plane specified by the radial angle ψ_i. The results correspond to taking an average of two measurements at equal angular phase for all samples of this experiment. The latter procedure also helps to compensate for errors due to misalignment.

37. Periodicity of Selected Samples. It may be noted that the cone-lattice structure (Figure 13) has an angular periodicity in ψ of $\pi/3$. A measurement in the plane of Section A-A corresponds then to the average of two measurements of the type $\psi = \psi_i = n\pi/3$ and a measurement in the plane of the Section B-B to the average of two measurements for $\psi = \psi_i = (n + \frac{1}{2})(\pi/3)$, where n is an integer. These two measurements were assumed to be sufficient to indicate approximately the variation of the reflection characteristics with ψ for the cone-lattice structure.

38. The periodicity in ψ for the Fafnir samples is π. If equal increments are desired one should take more increments for the Fafnir sample because of its larger period. However, measurements were only made in planes at 90 degrees for this preliminary investigation (corresponding to those for the cone-lattice sample).

C. Application of the Technique

39. The factors which influence the choice of measurement parameters in a practical application of the technique described above are the acoustical and geometrical characteristics of the specimens, the tank, the transducers, and the frequency range over which measurements are desired. The frequency range considered is from 20 kc to 1 Mc. Measurements at frequencies below 20 kc are of interest but could not be made satisfactorily in the existing tank.

40. Projector Parameters. There are two opposing requirements which govern the selection of the size of the projector. First, a uniform illumination over a sufficient portion of the specimen is necessary to obtain representative reflection measurements for the selection of a material for a tank lining. A reasonably uniform illumination is obtained with a piston-type projector if the projector radius, a, be small enough to allow operation

in the Fraunhofer region (reference (h)) i.e., that

$$a \leq \sqrt{\frac{D_p \lambda}{\pi}} \tag{30}$$

where D_p is the distance from projector to sample, and λ is the wave length of sound in water. For the cone structures, the minimum width of uniform illumination was selected at about 8 cm - the width of four cones. That this constitutes a sufficient portion of the lining was verified experimentally. The width of uniform illumination for a piston source was taken to be that between the half-power points, indicated by the angle β' in Figure 20. The pressure versus the polar angle β from a piston source for distances for which equation (30) is valid is given in reference (h) as

$$p = p_0 \left[\frac{2 J_1(ka \sin\beta)}{ka \sin\beta} \right] \tag{31}$$

The pressure is a maximum for $\beta = 0$ and decreases with increasing polar angle and reaches the half-power point when

$$\sin\beta' = \frac{\lambda}{4a}, \tag{32}$$

and passes through zero when

$$\sin\beta_0 = \frac{0.61\lambda}{a} \tag{33}$$

Let D_w be the distance in the plane of the sample between the two half-power points, i.e.,

$$D_w = 2 D_p \tan\beta' \tag{34}$$

For uniform illumination over the sample, it is advantageous to make D_p the distance from the projector to the sample, as large as the tank will allow. Since a space of 100 cm was maintained back of the sample in order to separate reflections between the sample and the back wall, a distance of 150 cm was

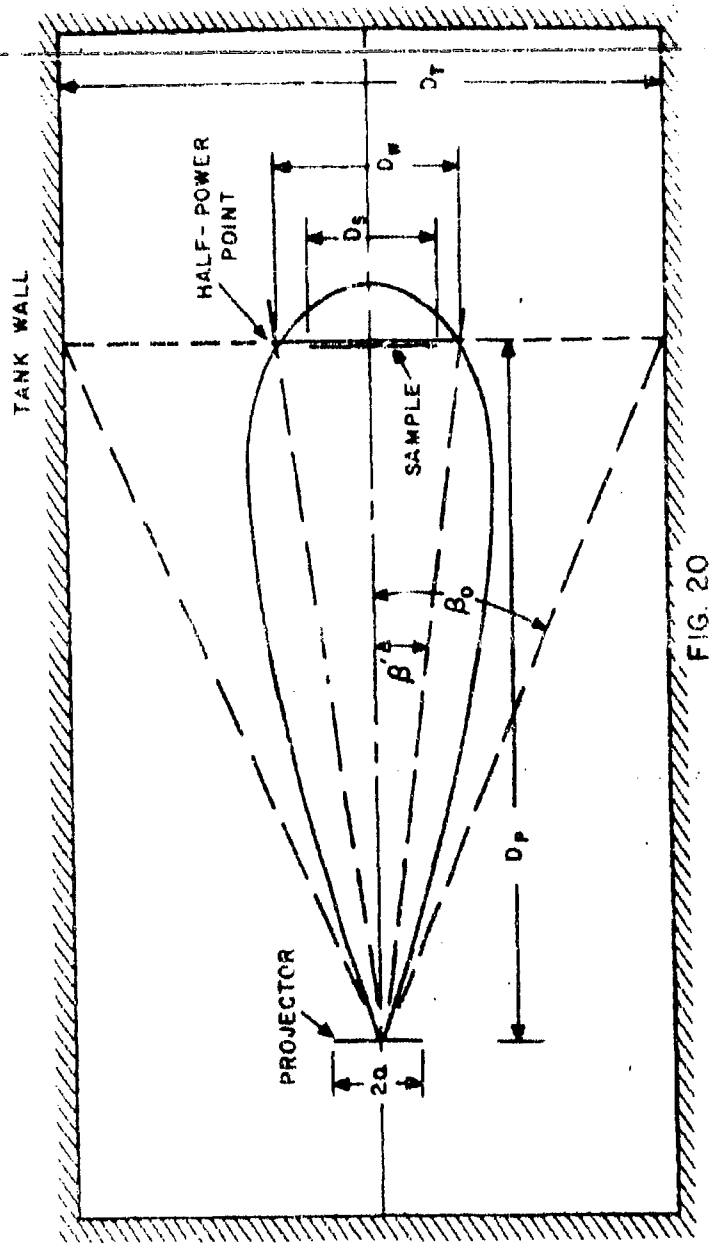

FIG. 20
DIAGRAM OF GEOMETRIC RELATIONSHIP OF PROJECTOR BEAM TO SAMPLE AND TANK

selected for D_p*. If $D_w/D_p \ll 1$, equation (34) can be written

$$D_w = 2 D_p \sin \beta' \tag{35}$$

The requirement given by equation (30), i.e., that the sample be in the Fraunhofer region, can now be expressed in terms of D_w, D_p, and λ as follows:

$$D_w \geq \sqrt{\frac{\lambda D_p}{2}} . \tag{36}$$

41. The second requirement on the size of the projector is that the intensity of the sound incident on the walls of the tank or the water surface be low. This is necessary because of the relatively low-level reflections from the samples. The condition that the main beam not illuminate the sides of the tank or the water surface between the projector and the sample can be expressed as

$$\beta_0 \leq \tan^{-1}\left(\frac{D_T}{2D_p}\right), \tag{37}$$

where D_T is the working width or depth, these being approximately equal for this tank. By using the relationship between the angles β_0 and β' given by equations (32) and (33) and by using equation (35), the requirement expressed by equation (37), which places a lower limit on D_w, becomes

$$D_w \leq \frac{D_p \sin\left[\tan^{-1}(D_T/2D_p)\right]}{1.22} . \tag{38}$$

It is convenient to express D_w relative to the sample width D_s as $\gamma = D_w/D_s$.

Thus, equations (36) and (38) can be written

$$\frac{1}{D_s}\sqrt{\frac{\lambda D_p}{2}} \leq \gamma \leq \frac{D_p \sin\left[\tan^{-1}(D_T/2D_p)\right]}{1.22\, D_s} . \tag{39}$$

* This value of D_w was found to be satisfactory for all frequencies except for the short interference from reflector side lobes [illegible] the use of 75 cm.

If D_p = 150 cm, D_f = 100 cm, and D_s = 22 cm, the above equation becomes

$$0.394\sqrt{\lambda} \leq a \leq 1.76 \ . \tag{40}$$

42. In terms of the projector radius, the above condition is

$$\sqrt{\frac{\lambda D_p}{2}} \leq a \geq \frac{0.61\lambda}{\sin[\tan^{-1}(a_f/2D_f)]} \ , \tag{41}$$

since

$$D_N = \frac{\lambda D_p}{2a} \ . \tag{42}$$

from equations (3) and (6); and if the numerical values listed above are inserted, the restriction on the projector radius is

$$8.67\sqrt{\lambda} \geq a \geq 1.93 \ . \tag{43}$$

Plots of equations (40) and (43) are given in Figures 21 and 22 respectively.

43 Hydrophone Radius. It is necessary to select a hydrophone of small radius in order that the shadow zone on the sample does not materially alter the reflection from the sample. The hydrophone shadow can be reduced by decreasing the ratio D_H/D_p where D_H is the distance of the hydrophone to the sample. On the other hand D_H must not be made too small or the uniformity of illumination of the sample will be appreciably affected. For the latter condition the radius of the hydrophone case must be

$$a_H \leq \sqrt{\frac{\lambda D_H}{2}} \tag{44}$$

The minimum value of λ is 0.146 cm at one Mc and the minimum value of D_H is 50 cm. Hence,

$$a_H \leq \sqrt{\frac{(0.146)(50)}{2}} = 1.91 \text{ cm} \tag{45}$$

The radius of the hydrophone case selected was 1.91 cm.

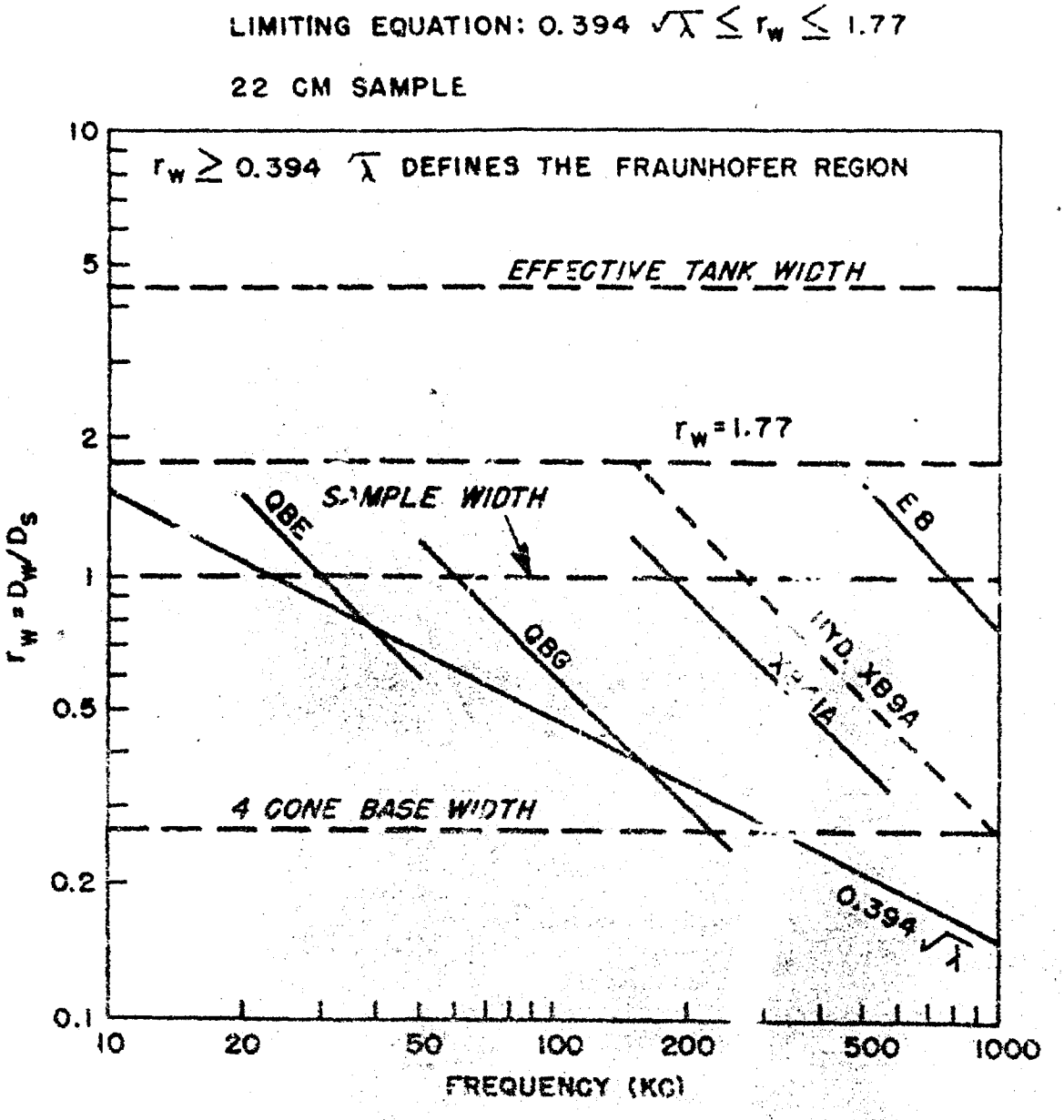

FIG. 21
RESTRICTIONS ON PROJECTOR BEAM WIDTH
BEAM WIDTH vs FREQUENCY

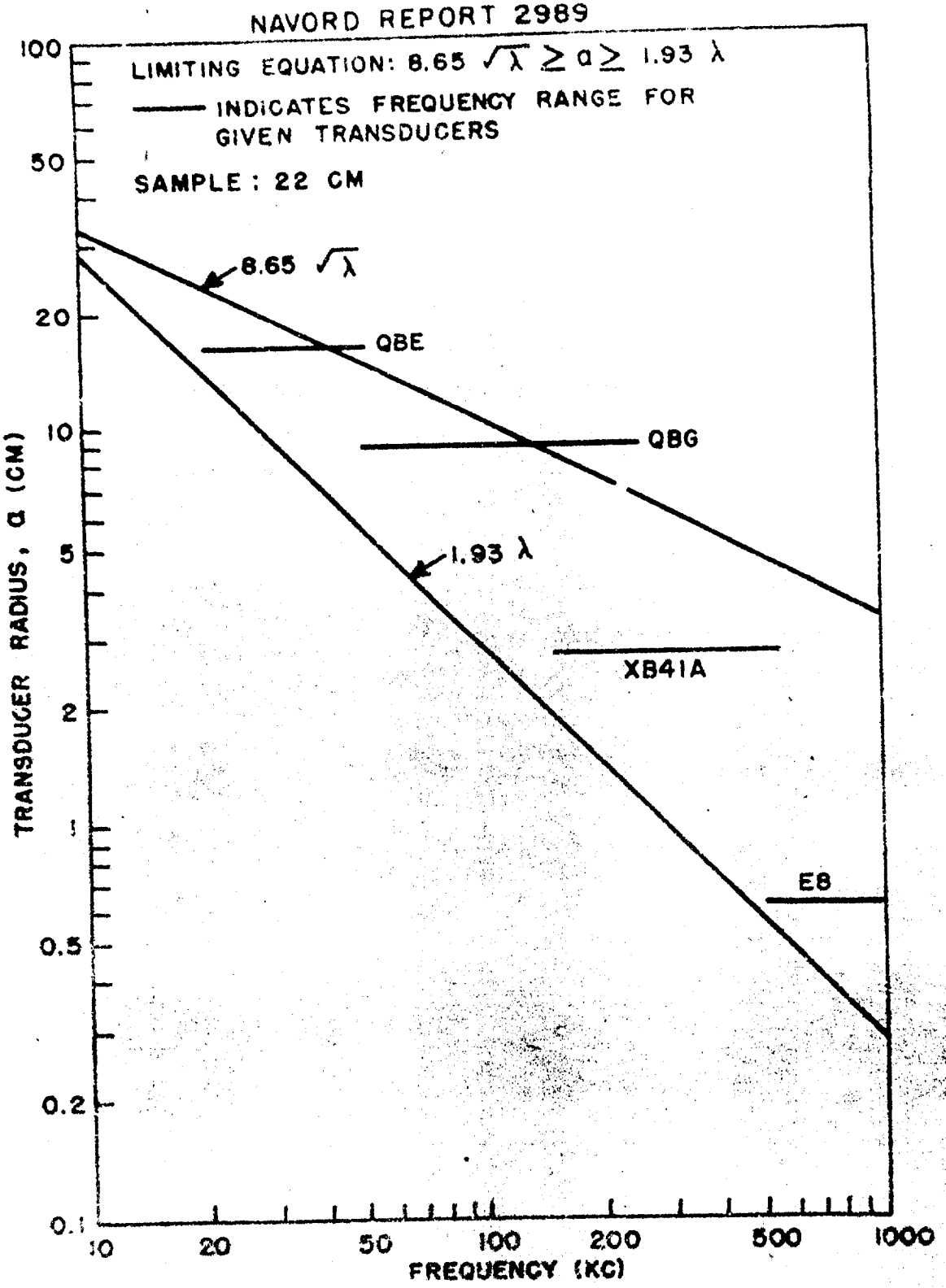

FIG. 22 RESTRICTIONS ON PROJECTOR BEAM WIDTH RADIUS vs FREQUENCY

44. It is desirable that the directivity pattern of the hydrophone be great enough to "see" the surface of the sample illuminated by the projector. The beam width is plotted as a dotted line in Figure 21 in accordance with the following equation

$$r_w = \frac{r_x D_w}{D_p}, \qquad (46)$$

$$= \frac{1.13\lambda}{D_p}$$

It may be observed that the beam width of hydrophone XB9A exceeded the beam width of all of the projectors except the E-8 which was used at the high frequencies. For these higher frequency measurements the hydrophone beam width was approximately a third of that of the E-8. The minimum hydrophone beam width (at 1 Mc.) was such that it intercepted sound from an area having a diameter equal to the width at the base of four adjacent cones This was tentatively accepted as the minimum width to get a representative reflection measurement.

45. Pulse Parameters. The pulse length in water should not exceed double the distance from the hydrophone to the specimen in order that the tail of the incident signal would not interfere with the reflection. Actually it was found to be more convenient to use about two-thirds of this value, which corresponds to a pulse duration of about 0.45 milliseconds. The repetition rate was set at about 150 pulses/sec as determined by the associated electronic equipment. The hydrophone rotation rate selected was 1/12 RPM to allow sufficient pulses per cm of hydrophone travel (approximately 90) for good pattern resolution.

VI. DISCUSSION OF RESULTS

46. The results of the present study are presented in the form of reflectivity patterns and plots of the computed values of R, Δ and S. In addition, plots of the normal reflectivity index, R_n, are shown for two of the samples, No. 21 and 22. Figure 19 shows a sample computation of R, Δ, and S. Patterns of Sample No. 21 and of a reference plate were chosen for this example. The pattern number is made up of the sample code number (see Table I) followed by a dash and a serial identification number. The special coordinate paper referred to previously is designed to cover -30^0 to $+30^0$ (Chart B) and -90^0 to $+90^0$ (Chart A). The latter was used only outside the range of Chart B. The use of the expanded scale of Chart B increased the accuracy of the power determination. After redrawing the polar plots on this special paper a planimeter is used to determine the areas under the curves, A_r for the reference plate and A_s for the sample as indicated in Figure 19. The peak pressures from the sample and from the reference plate are also read off the patterns and then S, Δ, and R are calculated as shown in the figure.

Comparison of Samples From 50 to 250 kc

47. Reflectivity of all samples at 100 kc. A comparison of the patterns for all samples at 100 kc is given in Figure 23. This figure is arranged to show the reflectivity patterns of the structured rubber samples on the left side and all other samples on the right. There is indicated on each pattern the identifying code number from Table I, the material, the structure, and the values of R, Δ, and S. The reference plate reflectivity pattern No. 01-136 shown in Figure 24, was used as the reference pattern for these computations.

48. The effect of sample material on the reflectivity pattern may be noted by comparing samples with the same structure but of different material. Patterns Nos. 21-162, 11-155 and 31-152, Figure 23, constitute such a group for lead-loaded butyl material with cone-lattice surfaces. The pattern for Sample No. 31, the lead-loaded sample with blowing agent, in contrast with the patterns of the two other samples, indicates a concentration of energy near the axis which might be called "negative scattering". Patterns for Sample No. 21, the aluminum-loaded sample and No. 11, the heavily-loaded lead sample, show scattering of the same order of magnitude as indicated by the scattering index, S. This is especially interesting since at 100 kc Sample No. 21 had a reflectivity index, R, approximately 25 db below that of No. 11. It should be observed that the system gain was adjusted to an arbitrary value to give nearly full scale at some point in all the polar plots. Otherwise pattern No. 21-162 would have been

FIG. 23 TYPICAL REFLECTIVITY PATTERNS

FREQUENCY 100 KC
PROJECTOR QBG

LOADED BUTYL RUBBER CONE LATTICE SAMPLES

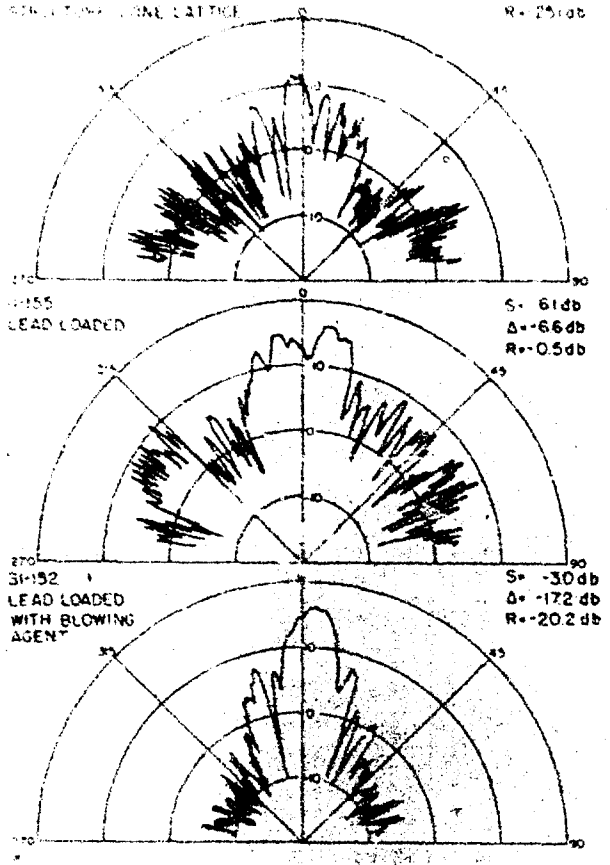

LOADED BUTYL RUBBER FLAT SAMPLES

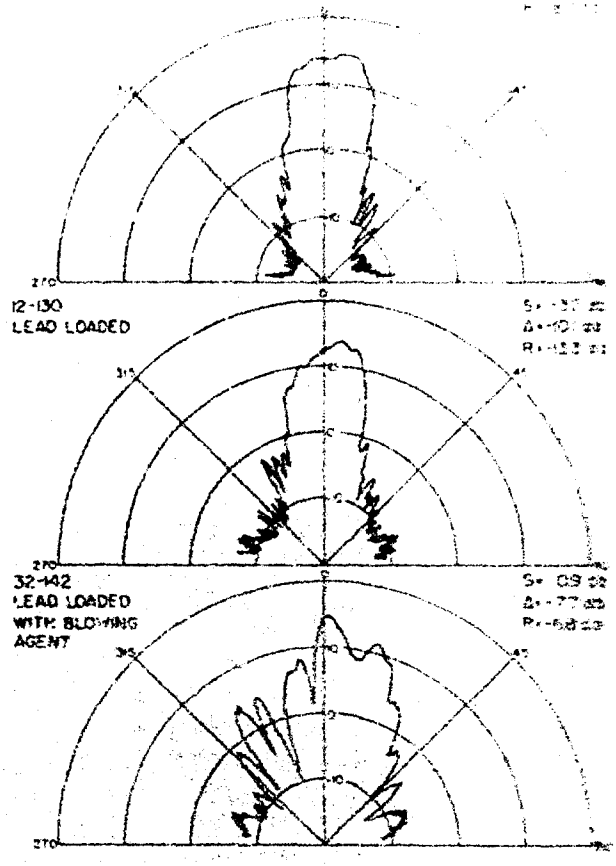

FAFNIR SAMPLES

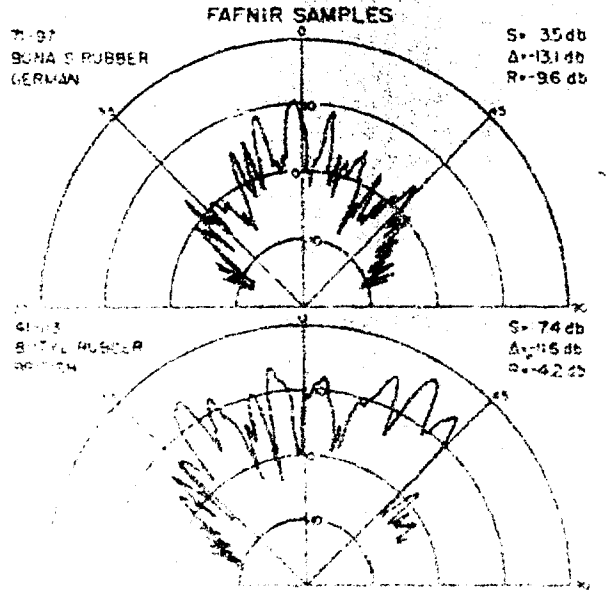

INSULKRETE AND CANVAS SAMPLES

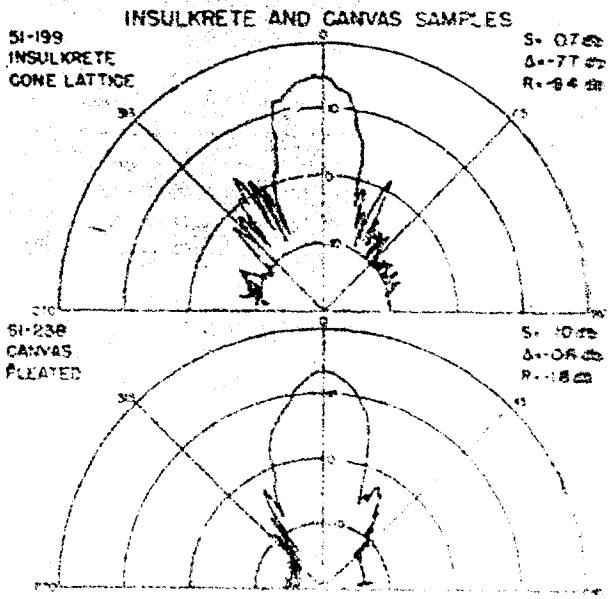

compressed [illegible] of the center of the group in Figure [illegible] and hence would have been unreadable. Patterns No. 24-115, 24-130 and 32-142, moreover, constitute a similar group of lead-butyl samples but with flat surfaces. None of these samples showed very much scattering. The lack of symmetry in the pattern for Sample No. 32, lead-loaded butyl rubber with blowing agent was caused by the poor mechanical nature of this material which caused irregularities on the surface. The asymmetry in the central lobe of Pattern No. 12 for the heavily lead-loaded butyl flat sample could not be so explained; the sample appeared to be structurally satisfactory. Furthermore, measurements at other frequencies on this sample exhibited asymmetry of comparable magnitude.

49. A comparison of samples having a cone-lattice structure with flat samples of the same material at 100 kc is shown in the upper portion of Figure 23. The difference in scattering between the two types of surfaces (structured values minus flat panel values) and also increased with heaviness of loading, being -3.9 db for the lead with blowing agent samples, +4.9 db for the aluminum-loaded samples, and +9.3 db for the heavily lead-loaded samples. As indicated in Table I, the cone structure sample having lead with a blowing agent had the lowest density, (1.07); the aluminum-loaded cone structure had a density of 1.23; and the heavily lead-loaded sample a density of 2.61. It should be noted that the flat lead-loaded sample with blowing agent, No. 32, had an anomalous density of 1.63. These results indicate that the type of material affects the scattering index.

50. It will be noted that the British Fafnir (Pattern No. 41-113) measured in the plane of Section B-B, Figure 10, seems to show more pronounced scattering off the acoustic axis than the other samples in Figure 23. This result is borne out by the fact that the British Fafnir had a high scattering index (S = 7.4 db) at 100 kc. In fact this value of S was the highest (at this frequency) for all of the samples tested.

51. The pattern for the German Fafnir, Sample No. 71 shown in Figure 23 is not necessarily typical of this structure because the narrow projector beam width illuminated too small a portion of the sample. The spacing of the elements and their dimensions were greater than in the case of the cone structure. The pattern was measured in a plane perpendicular to the wedge rows, i.e., along Section A-A, Figure 10.

52. Pattern No. 51-199, Figure 23, is for a cone-lattice [illegible] of Insulmate. The flat backing for this sample is [illegible] the cone elements are only 1 cm high as compared to [illegible] lead-butyl cone elements. Patterns of flat

[illegible] little difference [illegible] and the pattern for the cone [illegible] result shows that the 1 cm cones did not affect the acoustic performance.

54. The plotted curves [illegible] indicate a very small amount of sound concentration along the axis, as shown by the negative value of S. However, this appears to be a random phenomenon, since patterns at other frequencies indicate no definite trend.

54. The necessity for using the present technique in evaluating the scattering and absorption characteristics of structured specimens is evident from the fact that lateral spreading occurs for most of the patterns, and that the maxima occur at angles off normal for several of the structured samples. The use of the normal reflectivity index, R_n, instead of R as an indication of absorption would result in an error of 7.5 db for the British Fafnir Sample No. 41.

55. Patterns Versus Frequency. Reflectivity patterns for Sample No. 21 are compared in Figure 24 with patterns of the reference plate at corresponding frequencies. The scattering index, shown on Pattern No. 21-161, is a maximum at 150 kc, and decreases at both ends of the frequency band. The decrease at the low-frequency end may be attributed to the increase of wave length relative to the dimensions of the elements. The decrease at the high-frequency end is probably caused by reflection from the flat portion of the sample, as discussed in Section III, paragraph 23.

56. Reflection Parameters vs Frequency-Loaded Butyl Rubber Samples. Values for the scattering index, S, peak reflectivity index, Δ, and reflectivity index, R_0 for the various loaded-rubber samples are plotted in Figures 25 through 37. For any one sample these three parameters are plotted on the same figure. In addition, [illegible] for comparison purposes, each parameter for all samples is plotted on a separate figure. A negative value of the scattering index indicates a concentration of sound energy by the sample relative to that produced by the reference plate.

57. The three cone structure samples of loaded butyl rubber constitute a group which illustrates the effect of using different materials with a common type of structure. Figure 25 shows the parameters, S, Δ, and R_0, for the heavily lead-loaded butyl [illegible]. Interesting aspects of this material are the [illegible] peak reflectivity index and reflectivity index

FIG 24 REFLECTIVITY PATTERNS OF SAMPLE AND REFERENCE PLATE

FREQUENCY 50 TO 250 KC
PROJECTOR QBG
SAMPLE NO 21 ALUMINUM LOADED BUTYL RUBBER
STRUCTURE CONE LATTICE

SAMPLE NO 21

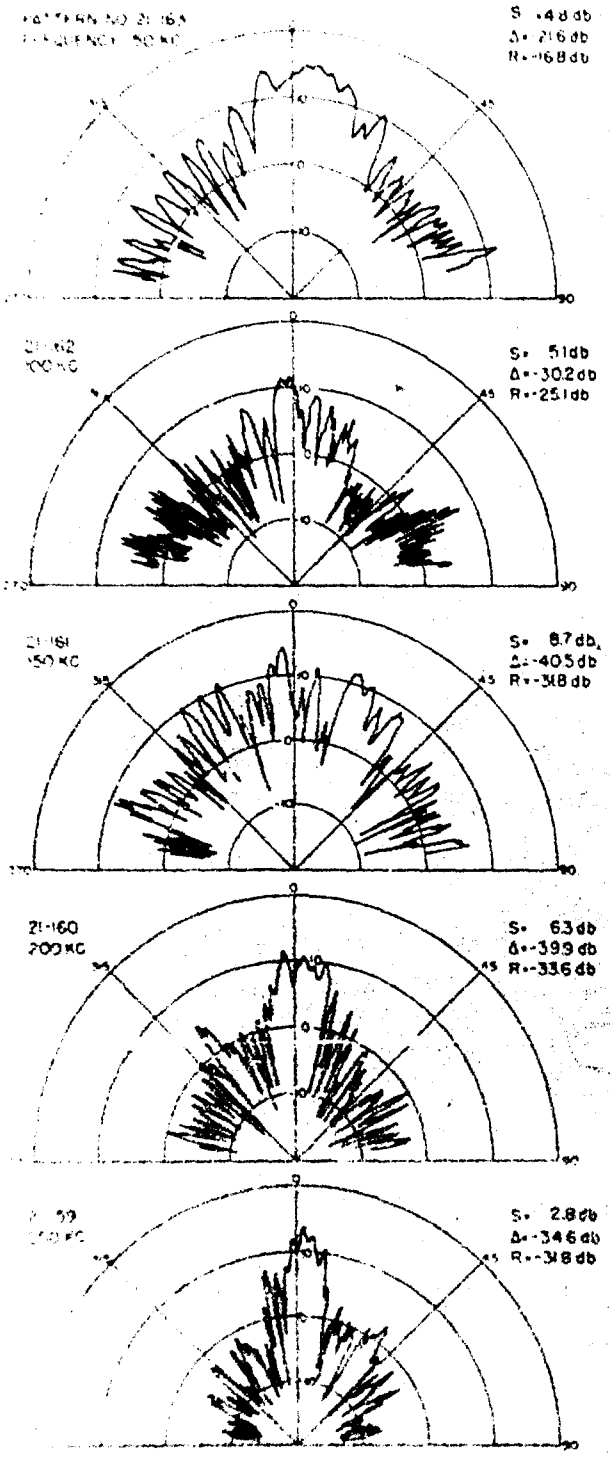

REFERENCE PLATE NO 01

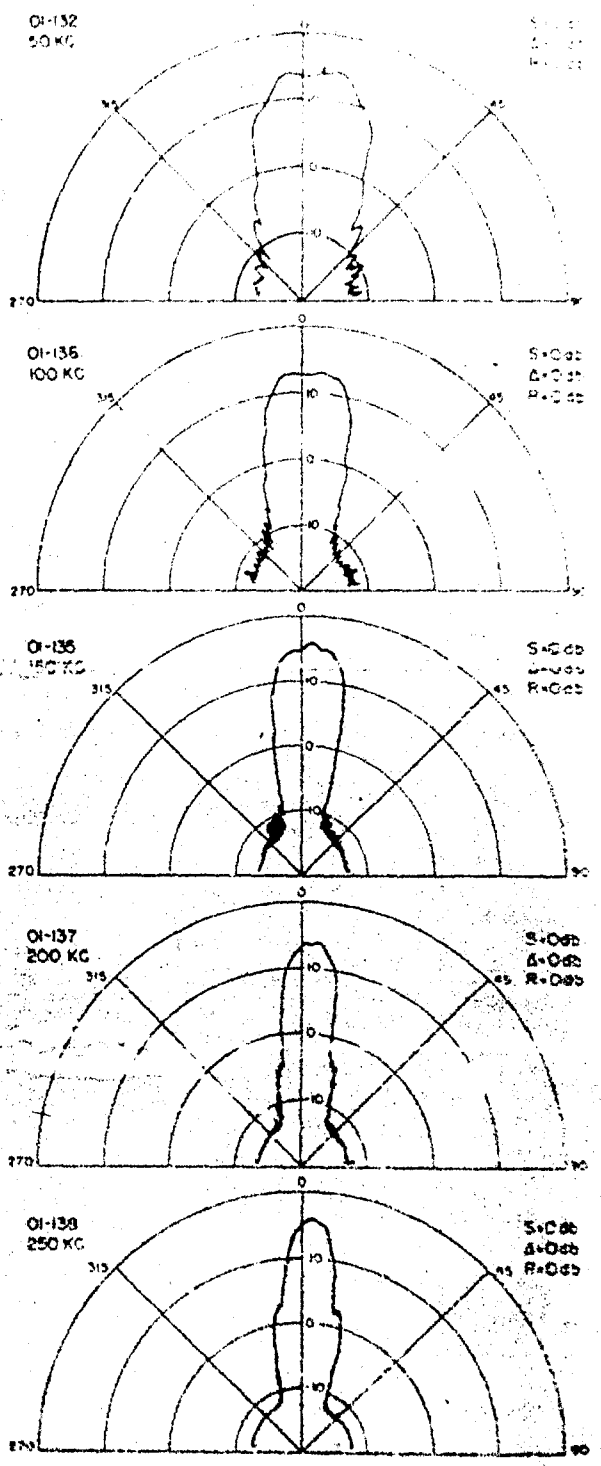

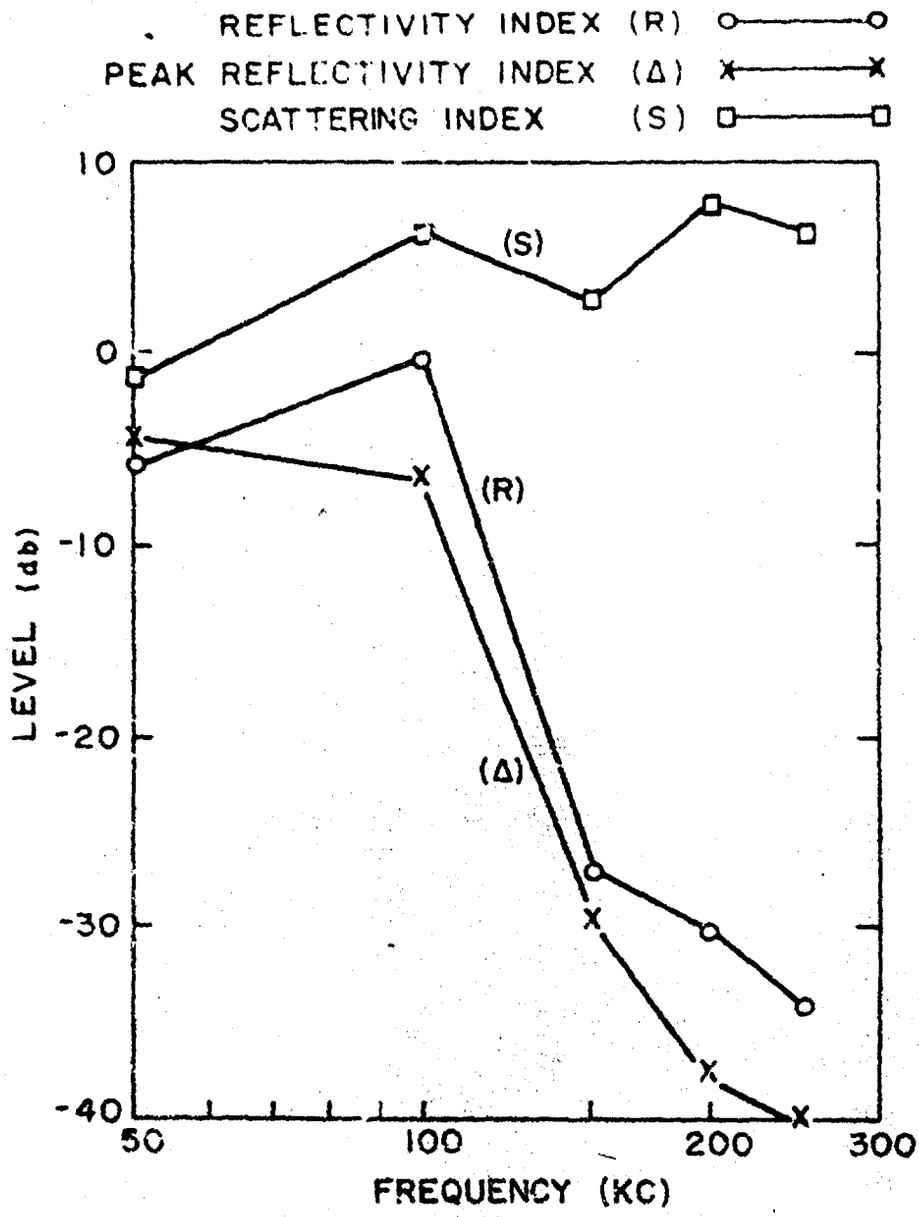

LEAD LOADED BUTYL RUBBER CONE LATTICE STRUCTURE

FIG. 25

REFLECTION CHARACTERISTICS VS FREQUENCY FOR SAMPLE NO. 11

[redacted]

[illegible] and the rapid decrease of other parameters above [illegible] This particular sample exhibited both the highest and lowest values of Δ and R of all of the loaded rubber cone structure samples as shown in Figures 35 and 36. The scattering increased from approximately -1 to +6 db over the frequency range 50 to 250 kc.

58. The reflection characteristics of the aluminum loaded cone structure Sample No. 21 are shown in Figure 26. The reflection from this sample was low throughout the frequency range, the reflectivity index decreasing from -24 db at 50 kc to -32 db at 250 kc. A similarity between this curve and that for the lead-loaded material No. 11 is that the major portion of the decrease occurs between 100 and 150 kc. One difference, however, is the apparent leveling off of the curve at 250 kc for Sample No. 21 compared to the relatively high slope of the curve for the lead-loaded sample. The peak reflectivity index for Sample No. 21 shows a minimum at 150 kc but the index is below -26 db throughout the frequency range. Also, at 150 kc the scattering is a maximum, 9 db, and drops to approximately 4 db at both the low and high ends of the frequency range.

59. The reflection characteristics for the cone-lattice sample of lead-loaded butyl rubber with blowing agent, Sample No. 31, is shown in Figure 27. Both the reflectivity and the peak reflectivity indices are fairly constant with frequency. The sample differs from the two materials discussed above by the negative values obtained for scattering for all frequencies except at 150 kc. It may be observed that the maximum value of the scattering index for this sample occurs at the same frequency as Sample No. 21.

60. Curves for three flat samples, No. 12, 22, and 32, each made from butyl rubber but with different metal loadings illustrate the effect of these materials on the acoustic properties of flat sheets. Figure 28 shows the reflection characteristics for the heavily lead-loaded sample. The reflectivity index, R, decreases from -7 db at 50 kc to -14.5 db at 250 kc. It may be noted by referring to Figure 35 that this sample is unique in that the reflectivity index of the flat sample is less than that for the cone-lattice sample for a portion of the frequency range, namely, from 50 to 100 kc.

61. Figure 29 gives the reflection characteristics for a flat sample of aluminum-loaded butyl rubber, No. 22. The reflectivity index for this sample decreases approximately 5 db through the frequency range shown. Since the scattering index is nearly zero, the peak reflectivity index, Δ, is approximately equal to the reflectivity index, R

[redacted]

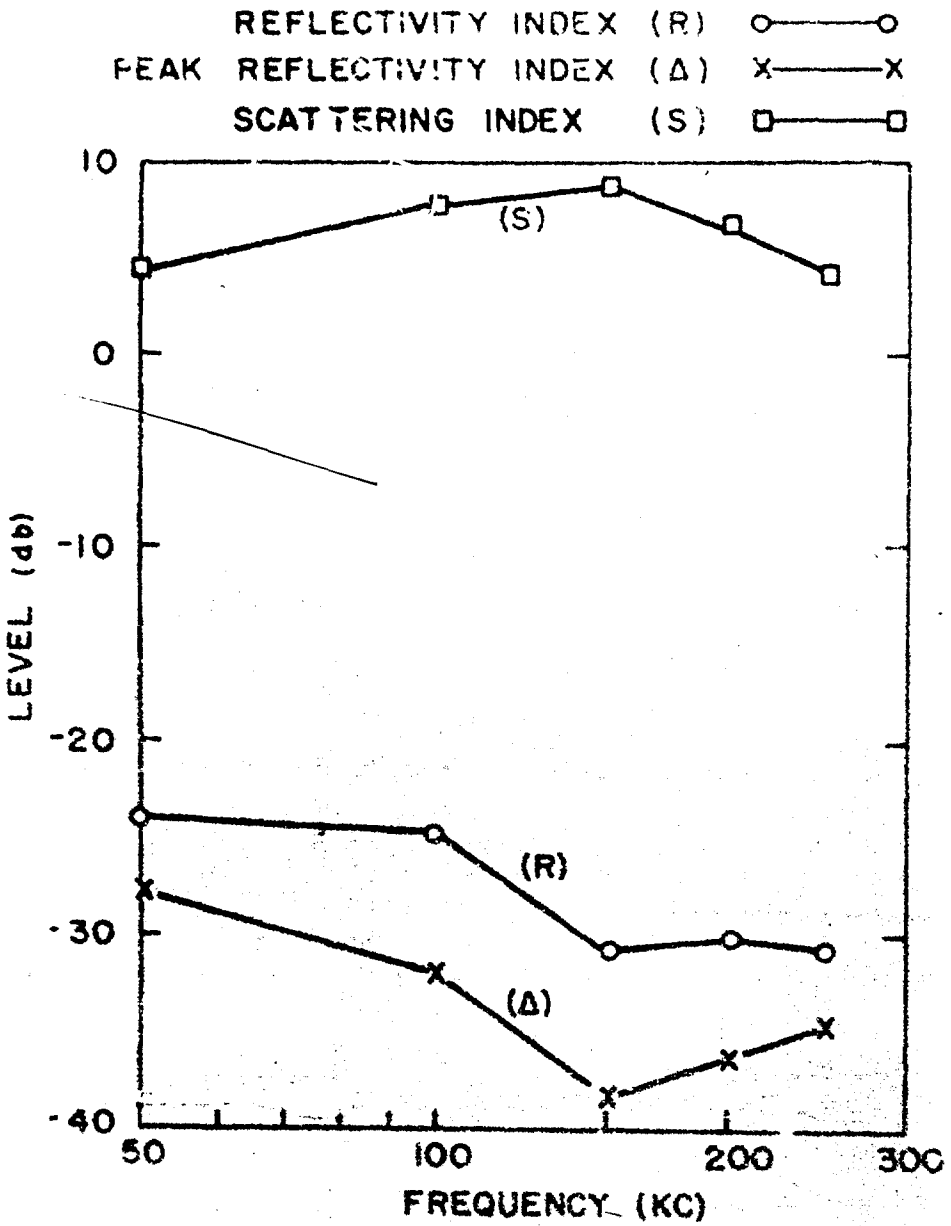

ALUMINUM LOADED BUTYL RUBBER CONE LATTICE STRUCTURE

FIG. 26

REFLECTION CHARACTERISTICS 'S FREQUENCY FOR SAMPLE NO. 21

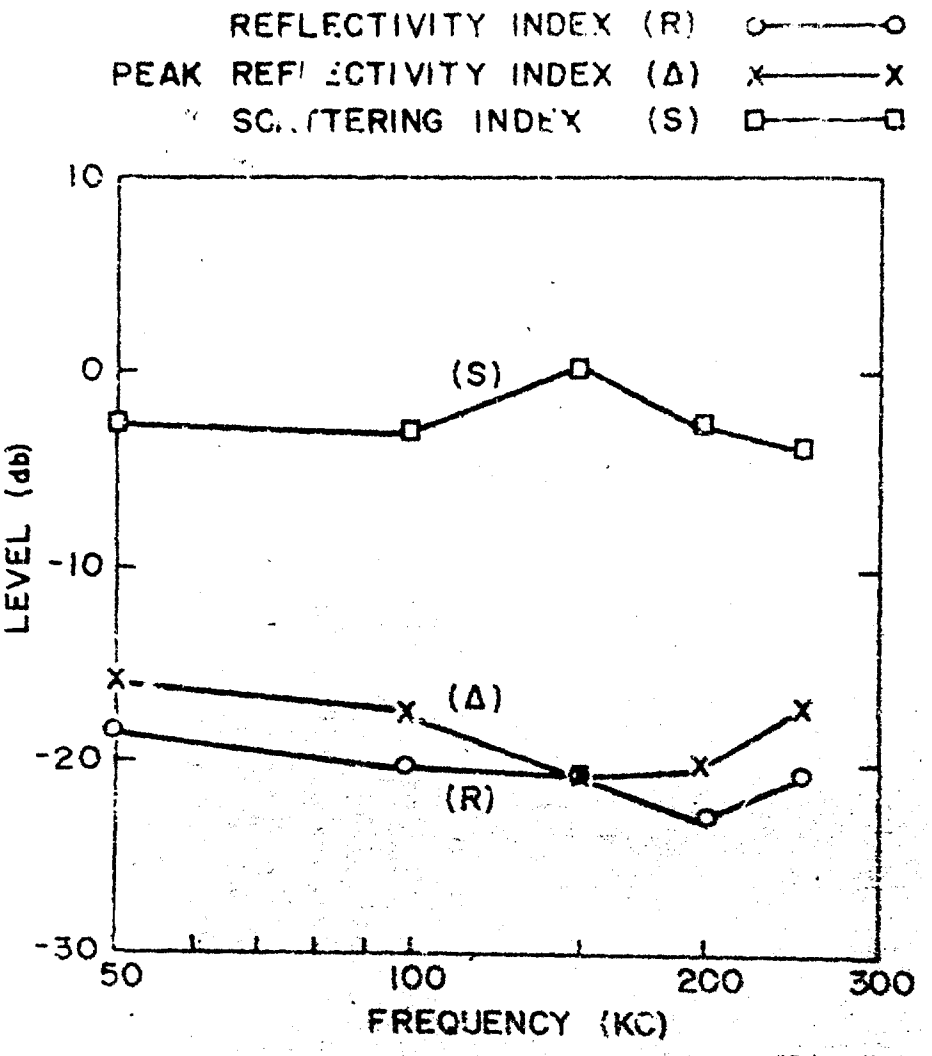

LEAD AND BLOWING AGENT LOADED BUTYL RUBBER CONE LATTICE STRUCTURE

FIG. 27

REFLECTION CHARACTERISTICS VS FREQUENCY FOR SAMPLE NO. 31

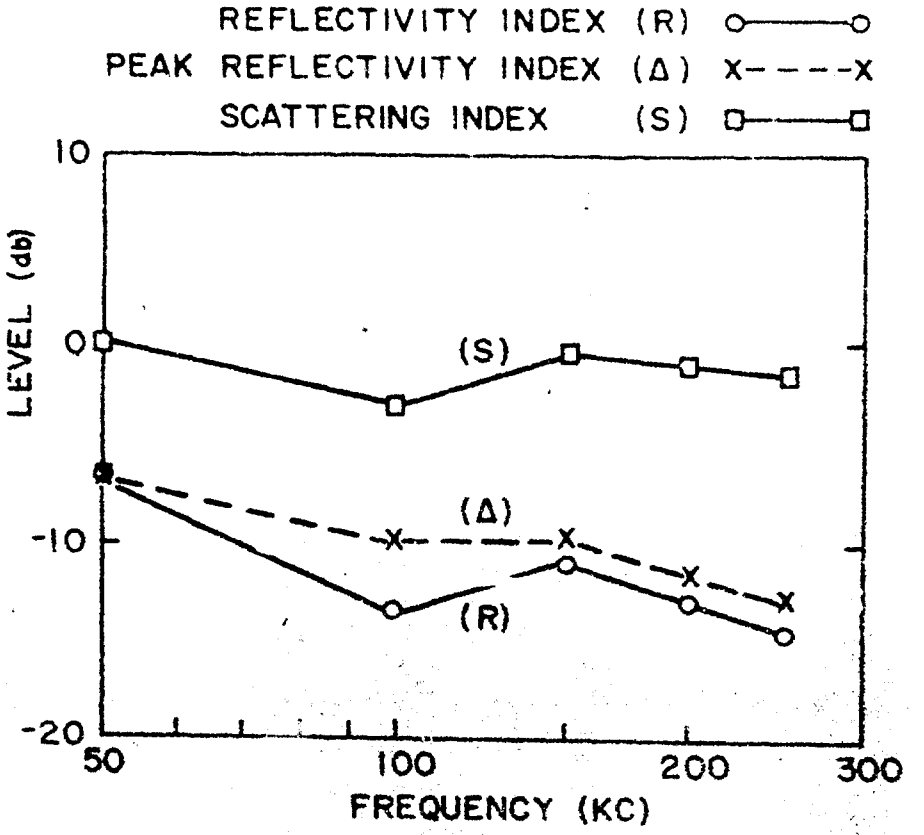

LEAD LOADED BUTYL RUBBER FLAT SAMPLE

FIG. 28

REFLECTION CHARACTERISTICS
VS FREQUENCY FOR SAMPLE NO. 12

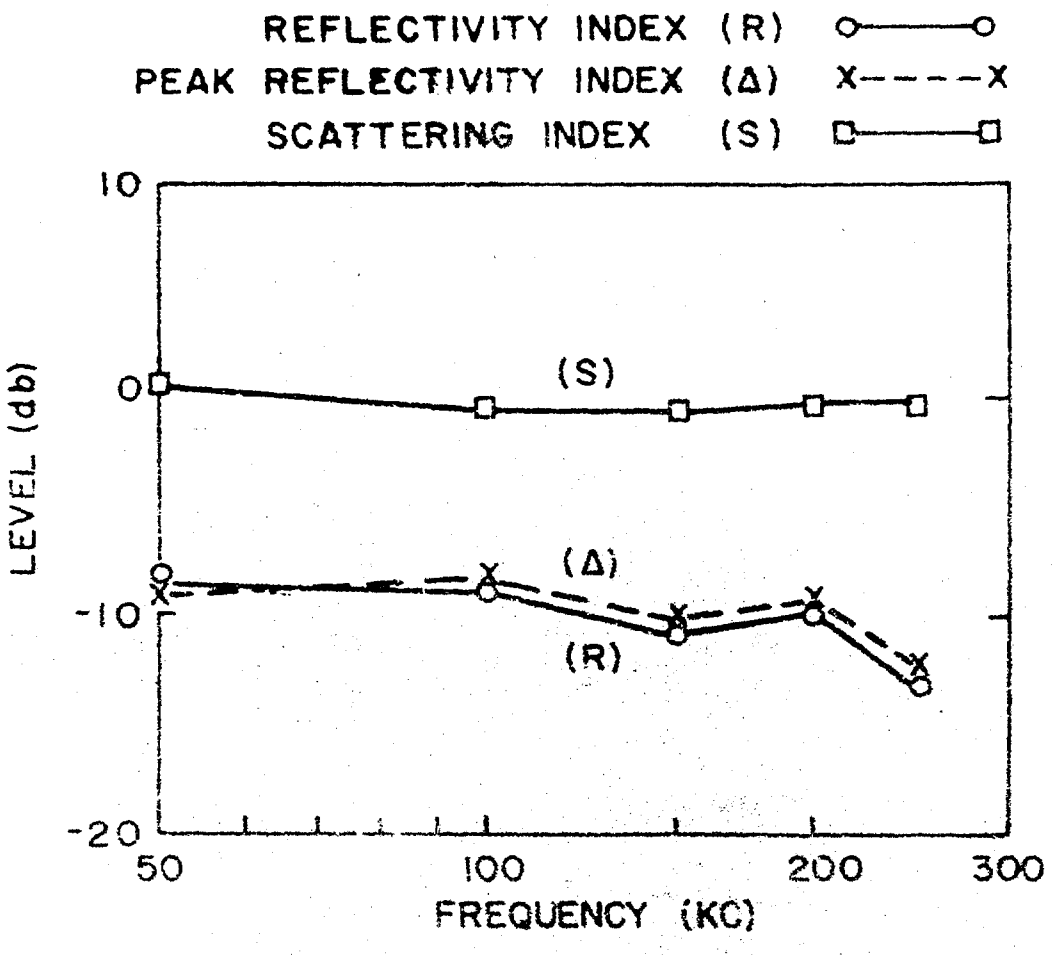

ALUMINUM LOADED BUTYL RUBBER FLAT SAMPLE

FIG. 29

REFLECTION CHARACTERISTICS
VS FREQUENCY FOR SAMPLE NO. 22

[illegible] tendency to [illegible] material exhibited a greater [illegible] reflectivity index and [illegible] materials. The reflectivity index decreased [illegible] from 50 to 250 kc.

[illegible] Figure 35 indicates that values of R for the cone-lattice samples (Nos. 11, 21, and 31) are two or more times (in db) [illegible] for the flat samples of the same material (Nos. 12, 22, and 32) except for Sample No. 11 at the two lowest frequencies and Sample No. 31 at the highest frequency. Since the base of the cone-lattice sample has the same thickness as the flat sample, this comparison is equivalent to noting the effect of inserting cones in front of the flat sample. The poor absorption characteristics of the cone-lattice sample of the lead-loaded material at the two lowest frequencies has not been explained. All loaded butyl rubber samples showed an increase of absorption with frequency over the range from 50 to 250 kc. It may be noted that curves of R for different materials are much more closely grouped for the flat samples than for the cone-lattice samples (Figure 35). Sample No. 21 was selected for a further study on the basis of a high value of absorption throughout the frequency range.

64. Samples other than Loaded Butyl Rubber. Reflection characteristics of samples other than loaded butyl rubber are shown in Figures 31 through 34. British Fafnir, Sample No. 41, shown in Figure 31, was the most absorbent of these materials except at a frequency of 100 kc. The correspondence between Δ and P may be noted. These parameters varied widely, as much as 25 db over the frequency band used. The minimum value of R was -32 db at 150 kc, which is almost the same as the corresponding value for Sample No. 21. It may be observed that the reflectivity index at 50 kc is -22 db, approximately the value claimed in reference [illegible] for German Fafnir in the frequency range for which it was designed, approximately from 10 kc to 35 kc. Furthermore, it may be noted that the high value at 100 kc is above the upper cutoff frequency considering the element spacing of the closely packed British Fafnir Sample No. 41 (see paragraph 22). The scattering index S, for this material is of interest because of the contrast between the geometry of the surface structure, periodicity and depth, and that of the cone lattice. Measurements were made parallel to the planes of the wedges (see Section B-B of Figure 10). The scattering index is about 3 db higher than the maximum value for the cone-lattice structures at all frequencies except one (100 kc), [illegible] frequency it is approximately the same.

[illegible] characteristics of four samples of Insulkote [illegible] These samples [illegible] cone lattice

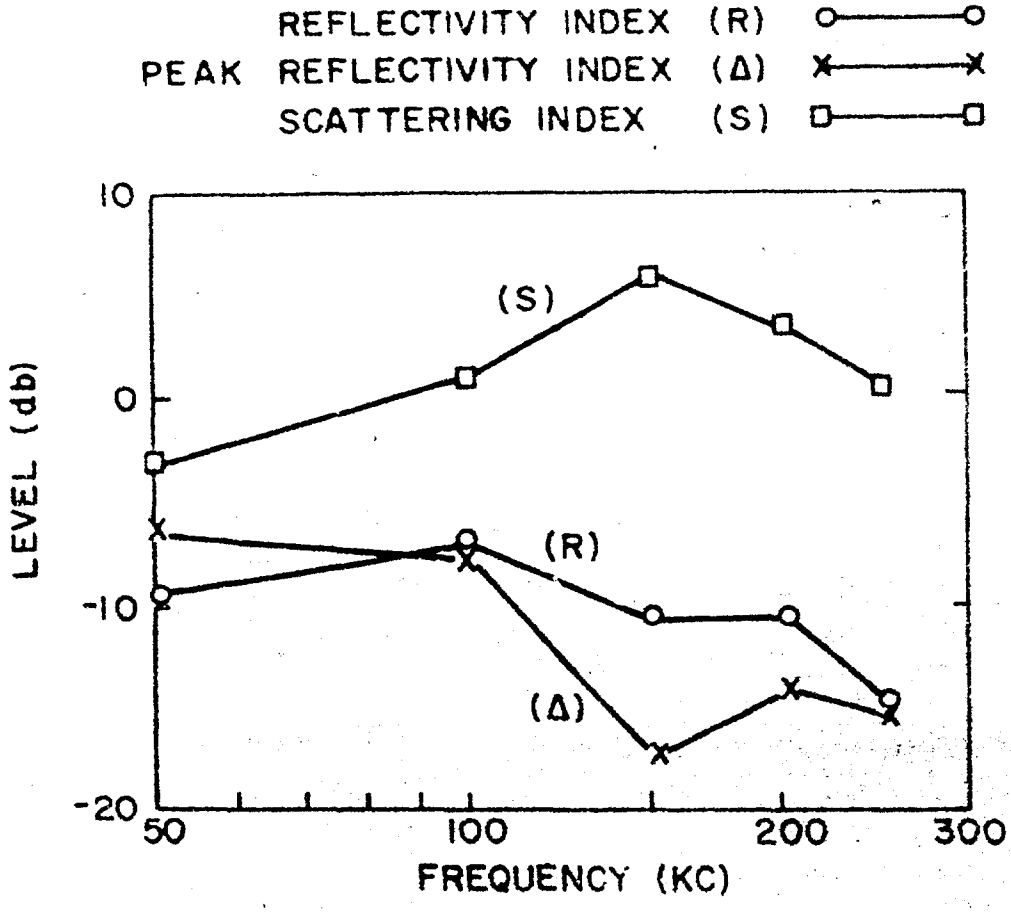

LEAD AND BLOWING AGENT LOADED BUTYL RUBBER FLAT SAMPLE

FIG. 30

REFLECTION CHARACTERISTICS VS FREQUENCY FOR SAMPLE NO. 32

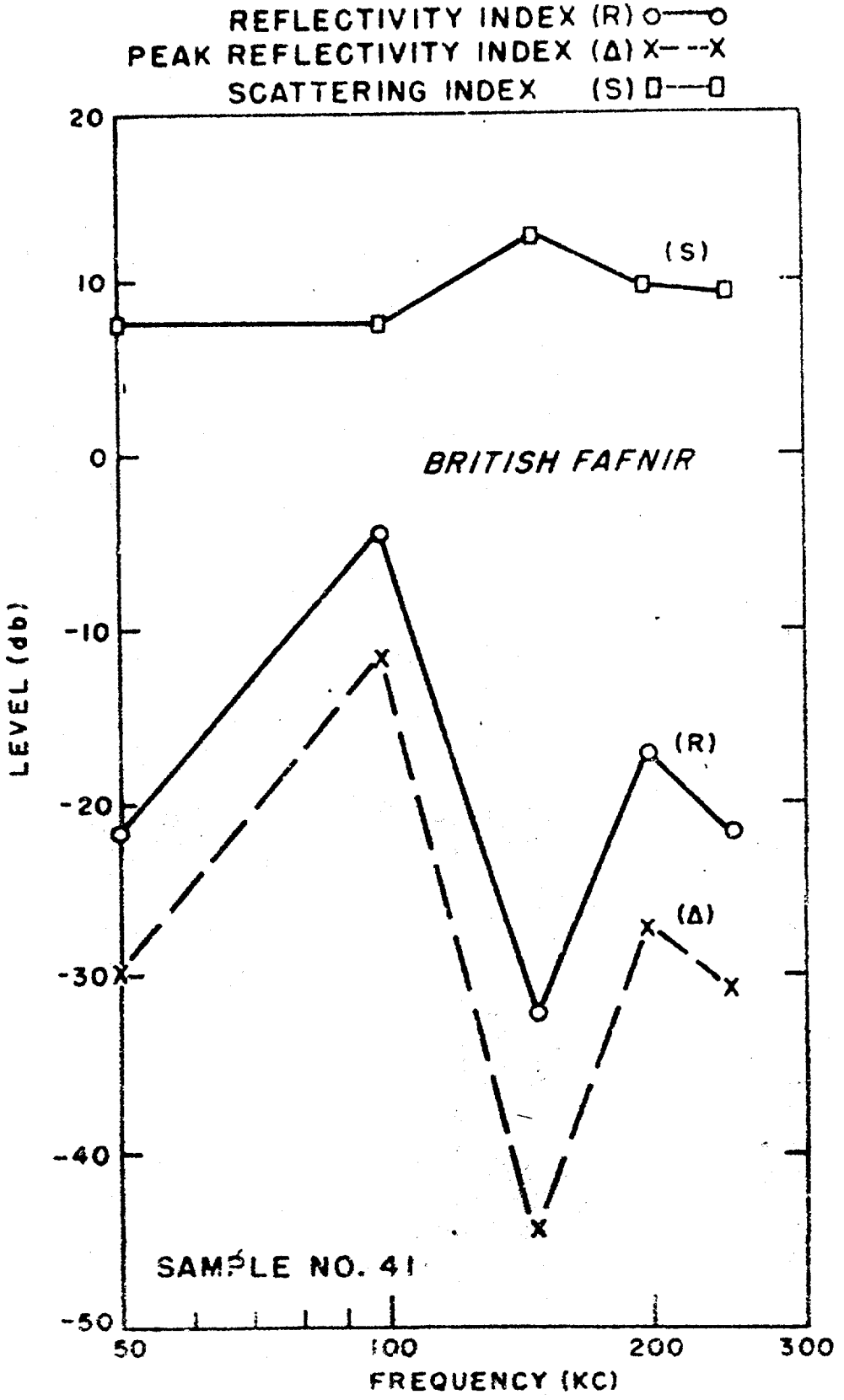

FIG. 31
REFLECTION CHARACTERISTICS vs FREQUENCY

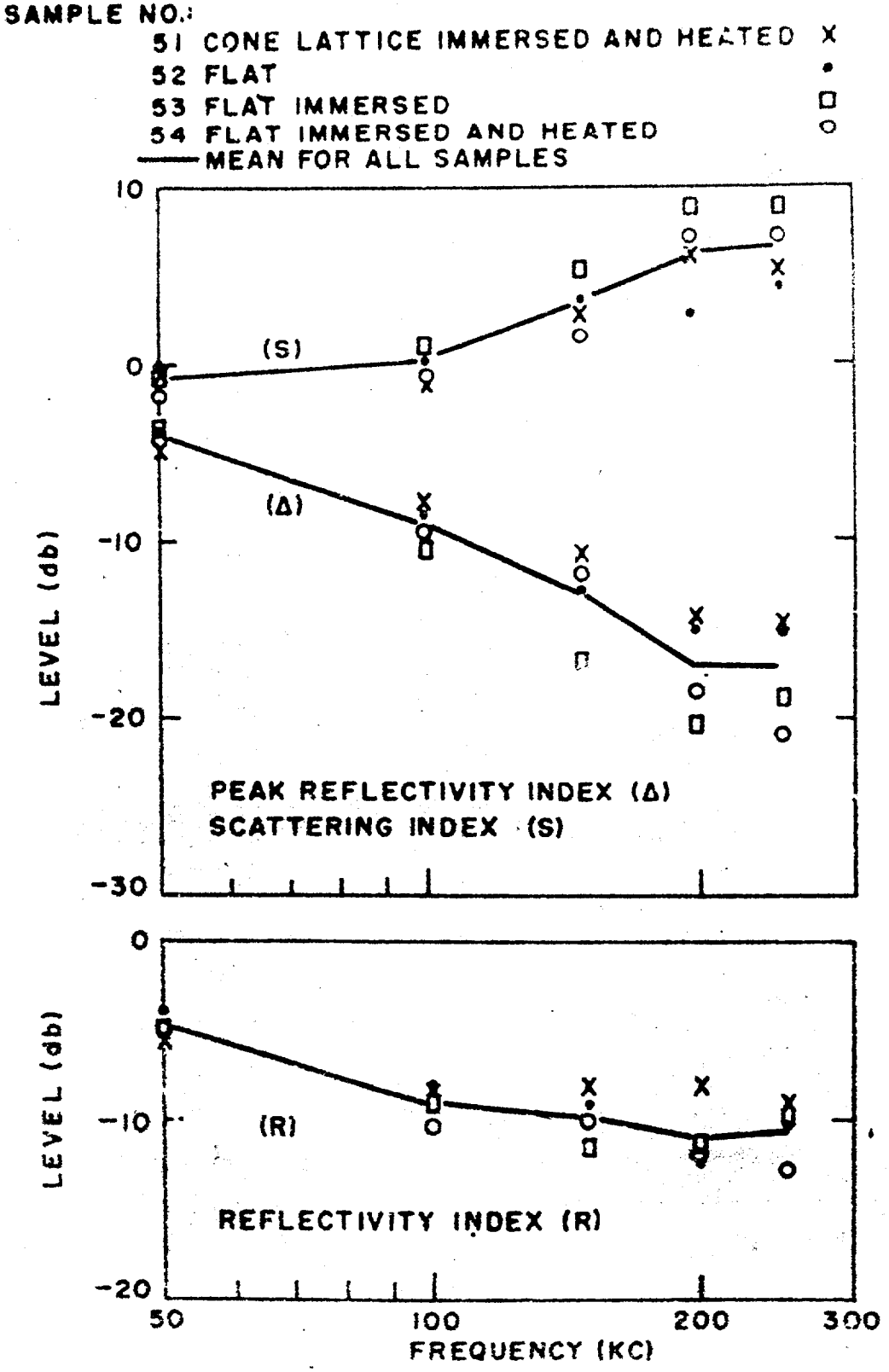

INSULKRETE

FIG. 32

REFLECTION CHARACTERISTICS vs FREQUENCY

surface, Sample No. 51; a flat surface which was measured without being previously immersed, Sample No. 52; a flat sample which was kept submerged for three days at room temperature before making measurements, Sample No. 53; and another flat sample which was kept submerged at 183°F for three days before measurement, Sample No. 54. As mentioned previously, the cones of the cone-lattice structure had the same base dimensions as the butyl cone lattice but could be made only one centimeter high because of the fragile nature of the material. Reference to Figure 32 indicates that for Insulkrete a corrugated surface provides very little benefit. This is in contrast to samples made from loaded butyl rubber. Immersing and heating the samples likewise appears to have little effect. The deviation of the reflectivity index from the mean for all samples except No. 51 was only a few db. If the reflectivity index of Sample No. 51 is adjusted for the difference in the volume of material, its deviation is also a few db. Since the reflectivity index decreased about 6 db and the scattering index increased about 6 db, the peak reflectivity index decreased approximately 12 db over the frequency range used. The value of the reflectivity index measured at 50 kc (approximately 5 db) on samples 5 cm thick agrees with measurements made by Trent and Darner, reference (b), on samples 12 in thick which indicated a reflection coefficient of about one percent or a reflectivity index of -20 db. It is evident from this agreement and also from the insignificant effect of a cone-lattice surface structure that for flat samples of Insulkrete the absorption is not limited by surface mismatch. This was not the case for flat samples of loaded butyl rubber.

66. Figure 33 shows the reflection characteristics of the pleated canvas, Sample No. 61. Before measurements were made the sample was immersed in water at 183°F for three days to remove as much entrapped air as possible. The reflectivity index is between -3 and -5 db over the frequency range. This lining had essentially no effect as a sound scatterer, the scattering index varying between small negative and positive values. This sample was included in the measurements since it has been tried as a cheap substitute for an absorbent lining in a small, high-pressure tank, the purpose being only to reduce the reverberation time. Even though the reflectivity index is only about -4 db it is of some value for the desired purpose.

67. Figure 34 illustrates the reflection characteristics of the German Fafnir lining used in the open tank at NOL. The material at one end of the tank is designated as Sample No. 71 and the material at the other end as Sample No. 72. It should be noted that these measurements were made above the frequency band for which this lining was designed. Measurements were made perpendicular to the plane of the ridges (see Figure 10). The reflectivity

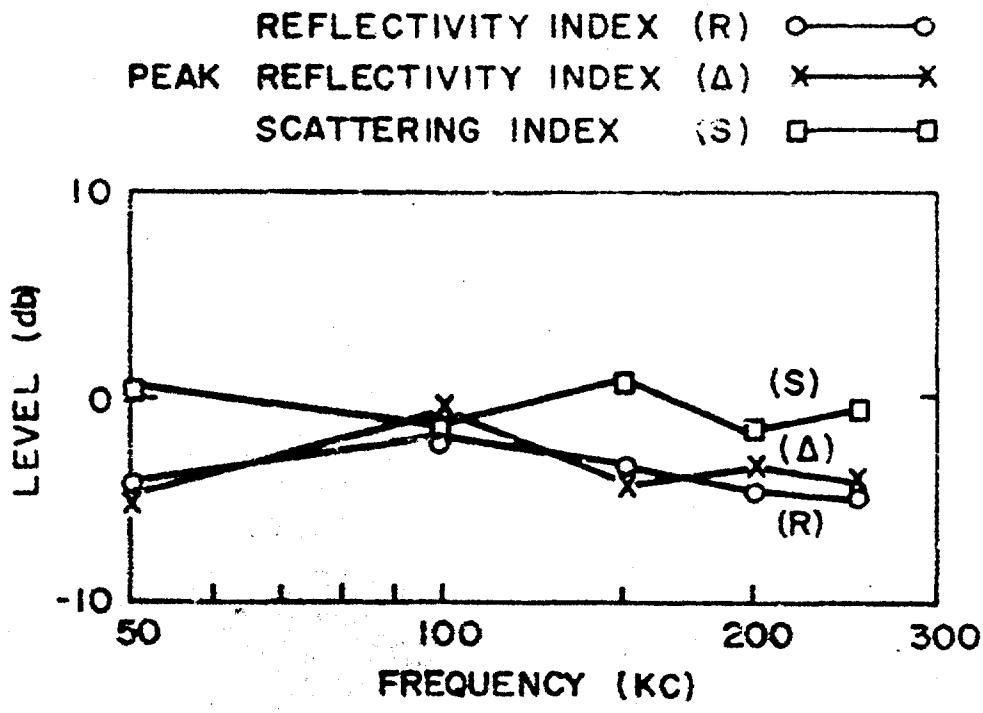

PLEATED CANVAS

FIG. 33

REFLECTION CHARACTERISTICS VS FREQUENCY FOR SAMPLE NO. 6

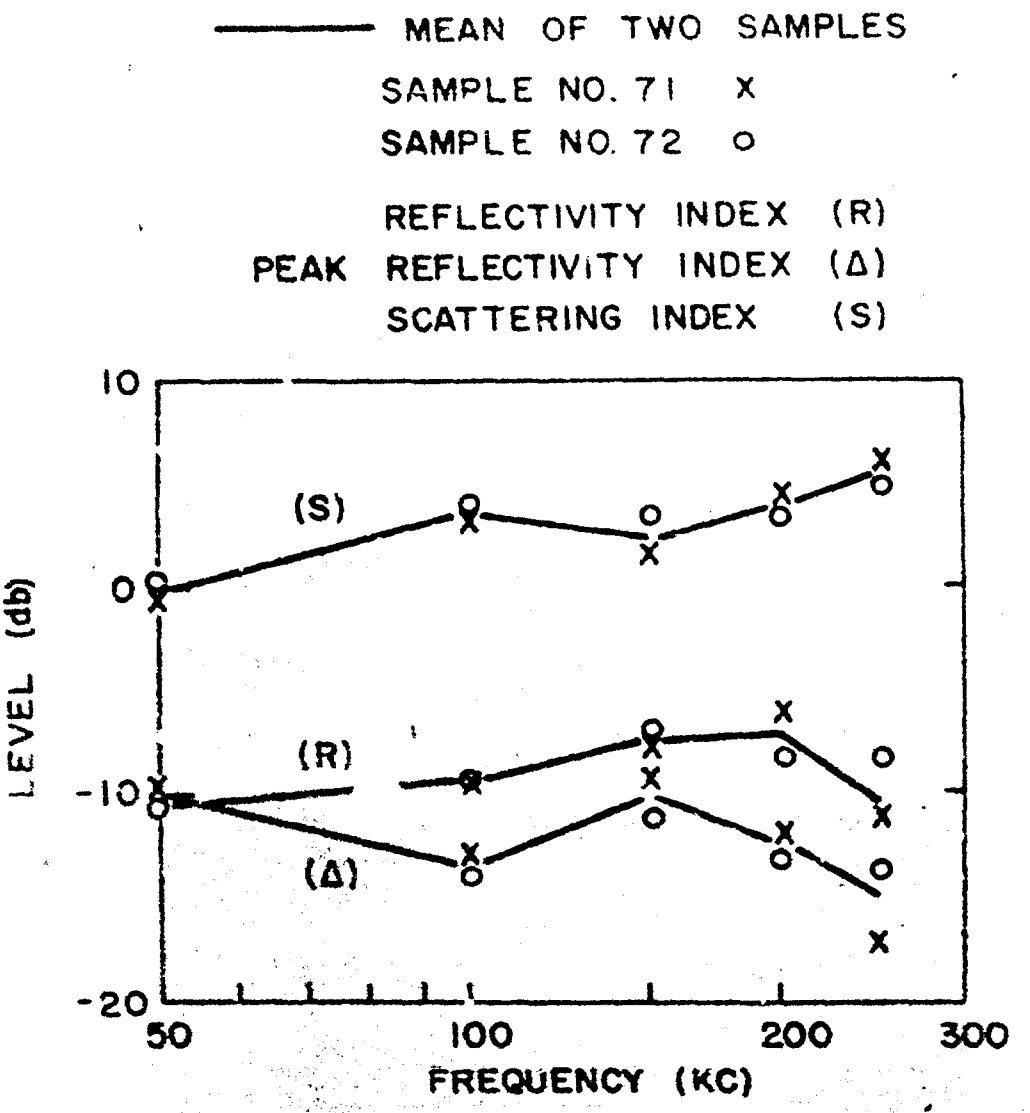

GERMAN FAFNIR SAMPLES (ENDS OF TANK)

FIG. 34

REFLECTION CHARACTERISTICS vs FREQUENCY

index for Samples No. 71 and 72 varies between about 6 db over the frequency range. As mentioned previously, considerable variation in reflection characteristics (R, Δ, and S) is to be expected because of the narrow beam width of the projectors relative to the dimensions of the elements. This is especially true at the upper end of the frequency band. The scattering index increases with frequency from 4 db at 50 kc to about 6 db at 250 kc. In addition to Sample Nos. 71 and 72, measurements were made on a German Fafnir panel identified as Sample No. 73. The reflection characteristics of this sample will be discussed later in the following section on sample orientation.

Measurements Considering Periodicity in ψ

68. The results presented heretofore on structured samples have been for a single orientation, $\psi = \psi_o$ which will be called the first orientation. Since in general these samples are periodic in the radial angle ψ, the measurements reported in this section were made to obtain a comparison between results based on a single orientation and results based on two orientations. For the second orientation the samples were measured in the plane $\psi = \psi_r = \pi/2$. The theory of these measurements is more fully described in Section III A, paragraphs 32 thru 34.

69. As usual, the symbols R, Δ, and S are used to denote the reflection characteristics in the plane $\psi = \psi_o = 0$; the symbols R_r, Δ_r, and S_r are used to denote reflection characteristics in the plane $\psi = \psi_r = \pi/2$; and R_a, Δ_a, and S_a are used to denote the average of the above values. These average quantities are defined by equations 27 through 29. Measurements were made on the cone-lattice sample, No. 21, and the German Fafnir sample, No. 73, through the frequency range from 50 kc to 250 kc and also on the British Fafnir sample, No. 41 at 250 kc. The ψ_o orientations chosen were for the cone-lattice sample a plane through Section A-A (Figure 13); for the German Fafnir sample a plane perpendicular to the parallel surfaces of the wedge elements (Section A-A of Figure 10) and for the British Fafnir samples it was in a plane parallel to the parallel surface of the wedge elements (Section B-B of Figure 10).

70. Figure 38, Sample No. 21 at 150 kc, illustrates Pattern No. 21-161 for ψ_o and No. 21-162 for ψ_r, respectively. The general shape of the patterns is similar; however, the pattern for ψ_r exhibits slightly more scattering than the ψ_o pattern. [illegible] these two orientations are plotted from 50 to 250 kc in Figure 39. The values of R and R_r show deviations from R_a of approximately one db. The deviation of S and S_r from S_a

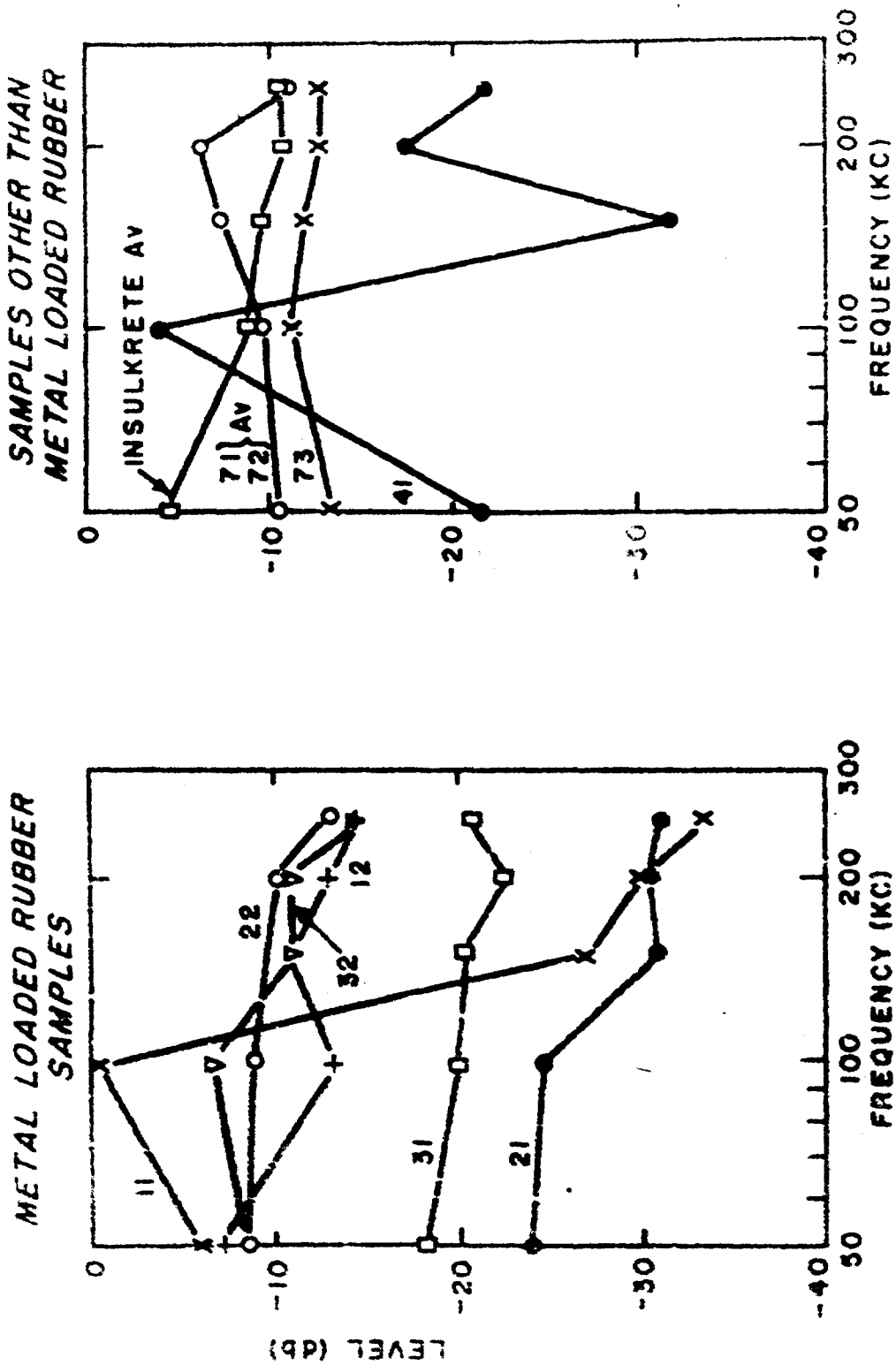

FIG. 35 REFLECTIVITY INDEX, R, FOR ALL SAMPLES vs FREQUENCY

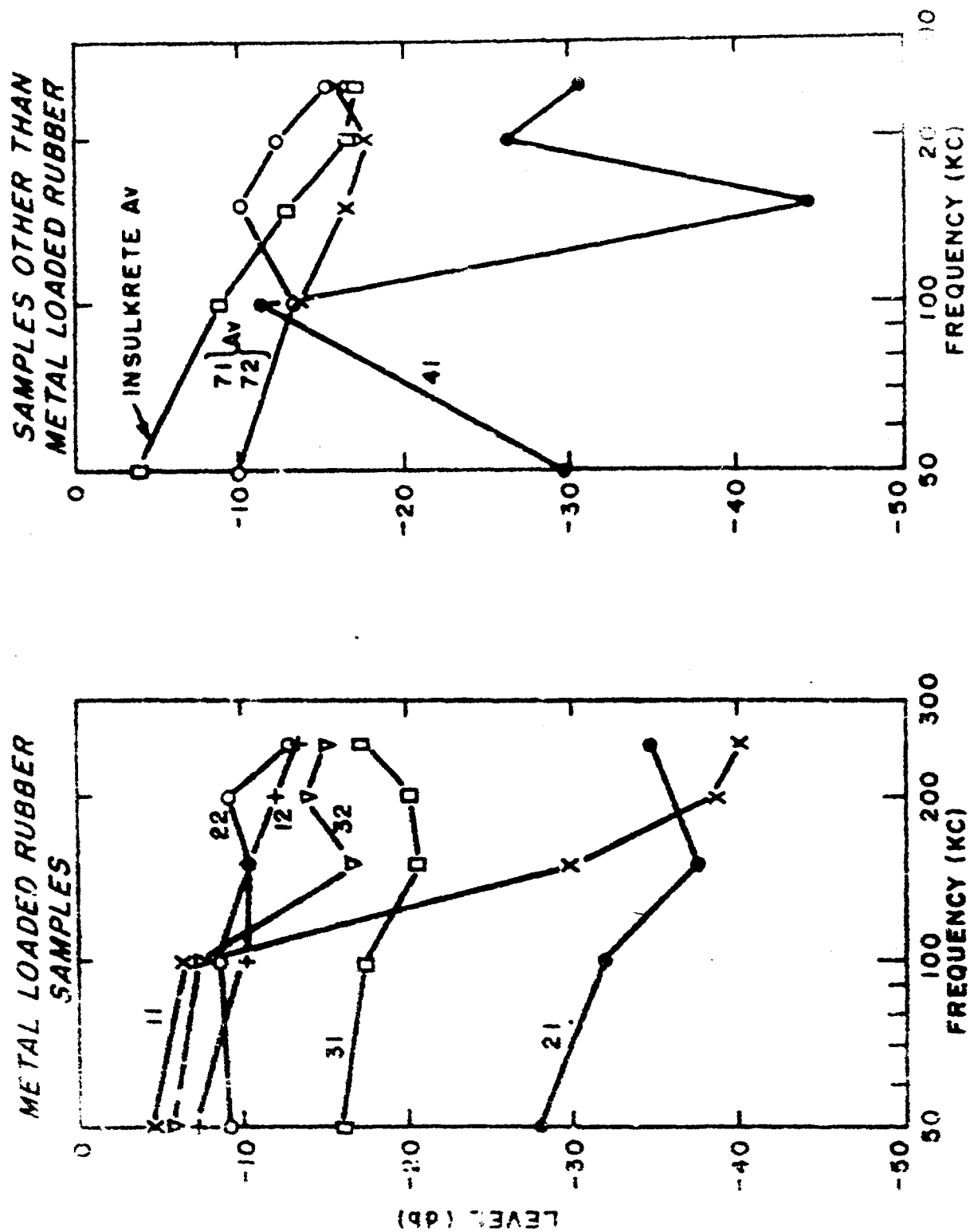

FIG. 36
PEAK REFLECTIVITY INDEX (Δ), FOR ALL SAMPLES vs FREQUENCY

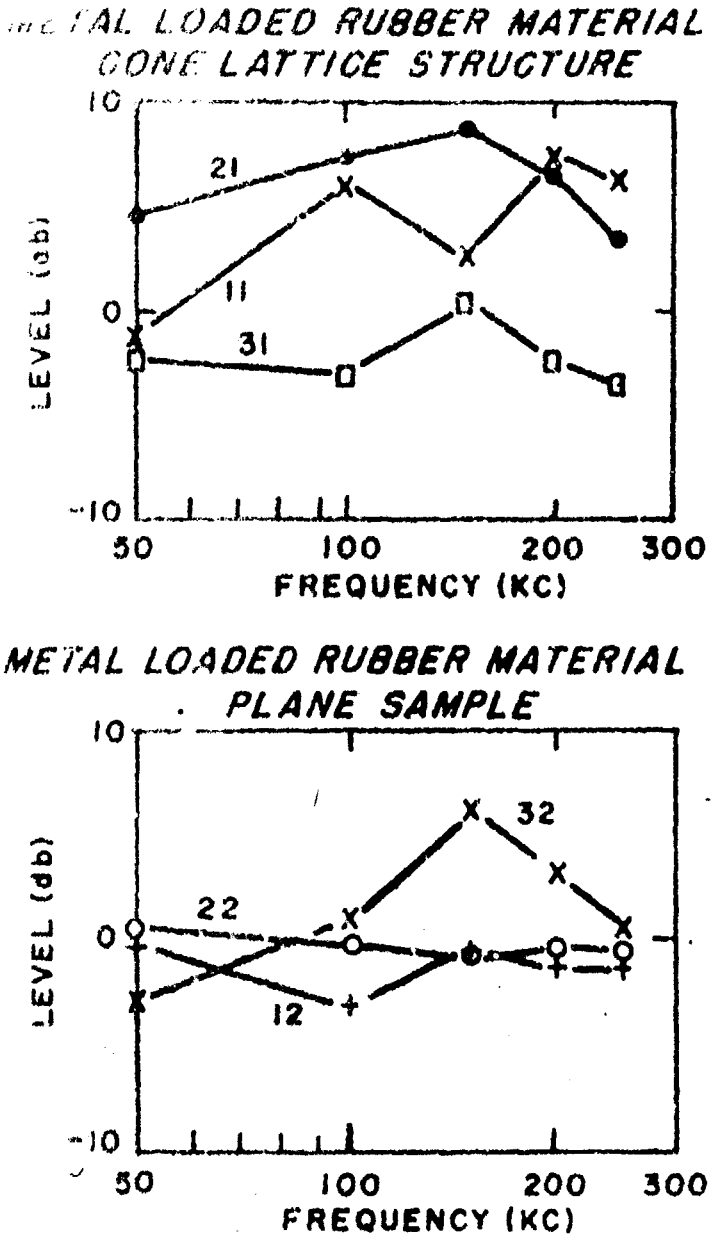

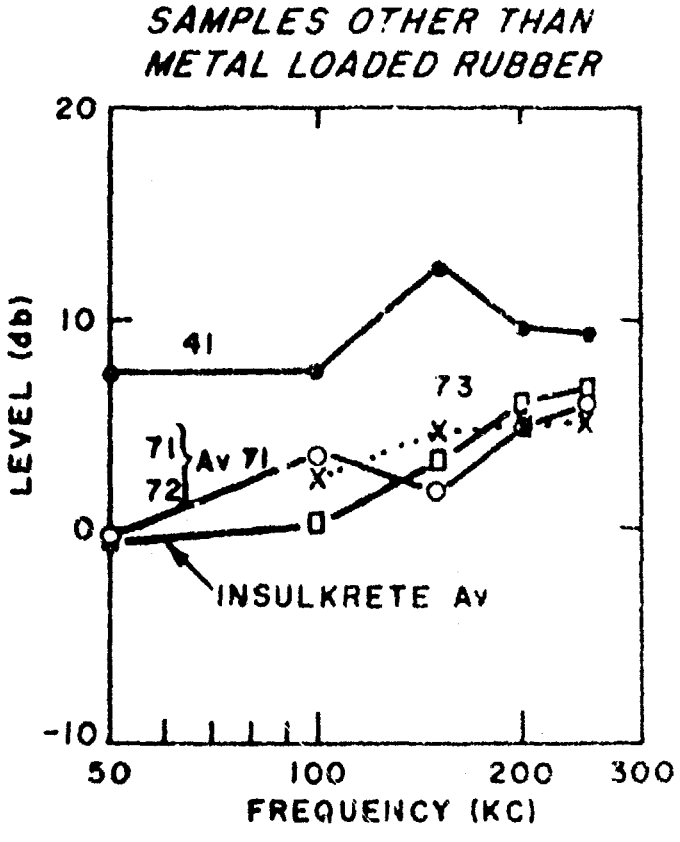

FIG. 37 SCATTERING INDEX, S, FOR ALL SAMPLES vs FREQUENCY

FIG. 38 REFLECTIVITY PATTERNS FOR PLANES Ψ_o AND Ψ_r

SAMPLE NO. 21: ALUMINUM LOADED BUTYL MATERIAL
STRUCTURE: CONE LATTICE
FREQUENCY: 150 KC
PROJECTOR: QBG

PLANE Ψ_r
SECTION B-B, FIG. 13

PATTERN NO. 21-166

S= 10.2 db
Δ=-42.3 db
R=-32.1 db

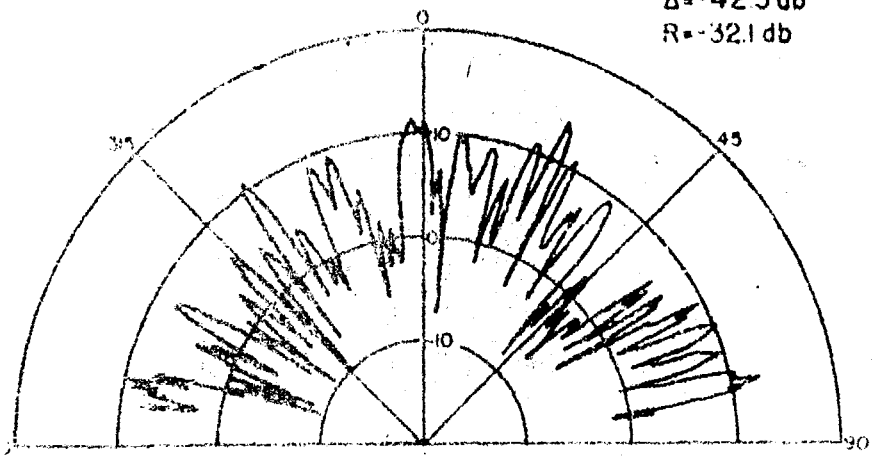

PLANE Ψ_o
SECTION A-A, FIG. 13

PATTERN NO. 21-161

S= 8.7 db
Δ=-40.5 db
R=-31.8 db

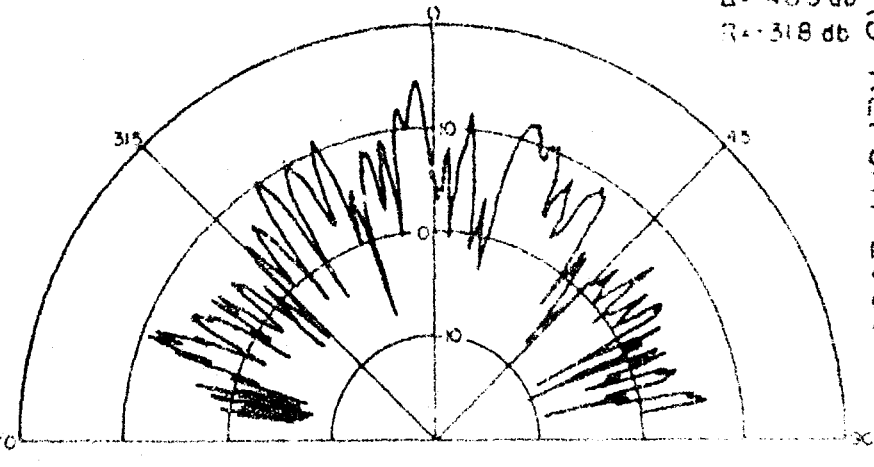

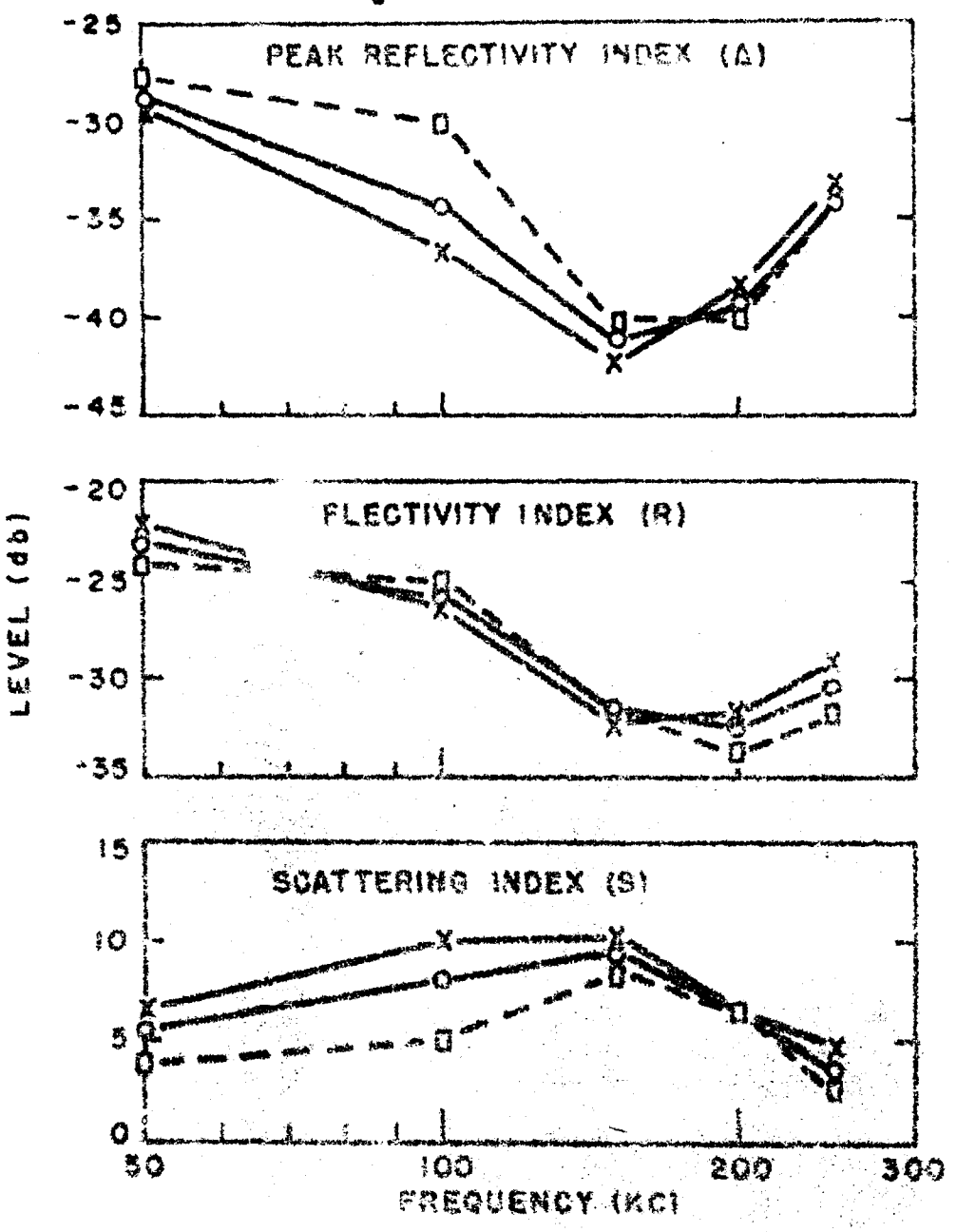

ALUMINUM LOADED BUTYL RUBBER CONE LATTICE

REFLECTION CHARACTERISTICS FROM MEASUREMENTS IN THE PLANES ψ_o AND ψ_r FOR SAMPLE NO. 21

FIG. 39

and Δ and Δ_r from Δ_a are also approximately one db with the exception of the values at 100 kc. At this frequency the maximum deviations are 3 db for S and 4 db for Δ. A comparison of the S_r and S curves indicates that the scattering increased slightly at the lower frequencies in the plane ψ_r which corresponds to a wider spacing of the elements.

71. Figure 40 compares reflection characteristics for Sample No. 73, German Refnir, from 50 to 250 kc. These curves illustrate the effect of averaging results for a sample which has a different geometry in the planes ψ and ψ_r. The maximum deviation of S and R_r from R_a is about 2 db; S and S_r differ from S_a about 2 db and finally Δ and Δ_r differ from Δ_a about 3 db.

72. Table II gives the average values of the reflection parameters for measurements on British Refnir at 250 kc.

TABLE II

Effect of Orientation on the Reflection Characteristics of British Refnir

(db)	(db)	Average (db)
S = 11.4	S_r = 8.0	S_a = 9.6 (see eq. (27))
Δ = -26.3	Δ_r = -25.0	Δ_a = -26.5 (see eq. (29))
R = -16.9	R_r = -17.0	R_a = -16.9 (see eq. (28))

It may be observed that the scattering is 3.4 db greater in the plane of ψ_r than in the ψ_r plane. The larger spacing of elements occurs in the ψ_r plane. Results shown in Figure 31 were made subsequent to those of Table II and since improvements had been made in the technique in the meantime, the reported values differ somewhat. The values in the table are presented to show only the effect of changing the plane of rotation of the probe hydrophone and are considered to be sufficiently accurate for this purpose.

Experimental Measurements on Samples No. 21 and No. 22

Figure 41 shows the reflection characteristics of Sample No. 21 in the frequency range from 140 to 260 kc taken in 5 kc increments. It may be observed that the scattering index S is quite small and hence the values for Δ and R are approximately

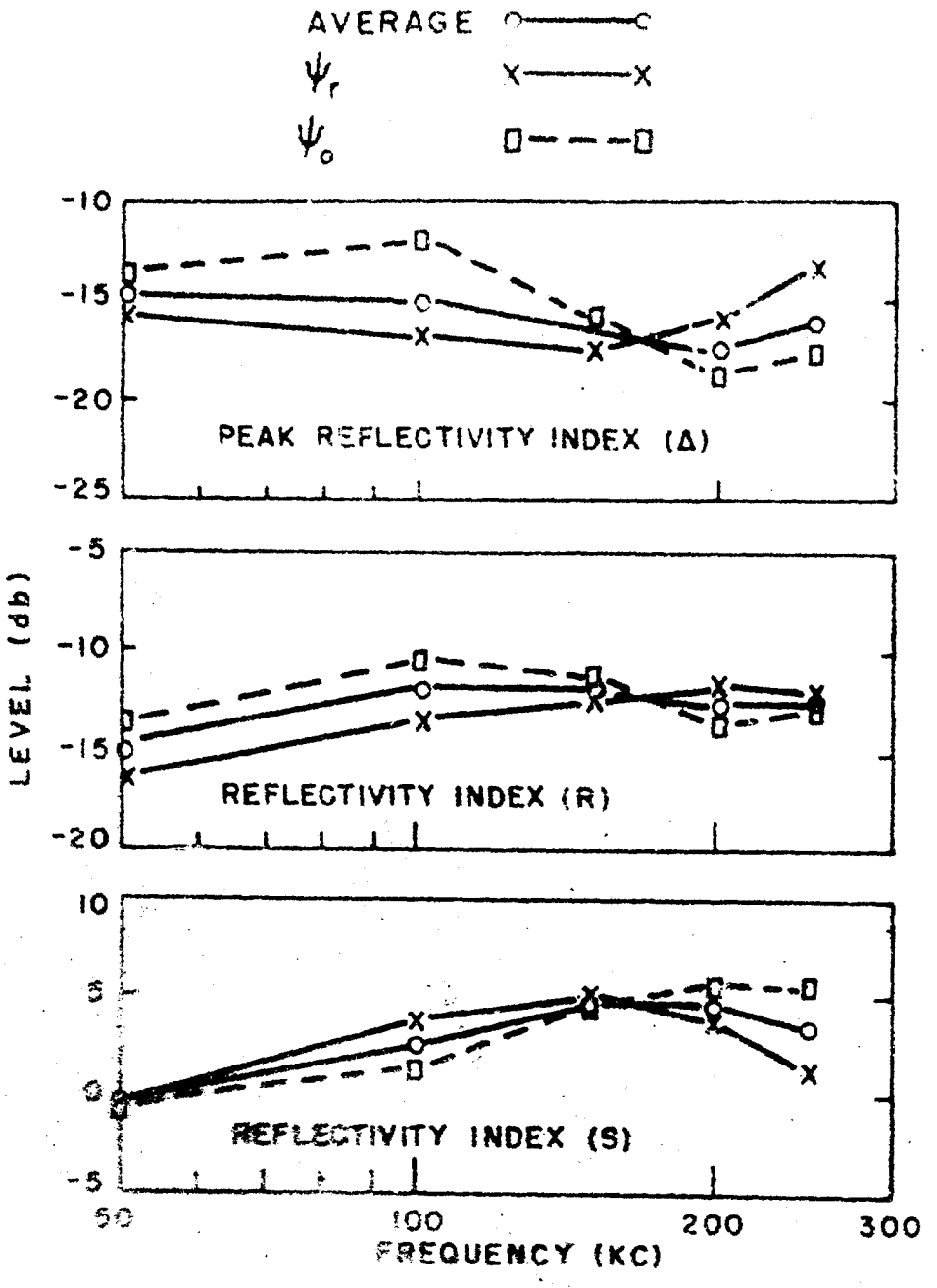

GERMAN FAFNIR SAMPLE

REFLECTION CHARACTERISTICS FROM MEASUREMENTS IN THE PLANES ψ_o AND ψ_r FOR SAMPLE NO. 73
FIG. 40

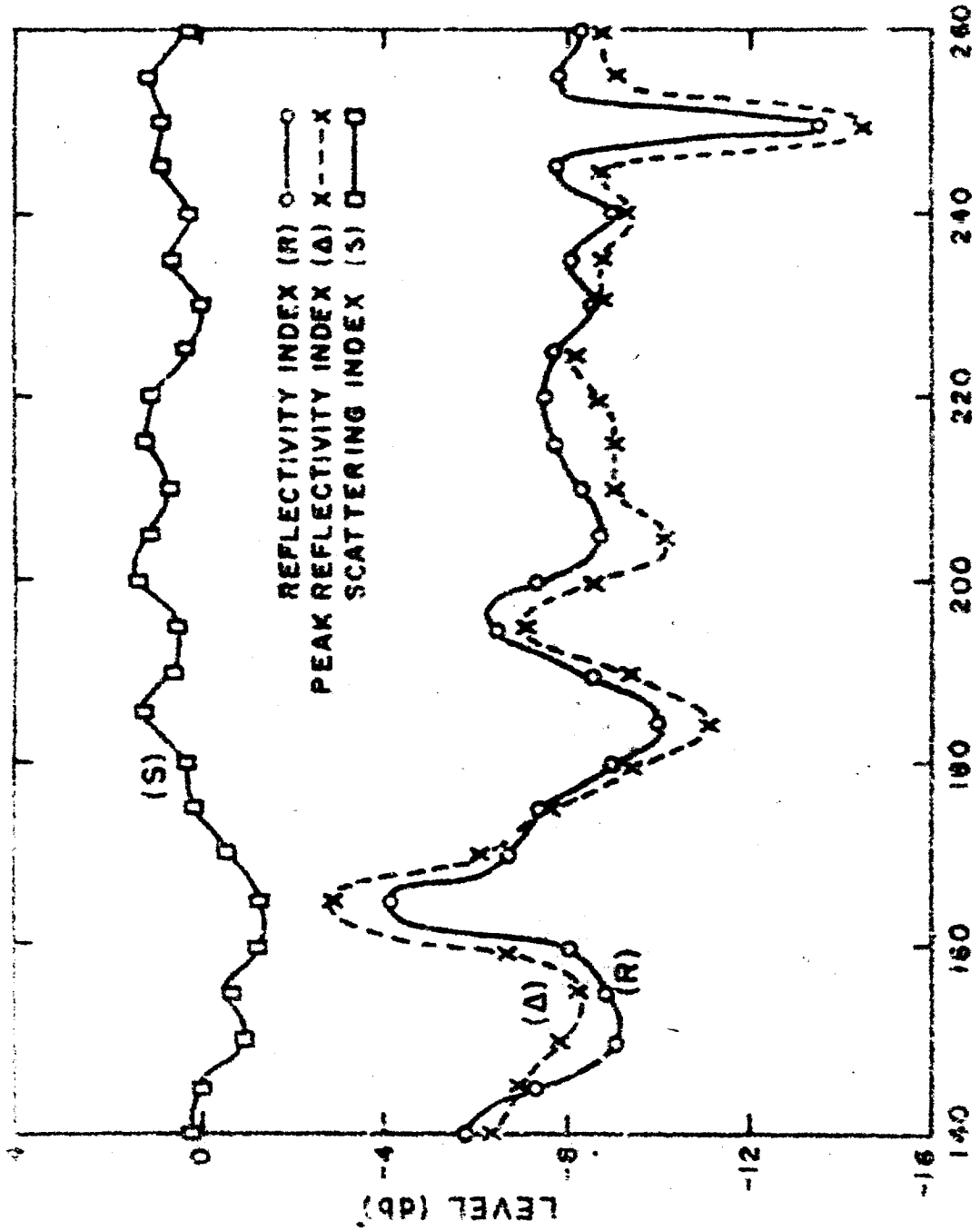

ALUMINUM LOADED BUTYL RUBBER FLAT SAMPLE

REFLECTION CHARACTERISTICS VS FREQUENCY FOR SAMPLE NO. 22
FIG. 41

the same, but vary as much as 5 db in a frequency interval of 5 kc. This variation places a limitation on the interpolation of Δ and R between values measured at intervals of 50 kc.

74. The curve for R shows a roughly periodic variation with frequency from 150 to 200 kc, but from 200 to 245 kc R shows little variation except at 250 kc where there is a pronounced minimum.

75. Figure 42 shows the reflection characteristics of Sample No. 21, the cone-lattice sample corresponding to the plane-surface Sample No. 22, measured at 5 kc increments over the frequency range from 140 to 260 kc. The scattering index for this cone sample is approximately 8 db at 140 kc and decreases to a value of about 4 db at 260 kc. As has been mentioned previously this decrease in scattering is believed to be caused by the increase of reflection with frequency from the flat surfaces between the cone bases. The peak reflectivity index, Δ, is a minimum, -41 db, at around 170 kc; it is about -37 db at 140 kc and increases to -34 db at 260 kc. The reflectivity index, R, is approximately -30 db at both ends of the frequency band (140 kc and 260 kc) and is a minimum (-37 db) at 250 kc.

Comparison of R and R_n. Figures 43 and 44 show the normal reflectivity index, R_n, for the flat sample and the cone-lattice sample, respectively. The corresponding curve for the reflectivity index R is plotted on each curve for comparison. It may be observed that R_n is more nearly equal to R for the flat sample than for the structured sample. The necessity for using the present technique for measuring structured samples may be noted by observing that the difference between the two curves shown in Figure 44 is about 28 db at the low-frequency end.

Broad Frequency Range Measurements - Sample No. 21

77. Measurements were made on Sample No. 21, the aluminum-loaded butyl rubber sample with a cone-lattice structure over the frequency range from 20 kc to 1 Mc, in 50 kc increments. Four projectors (QBG, KB41A, H8 and QHE) were used in order to cover the wide frequency range. Figure 21 shows the beam widths versus frequency of these four transducers.

78. Typical Reflectivity Patterns. Figure 45 shows reflectivity patterns for Sample No. 21 as well as for the reference plate at five representative frequencies. The reflection indices R, Δ, and S, the pattern number, the frequency, and the projector used are indicated on each pattern. Since the values of R, Δ and S obtained with the KB41A transducer do not agree with the averages from 150 kc to 200 kc, the measurements made with this transducer may not be as reliable as the other measurements.

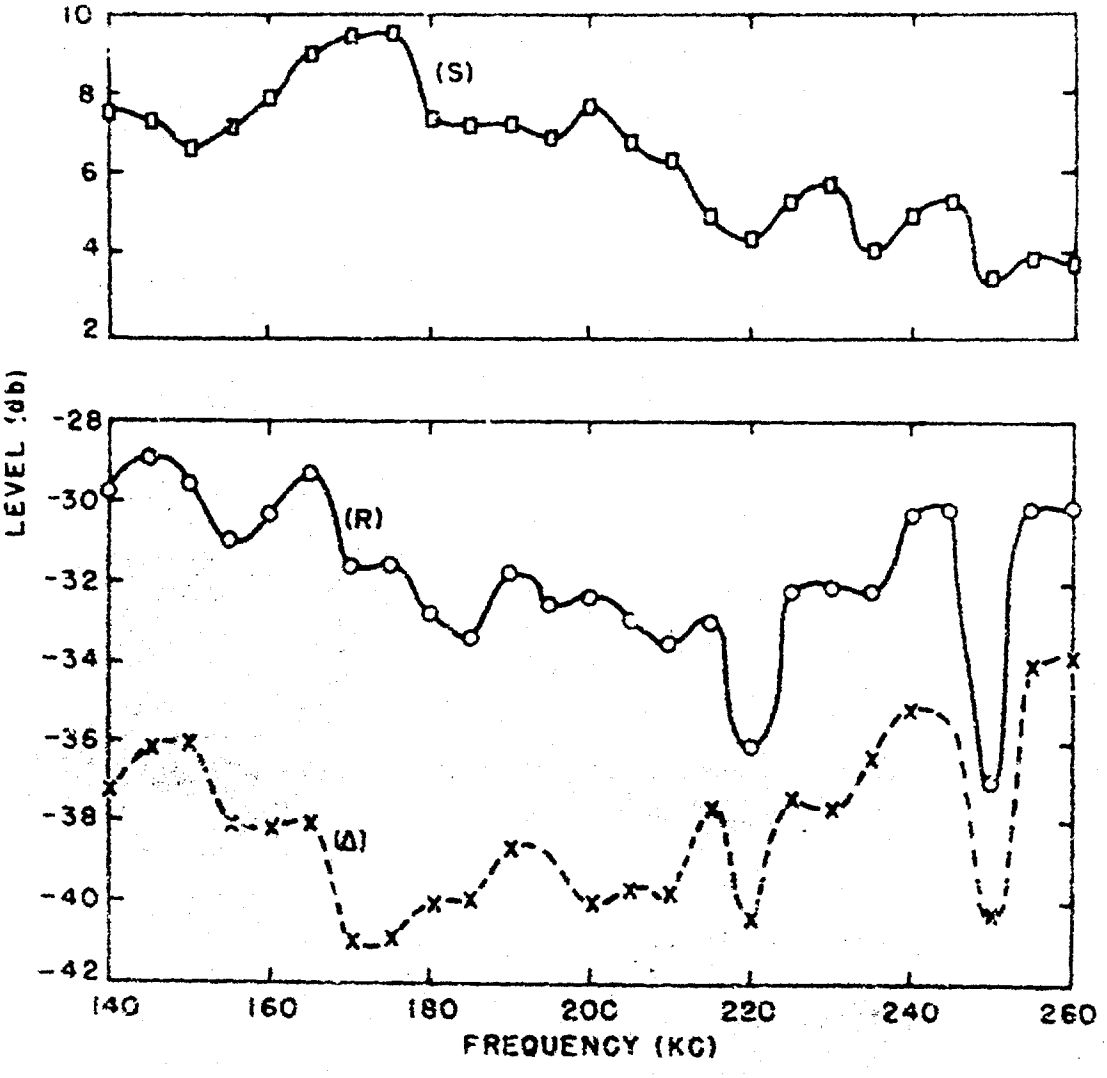

ALUMINUM LOADED BUTYL RUBBER CONE LATTICE SAMPLE

REFLECTION CHARACTERISTICS vs FREQUENCY
FOR SAMPLE NO. 21

FIG. 42

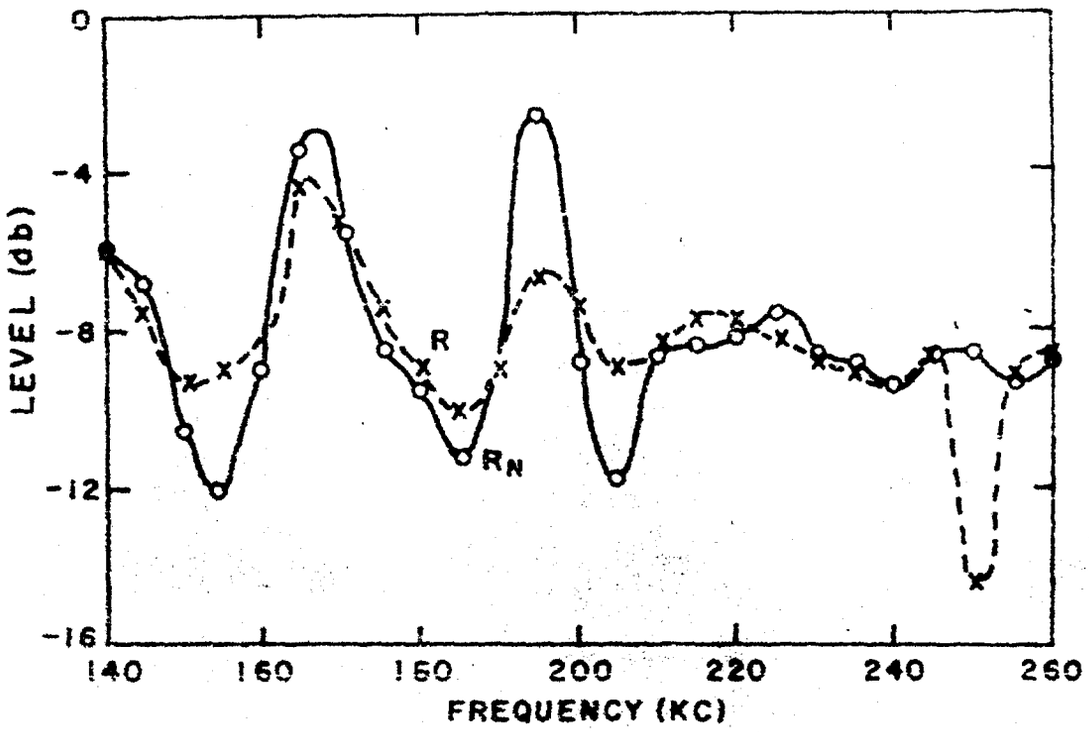

ALUMINUM LOADED BUTYL RUBBER FLAT SAMPLE

COMPARISON OF NORMAL REFLECTIVITY INDEX, R_N, AND THE REFLECTIVITY INDEX, R, OF SAMPLE NO. 22

FIG. 43

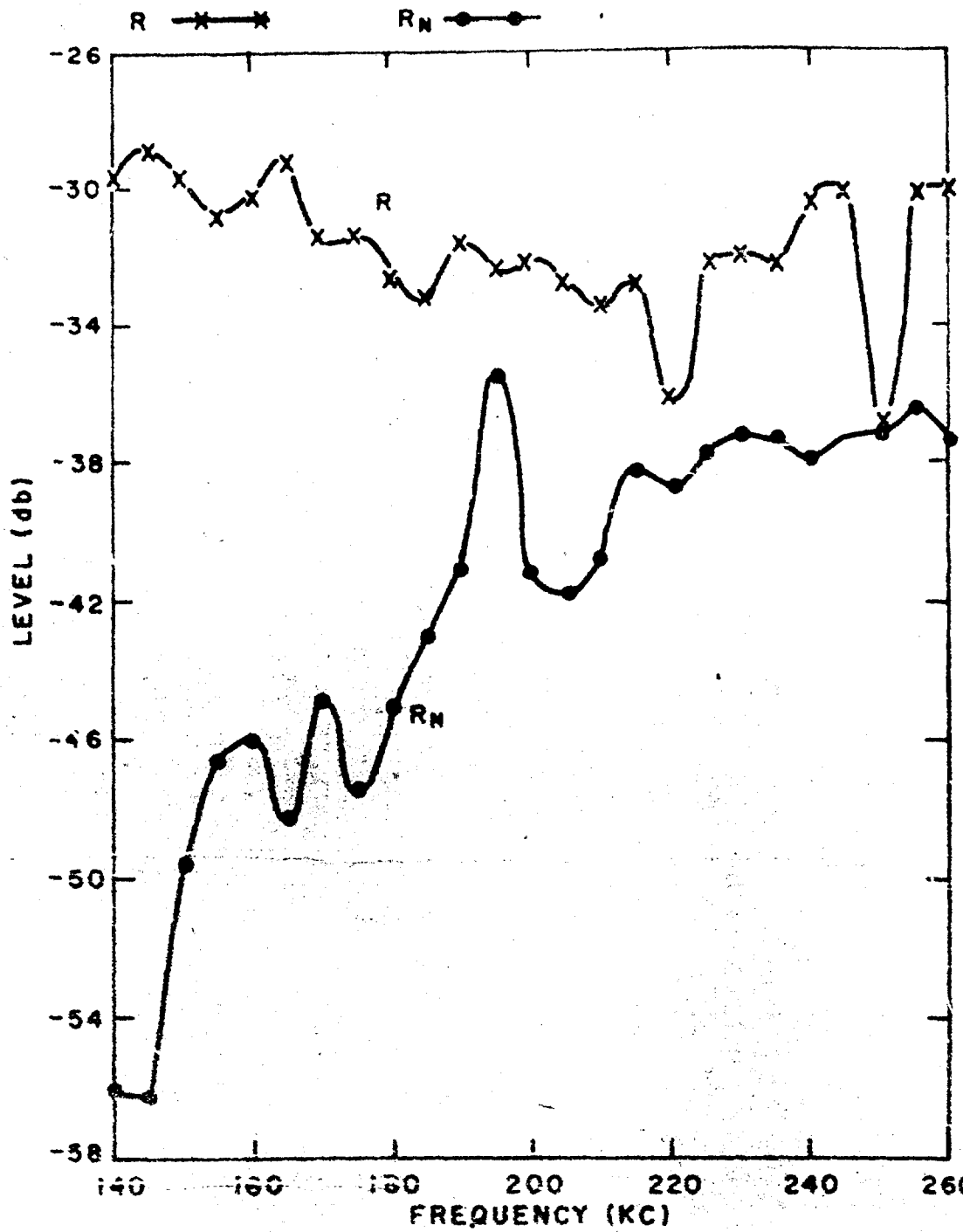

ALUMINUM LOADED BUTYL RUBBER CONE LATTICE SAMPLE

COMPARISON OF NORMAL REDUCTIVITY INDEX, R_N AND THE REFLECTIVITY INDEX, R OF SAMPLE NO. 21

FIG. 44

FIG 45 REFLECTIVITY PATTERNS OF SAMPLE AND REFERENCE PLATE

FREQUENCY 35 KC TO 1 MC
SAMPLE NO 21: ALUMINUM LOADED BUTYL RUBBER
STRUCTURE CONE LATTICE

SAMPLE NO. 21

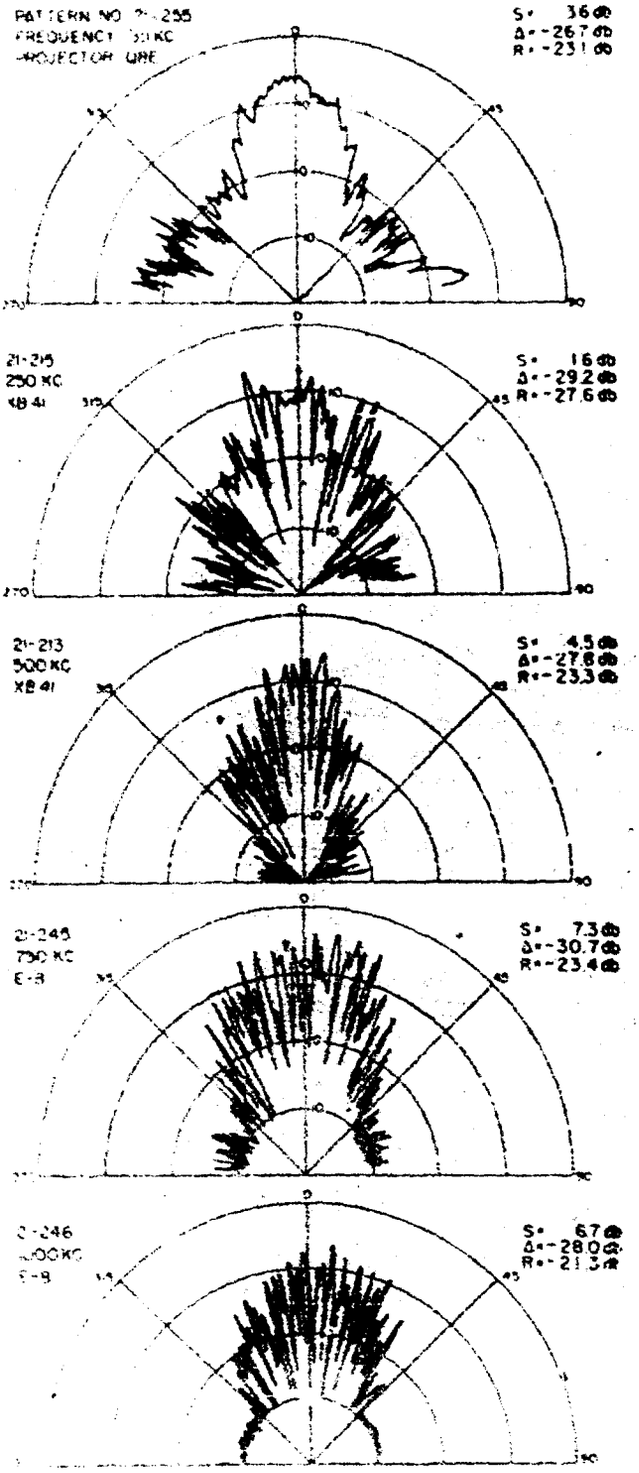

REFERENCE PLATE NO 01

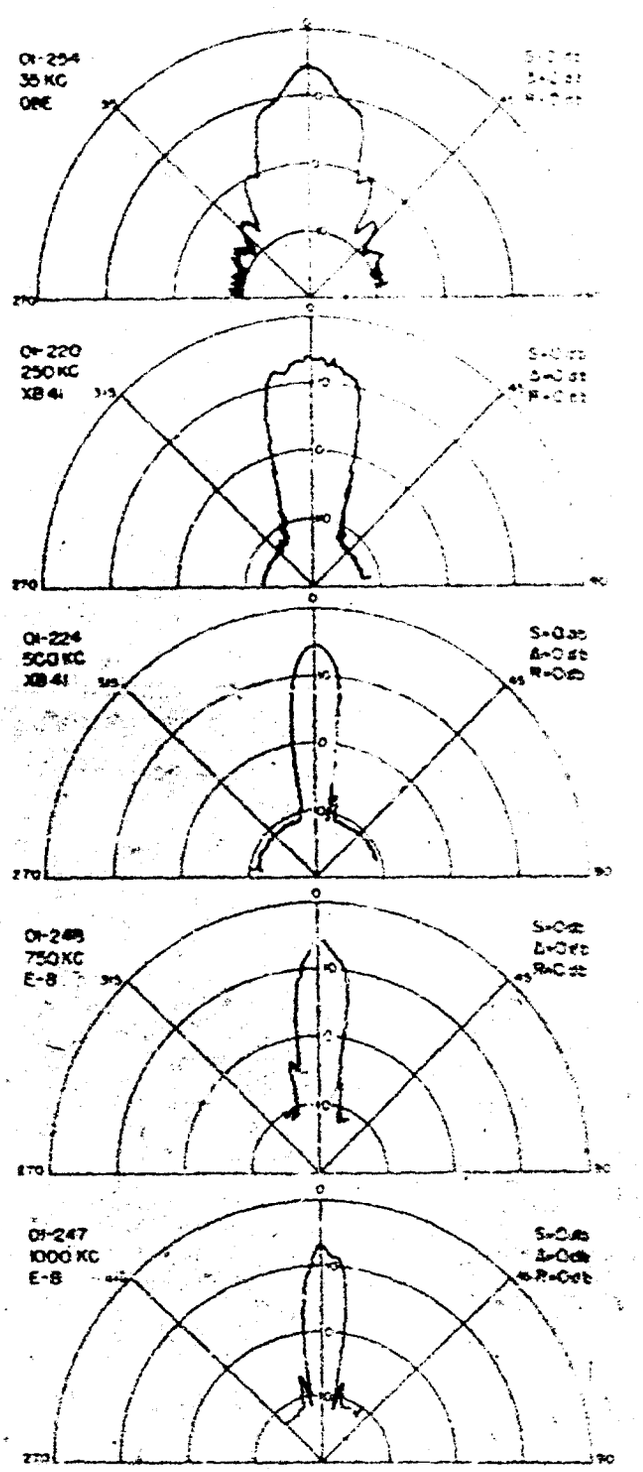

79. A comparison of the patterns for the four transducers at overlap frequency points is shown in Figure 46. The values of R for the patterns at 250 kc differ by 4.5 db. However, the differences in R are only about 1.5 db for the sets of patterns at 50 and 500 kc. Δ differs by 1.4 db at 250 kc but falls within 1 or 2 db at the other two frequencies.

80. Reflection Characteristics. Figure 47 is a plot of the reflection characteristics of Sample 21 throughout the frequency range from 20 kc to 1 Mc. Measurements made with the different projectors are indicated by different symbols. The plotted curves represent an average of all available points except the points marked X. The latter are for the rotated plane $\psi_r = \pi/2$. The curves thus represent measurements made in the plane $\psi_r = 0$. It is considered probable that the decrease in S and the increase in Δ and R over the range from 200 kc to 500 kc are caused by the plane portions of the structure between the cones. The average value of R is below -20 db for the entire range and the average value of Δ is below -25 db for all but the two lowest frequencies. The increase in scattering from 25 kc to 150 kc is in agreement with the theory given by Rayleigh concerning corrugated surfaces, reference (c). Values of R, Δ, and S at the two highest frequencies are somewhat doubtful because of the narrow hydrophone pattern.

Interpretation and Reliability of Results

81. The overall system was checked for linearity and drift as part of the procedure for each run. The drift was checked by retracing an initial low-level portion of the reflectivity pattern and the maximum deviation allowed without discarding a run was approximately 1/2 db. Usually, the retrace did not deviate a measurable amount. The linearity was checked by noting recorder deflection versus oscillator output (see Figure 15 for a block diagram of the equipment). Acceptable values of recorder deflection were -20 $\pm$ 1 db for a 20 db decrease of oscillator output. The deviation was usually about 0.5 db. It was established that this deviation usually occurred in the range from -15 to -20 db, corresponding to low-level portions of the patterns.

82. The ability to duplicate measurements was checked as thoroughly as the limited time available allowed. However, this did not permit very many repeat runs to be made. Repeat runs were made under similar conditions on Sample No. 21 in the frequency range from 50 to 250 kc. The results showed an average deviation for values of R, Δ, and S of $\pm$ 1 db. Comparison runs were made at intervals of several days. The sample was removed and then [illegible] for these comparisons.

FIG 46 REFLECTIVITY PATTERNS OF SAMPLE NO 21 VS PROJECTOR BEAM WIDTH

SAMPLE NO 21 ALUMINUM LOADED BUTYL RUBBER MATERIAL
STRUCTURE CONE LATTICE

NARROW BEAM

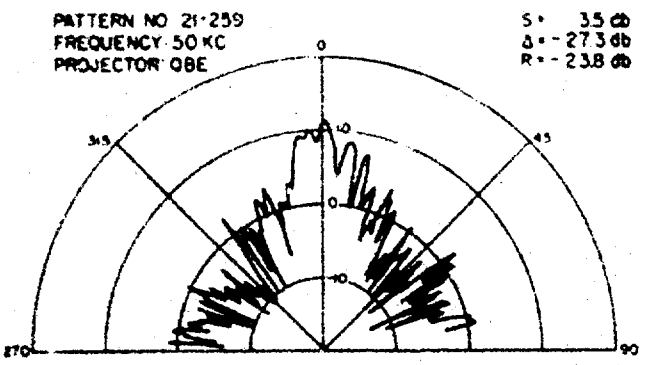

BROAD BEAM

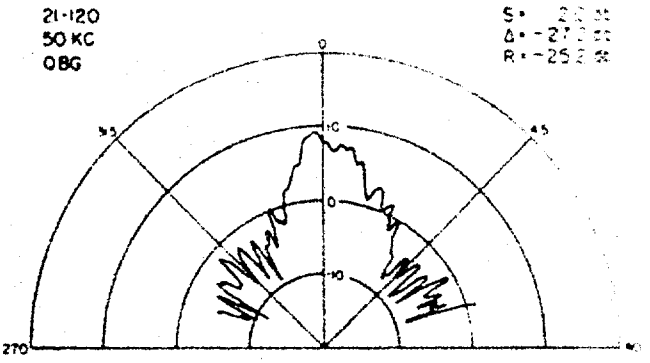

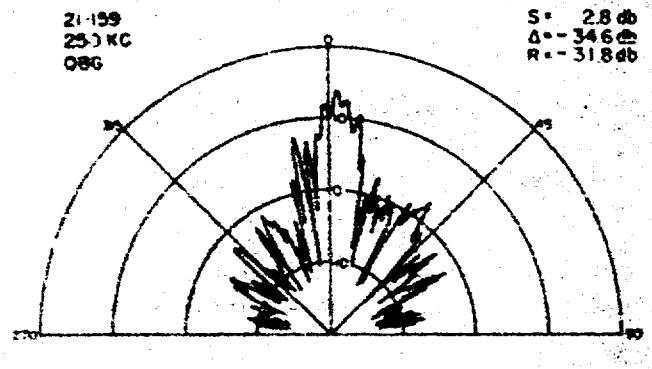

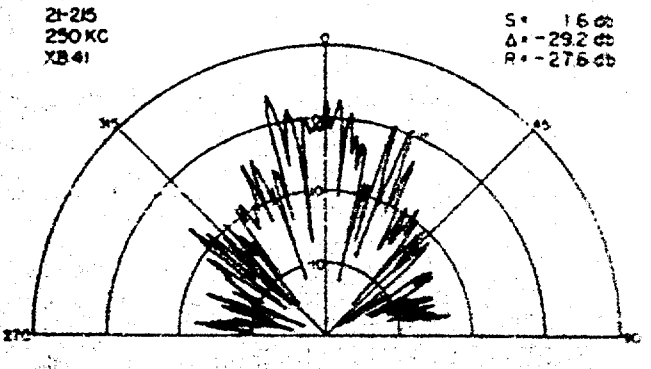

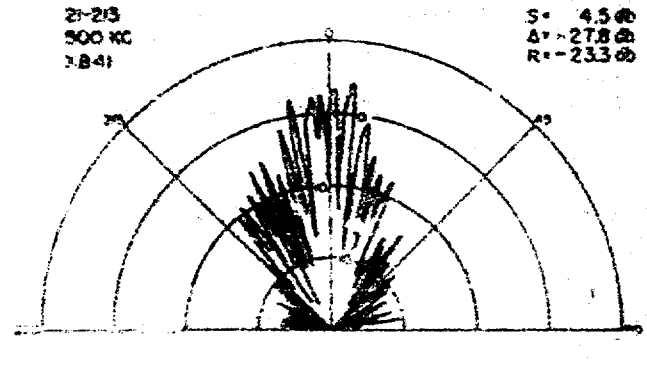

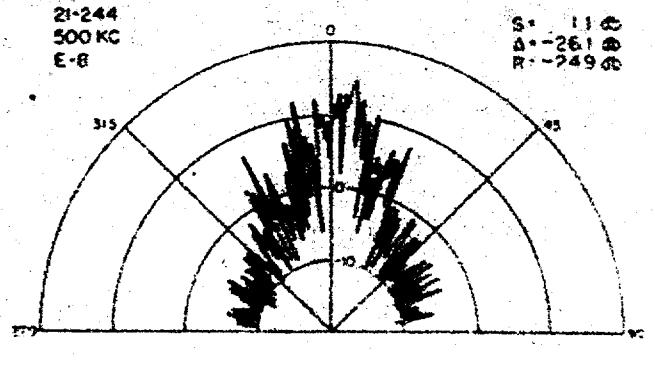

PROJECTOR	SYMBOL	Ψ
QBG	O	O
XB41A	+	O
E8	Δ	O
QBE	□	O
QBG	X	$\pi/2$

—— AVERAGE OF ALL POINTS FOR Ψ_0 PLANE

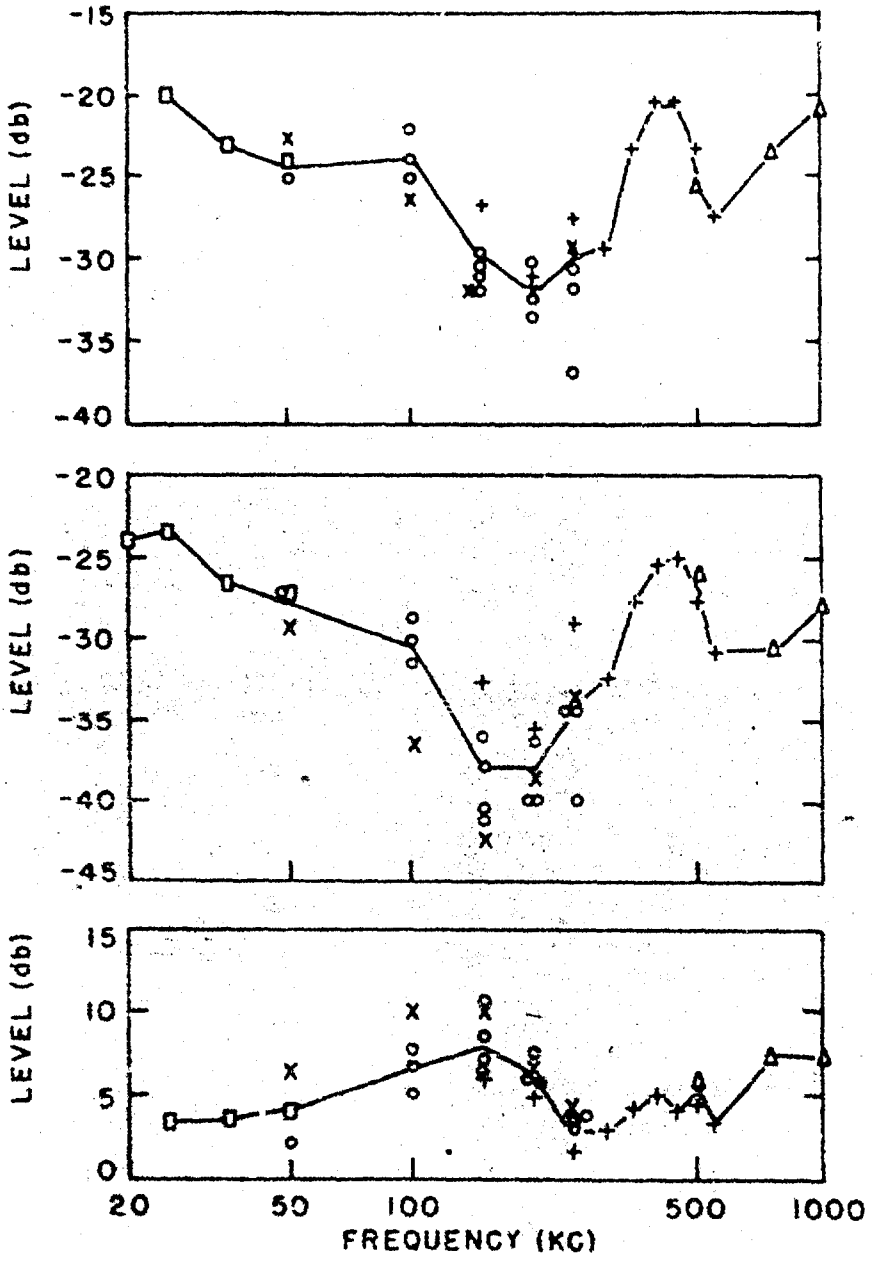

ALUMINUM LOADED CONE LATTICE

REFLECTION CHARACTERISTICS vs FREQUENCY FOR SAMPLE NO. 21

FIG. 47

85. [illegible] in this report is relative to the [illegible] reflected from the reflection plate. Therefore, the scattering index will be dependent on beam width.

VII. CONCLUSIONS AND RECOMMENDATIONS

86. The results of the present study indicate that Sample No. 21, the cone lattice structure of aluminum-loaded butyl rubber, shows outstanding promise as a tank lining over the frequency range from 20 kc to 1 Mc. It would probably be useful at both higher and lower frequencies also.

87. It appears that this lining could be improved for high frequencies by eliminating the discontinuity caused by the plane portion of the lining. Results indicate that reflections from these small plane surfaces are significant at frequencies for which the width of this flat surface is greater than a half-wave length of the sound. For Sample No. 21 this frequency was about 200 kc. These plane surfaces could be replaced by properly shaped depressions.

88. Further improvement of the lining at low frequencies will probably be more difficult than at high frequencies. One possibility is to use included air spaces to permit more deformation of the material and in turn increase the loss. This method was used effectively for Fafnir.

89. Another possible means for improving the absorption of the material at low frequencies is to increase the length of the cones. This would probably have the additional advantage of increasing the scattering at the lower frequencies. The disadvantages are that such a lining would occupy more space, and require more material.

90. It is probable that absorption can be increased somewhat at all frequencies by the selection of better materials. The material consisting of 100 parts of aluminum to 100 parts (by weight) of butyl rubber was selected for the conical structure panels on the basis of reflection measurements made on flat samples. This proportion may not be optimum for a cone-lattice sample. It could be determined by an experimental investigation of a series of cone-lattice samples in which the proportion of metal was varied. There is some indication that the heat treatment during the molding process has considerable effect on the characteristics of the material. Measurements on samples having the same formula indicate differences in reflection characteristics. For example, the flat samples consisting of 100 parts aluminum to 100 parts of butyl rubber, [illegible], indicate approximately 3 db lower [illegible] reflectivity [illegible] than Sample No. 22, Figure 29, although [illegible] approximately 50% thicker than the former.

Experimental investigation of the acoustic properties of cone-lattice samples subjected to a variation of heat treatment during the molding process should be made and the processing technique standardized as far as practicable.

89. In order to extend and refine the knowledge of the applicability of this lining to acoustic tanks, the following additional measurements are recommended:

a. The measurement of reflection characteristics versus the angle of incidence.

b. The measurement of normal reflection reduction versus pressure. These measurements would indicate the applicability of linings for use in acoustic pressure tanks.

c. The measurement of reflection characteristics below 20 kc. Results of these measurements would indicate the lower frequency limit of a tank lined with a cone-lattice structure of aluminum-loaded rubber.

ACKNOWLEDGMENTS

90. The author wishes to express his appreciation to the following individuals of the Acoustics Research Division: Mr. Jacob Pomerantz for comments and help throughout the work on theory, analysis, and presentation; Miss Frances Fergbee for the computation and preparation of the graphs; Mr. P. C. Rand for assistance in making the measurements; Mr. A. T. Jaques and Dr. W. S. Cramer for helpful suggestions in interpreting the results. The loaded butyl rubber was formulated by Mr. Irving Silver, and the molding process was carried out under the supervision of Mr. S. P. Prosen, both of the Chemistry Division.